Effects of Power and Heating Sector Integration for the Future Dutch High-Voltage Electricity Grid

Development of a Representative Model of the Dutch High-Voltage Electricity Grid

W. Zomerdijk

Technische Universiteit Delft

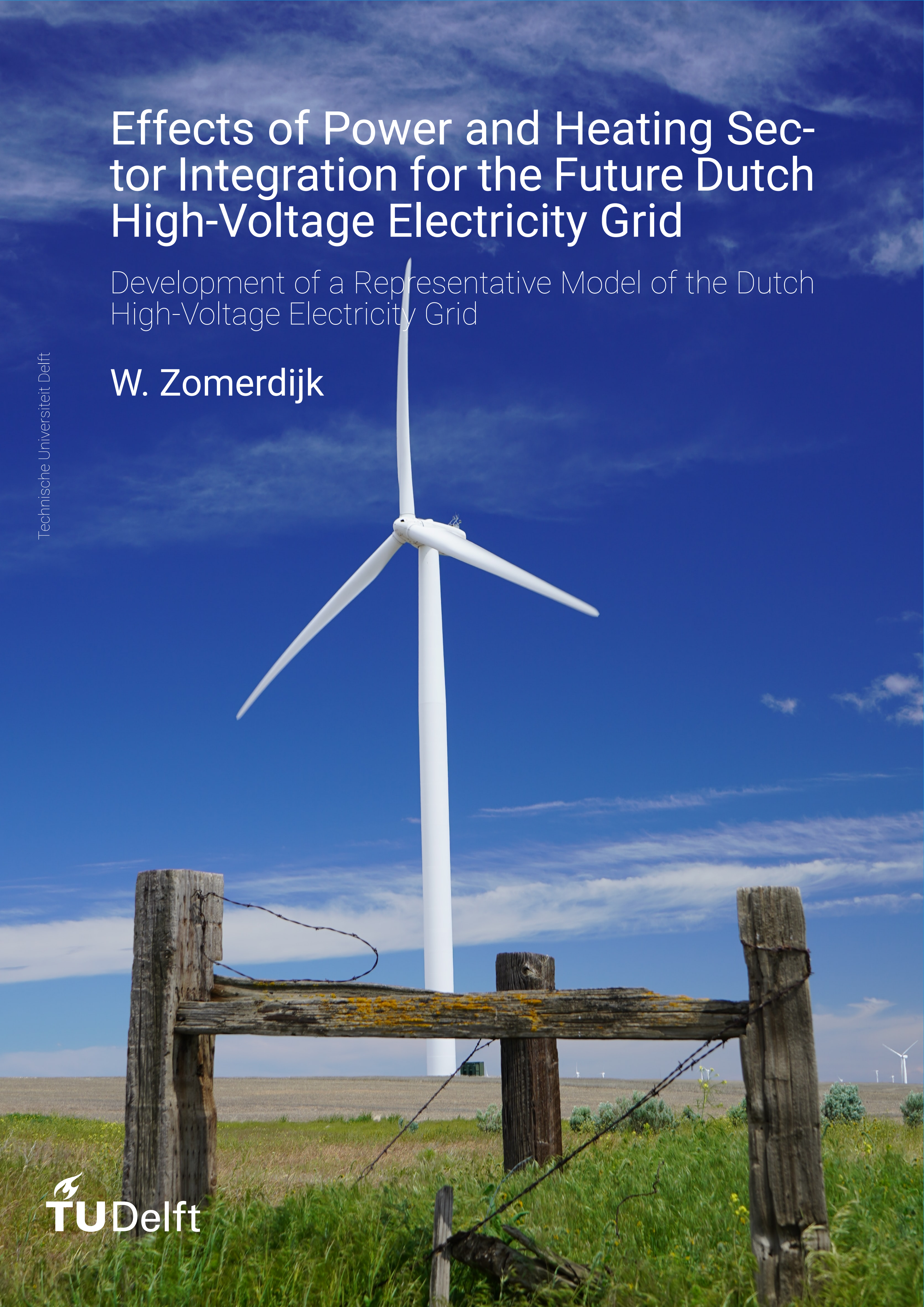

TU Delft

Effects of Power and Heating Sector Integration for the Future Dutch High-Voltage Electricity Grid

Development of a Representative Model of the Dutch High-Voltage Electricity Grid

by

W. Zomerdijk

to obtain the degree of Master of Science
at the Delft University of Technology,
to be defended publicly on Friday December 10, 2021 at 14:00.

Student number:	4319370	
Project duration:	January 4, 2021 – December 10, 2021	
Thesis committee:	Prof. dr. ir. P. Palensky,	TU Delft
	Dr. ir. M. Cvetkovic,	TU Delft, supervisor
	Dr. ir. A. Shekhar,	TU Delft

TU Delft

Abstract

We are on the verge of a global energy system revolution. By signing and ratifying global treaties, the groundwork for this revolution is laid. The objective is to limit global warming to two degrees Celsius above pre-industrial levels and stabilise greenhouse gas concentrations at a level that would prevent dangerous anthropogenic interference with the climate system, before 2050. This requires a carbon-free electricity system, which implicates that existing fossil sources of electricity need to be replaced by renewable sources. Most of these sources are weather-dependent and follow seasonal patterns. This leads to a variable, uncertain, and uncontrollable electricity supply. Energy system integration is posed as a key concept to provide the much-needed flexibility to the electricity grid and has been the subject of extensive research. However, there still is a considerable need for further research in the field of energy system integration. Part of the research gap is validation and substantiation of the proposed energy system integration policies and investment decisions. An indispensable component for filling the research gap is a numerical model of the energy system.

In this context, the author of this thesis developed a numerical model of the Dutch high-voltage electricity grid. The model can be used to analyse proposed energy system integration policies, optimise the electricity system investment decisions, and prioritise the bottlenecks in the electricity system. The model is used to analyse the effects of several power and heating sector integration scenarios for 2050.

The model is constructed in the pandapower framework. The framework is coded in the Python programming language. The model parameters are based on open data and the model input is derived from national sector outlooks and the Energy Transition Model from Quintel Intelligence. Due to the unavailability of operational data from the reference system, the accuracy of the model is determined by evaluating the underlying assumptions and performing a sensitivity analysis. Once the model is validated, the effects of power and heating sector integration on the Dutch high-voltage electricity grid are analysed and the bottlenecks are identified. The results show a substantial increase in grid loading. The highest grid loading occurs when a large portion of the heating demand is electrified, and a large portion of the electricity supply is generated by variable renewable energy sources.

The bottleneck analysis of power and heating sector integration scenarios presents one of the use cases of the created representative model of the Dutch high-voltage electricity grid. As the model is based on open data, it is the intention of the author to make the model publicly available as well. This allows other entities to perform a broad range of analysis on the electricity system.

Preface

During the last eleven months I worked on the development of a representative model of the Dutch high-voltage electricity grid to study the effects of heating sector electrification on the Dutch electricity grid. This thesis does not only fulfil the final requirement to finish the Master Sustainable Energy Technology, but also marks the end of my time as a student. The last eight and a half years have been a roller coaster with ups and downs, and I am grateful for all the opportunities that I was given. This work would not have been realised without the support of many friends, family and colleagues. Therefore, I would like to take this opportunity to express my gratitude. Foremost, I would like to thank my supervisors and committee members. Unfortunately, we haven't met in person yet, but hopefully that will follow soon! Digvijay, thank you for your daily supervision. Your knowledge and experience turned out to be essential. I want to thank Milos for all the valuable feedback and expertise. And lastly, I would like to thank the chair of my committee, Peter, for believing in my capabilities.

A special thanks to Daniël and Lennart, for their unconditional support. We have known each other since the start of my life as a student in Delft. Thank you for all your advice, solicited and unsolicited. Furthermore, I would like to give special thanks to my father Timo, my mother Yvonne, and my twin brother Pim. You always had a positive note that kept me going – I would not be here without you.

W. Zomerdijk
Rotterdam, December 2021

Contents

Glossary

Alternating Current (AC)	an electric current which periodically reverses direction and changes its magnitude continuously with time. The number of reversals per second is referred to as the frequency. The European electricity system runs on AC at a frequency of 50 Hz.
Anthropogenic	caused by humans or their activities.
Capacity factor	a measure of how often an electricity generator runs for a specific period of time. Expressed as a percentage and calculated by dividing the actual electricity output by the maximum possible output.
Circuit	the high-voltage electricity grid operates at alternating current in three separate phases. A high-voltage line consists of one circuit with three conduits, one conduit per phase [1].
Convertor station	a station where direct current is converted to alternating current and vice versa [1].
Demand side response	providing the possibility of shifting demand away from the peak, although the average daily consumption is not altered [2].
Direct Current (DC)	an electric current that is uni-directional, so the flow of charge is always in the same direction.
Energy sector integration	linking the various energy carriers—electricity, heat, cold, gas, solid and liquid fuels—with each other and with the end-use sectors, such as building, transport or industry [3].
Energy system integration	the coordinated planning and operation of the energy system across multiple energy carriers, infrastructures, and consumption sectors, for a more efficient, circular, and reliable energy system [3].
European Green Deal	a new growth strategy that aims to transform the EU into a fair and prosperous society, with a modern, resource-efficient and competitive economy where there are no net emissions of greenhouse gases in 2050 and where economic growth is decoupled from resource use [4].
Flexibility	the capability of a power system to cope with the variability and uncertainty that solar and wind energy introduce at different time scales, from the very short to the long term, avoiding curtailment of power from these variable Renewable Energy Sources (RES) and reliably supplying all customer energy demand [5].
Full-load hours	represents the number of hours a generator would need to produce a certain amount of energy if it is operating at full capacity.
Grid reliability	the ability of power system components to deliver electricity to all points of consumption, in the quantity and with the quality demanded by the customer [6].
High-voltage	in the Netherlands referred to as all voltage levels of 110 kV and up.
High-voltage lines	the lines responsible for the transportation of electricity from and to the high-voltage stations and neighbouring countries.

High-voltage stations	a location where generators, transformers, protection equipment, and lines are connected to.
kV	1 kiloVolt [kV] = 1,000 Volt [V].
MVA	1 MegaVoltAmpere [MVA] = 1,000,000 VoltAmpere [VA] = 1 Watt [W] = 1 Joule per second [J/s]. It represents the amount of electric energy that can be transported via a conduit.
National Climate Agreement	an agreement ratified by the Dutch government containing a package of measures which has the broadest possible base of societal support, which has the active support of as many contributing parties as possible and which will achieve the political reduction target of 49% in 2030 [7].
Network expansion planning	determine the optimal network expansion investments to expand the existing power system to serve the growing demand in the future.
Optimal power flow	a loadflow computation, in which the calculation of the node voltages and the optimisation of the controllable variables are carried out simultaneously [8].
Paris Climate Agreement	a legally binding international treaty on climate change which goal is to limit global warming to well below 2, preferably to 1.5 degrees Celsius, compared to pre-industrial levels [9].
Power-to-Heat	the use of systems (e.g. heat pumps and/or boilers) that can convert renewable electric power into efficient heating or cooling [10].
Power-to-Hydrogen	the use of systems (e.g. PEM and/or alkaline electrolysers) that can convert renewable electric power into hydrogen [10].
Power-to-X	the process of converting the power generated from renewable sources to different types of energy carriers for use across multiple sectors, or to be reconverted back into power [10].
Security of supply	the ability of an electricity system to guarantee supply to customers with a clearly established level of performance [11].

List of Acronyms

AC	Alternating Current
CBS	Statistics Netherlands
CCGT	Combined Cycle Gas Turbine
CCS	Carbon Capture and Storage
CHP	Combined Heat and Power
DC	Direct Current
DSO	Distribution System Operator
EF	Emission Factor
ETM	Energy Transition Model
ETS	Emmissions Trading System
GEP	Generation Expansion Planning
HV	High-Voltage
IRENA	International Renewable Energy Agency
LCA	Life Cycle Assessment
LT-LEDS	Long-Term Low Emission Development Strategy
NDC	Nationally Determined Contributions
OPF	Optimal Power Flow
P2H	Power-to-Heat
$P2H_2$	Power-to-Hydrogen
P2X	Power-to-X
PBL	Netherlands Environmental Assessment Agency
PFO	Paper, Food, and Other
PV	Photovoltaic
RES	Renewable Energy Sources
SCGT	Simple Cycle Gas Turbine
TSO	Transmission System Operator
UCM	Unit Commitment Model
UIC	Unit Investment Costs
UNFCCC	United Nations Framework Convention on Climate Change
VRES	Variable Renewable Energy Sources

List of Figures

List of Tables

1
Introduction

This chapter provides the reader with a general overview of the scope, goal, and outline of this thesis. In the first section, Section 1.1, background information is presented, followed by stating the problem definition in Section 1.2. In the subsequent section, Section 1.3, the research objective is introduced, leading to a formulation of the research questions in Section 1.4. Section 1.5 sketches the approach for answering the posed research questions. Finally, the content of this document is outlined in Section 1.6.

1.1. Background

We are on the verge of a global energy system revolution. The groundwork for this revolution is laid by signing and ratifying global treaties. The treaties underpin the need for research in general, and this thesis' research in specific. The beginning of this global revolution dates back tens of years ago. Below, a timeline composed of milestones is presented.

Rio de Janeiro, 1992

An international environmental treaty addressing climate change, known as the United Nations Framework Convention on Climate Change (UNFCCC), is negotiated and signed by 154 states. The objective of the convention is to stabilise greenhouse gas concentrations at a level that would prevent dangerous anthropogenic interference with the climate system [19]. Since then, almost all the members of the United Nations have signed and ratified the treaty.

Paris, 2015

A legally binding international treaty on climate change, known as the Paris Agreement, is adopted by 196 signatory parties of the UNFCCC. The objective of the Paris Agreement is to limit global warming to 2 degrees Celsius above pre-industrial levels and to pursue efforts to limit the temperature increase even further to 1.5 degrees Celsius. Therefore, as stated in the treaty, the global emissions need to peak as soon as possible, whereafter rapid reductions need to be undertaken [20].

As part of the Paris Agreement, all the participating countries had to submit their climate action plans, known as the Nationally Determined Contributions (NDC), by 2020. To provide a long-term horizon to their NDC, the countries were also invited to submit their Long-Term Low Emission Development Strategy (LT-LEDS). In their NDC, the countries communicate the actions they will take to reduce their greenhouse gas emissions and to build resilience to adapt to the impacts of rising temperatures. The LT-LEDS places the NDC into the context of a countries' long-term planning and development priorities, providing a vision and direction for future development [9].

Brussels, 2016

The European Commission submitted their first version of the NDC in October 2016, and an updated version on December 2020, which states that its Member States are committed to a binding target of a net domestic reduction of at least 55% in greenhouse gas emissions by 2030 compared to 1990 [21]. The LT-LEDS submitted by the European Commission in March 2020, states that its Member States are committed to achieving a climate-neutral EU by 2050 [22]. Both of which have been incorporated in the European Green Deal; a new growth strategy that aims to transform the EU into a fair and prosperous society, with a modern, resource-efficient and competitive economy where there are no net emissions of greenhouse gases in 2050 [4].

The Hague, 2019

As an EU Member State, the Netherlands is committed to achieving both the 55% reduction in emissions by 2030 and climate-neutrality by 2050. The long-term planning and development priorities of the Netherlands for achieving these goals are documented in the National Climate Agreement and were published in June 2019 [7]. Among other things, it states that between now and 2050, limiting climate change will require a carbon-free electricity system, which implicates that existing fossil sources of electricity need to be replaced by renewable sources. Sources which, in the case of the Netherlands, will comprise offshore and onshore wind turbines, solar panels, and sustainable molecules. Most of these sources are weather-dependent and follow seasonal patterns, leading to a variable, uncertain, and uncontrollable electricity supply. Moreover, it states that due to the electrification—often introduced as a simple pathway to sustainability—in the industry, mobility, and buildings sectors, there will be a growing demand for electricity generated from renewable sources. Furthermore, as climate-neutrality applies to the entire energy system and as some energy end-use sectors are difficult to electrify, conversion of electricity to sustainable molecules (e.g. hydrogen and methane) will be necessary to achieve the overall energy policy goals. Difficult-to-electrify end-use sectors include, among others, high-temperature industries, aviation, and heavy and long-haul transport. This will further increase the electricity demand. Finally, a more circular energy system is envisioned. Waste streams will need to be reused for energy purposes. A common example is the use of waste heat from industrial processes and data centres for district heating networks.

To summarise, the key characteristics of the Dutch future energy system will be threefold: (1) electricity fully supplied by renewable energy sources, (2) increase in demand for electricity, due the electrification of energy in end-use sectors and the conversion of electricity to other sustainable energy sources, and (3) reduction of energy waste streams by creating a circular energy system.

In general, there are radical changes required for every energy sector and research has to be done in identifying the bottlenecks, increasing the energy efficiency, building a roadmap, and devising policies for the way forward in all of them. For the power sector specifically, there is a need for added flexibility to balance the variable electricity supply and increasing demand. Multiple policies have been proposed to increase the flexibility, such as energy sector integration, large-scale storage integration, demand side response, network expansion planning, and European interconnection.

In the envisaged energy system sketched in the Dutch climate agreement and shared by the findings of a joint study by TenneT TSO B.V. and N.V. Nederlandse Gasunie [23, 24], energy sector integration is posed as a key concept to provide flexibility to the electricity grid, and decarbonise other energy sectors through extensive electrification and the use of sustainable fuels. In recent studies related to energy sector integration, the effects of linking the power and gas sector are often researched. However, a detailed analysis of the effects of linking the power and heating sector in the Dutch future energy system has not been performed.

According to research performed by the Aalborg University, data for energy use in the Netherlands in 2015 shows the final energy demand for heating and cooling applications to be 50% of the final Dutch energy demand [25]. With the goal of achieving climate-neutrality in 2050, part of the energy demand for these applications will need to be provided by electricity. This is where Power-to-Heat (P2H) comes in. P2H is the use of systems (e.g., heat pumps and boilers) that can convert renewable electric power into efficient heating or cooling [26].

1.2. Problem Definition

The integration of P2H resources in the Dutch energy system has two major advantages: (1) P2H can provide extra flexibility to the electricity system, and (2) P2H can decarbonise the heating sector by extensive electrification of the heat sources. However, the adoption of P2H resources in the Dutch energy system will impact the existing final electricity demand and electricity peak loads. While P2H technologies enable a decarbonised future, they can have a significant impact on the electricity grid. One method applicable for analysing the effect of energy sector integration in general, and more specifically heating sector electrification by P2H integration, is the use of energy system modelling frameworks. However, one of the drawbacks shared by the modelling frameworks is the absence of a detailed Dutch power system model applicable for performing an electricity grid impact analysis.

1.3. Research Objective

An indispensable component for filling this research gap is a numerical model of the Dutch electricity grid. A numerical model of the grid can be used to get accurate insights into the impact of policies and investment decisions regarding the decarbonisation and transformation of the energy system, while also helping in identifying bottlenecks in implementing decisions. For this thesis, the focus lies on creating a model of the national high-voltage electricity grid and analysing effects of nationwide energy demand transformation. More specifically, the impact of heat electrification scenarios in 2050 on the Dutch high-voltage electricity grid are analysed to identify the bottlenecks and evaluate grid investment decisions.

1.4. Research Questions

In order to evaluate the effects of electrification of the heating sector on the Dutch high-voltage electricity grid, the following research question and sub-questions are proposed:

1 **How do we create a representative model of the Dutch high-voltage electricity grid for assessing energy sector integration?**

- How do we create a model of an electricity grid at a national scale?
- How do we validate a model of the Dutch electricity grid?

2 **How do we create scenarios for power and heating sector integration?**

- What are the national outlooks for the heating sector?
- Which energy sectors need to be considered for future heating sector electrification?

3 **How does heating sector electrification impact the investments in the electricity grid?**

- What are the bottlenecks of heating sector electrification for the Dutch high-voltage electricity grid?
- Will grid investments be needed to overcome these bottlenecks in 2050?

1.5. Research Approach

The main research questions revolve around three different aspects of this thesis' work. The first research question focuses on the model of the Dutch high-voltage electricity grid. The model is created by analysing all available open data sources to obtain information on the critical high-voltage stations, high-voltage and interconnection lines, transformers, renewable and non-renewable generators, and demand load. The model is validated using available validation and verification approaches in literature.

Having validated the model, the next research question focuses on the scenario study for power and heating sector integration. The national outlooks for the power and heating sector are analysed and the potential for heating sector electrification is researched. Multiple scenarios are created to analyse both the effects of low and high penetration of variable renewable energy sources, and low and high electrification of the heating sector. The stability of the grid is tested by imposing extreme weather in the different scenarios.

The final part of this research revolves around analysing the impact of heating sector electrification on the high-voltage electricity grid. The bottlenecks are identified and grid investments are proposed to resolve them. The main objective of doing such an impact analysis is to prove the agility and abilities of the created model.

1.6. Thesis Outline

The findings of the literature review and the context of the proposed energy sector integration policies are presented in Chapter 2. Chapter 3 explores the physical infrastructure and the organised electricity market of the Dutch power system. The modelling and validation methods used to create a representative model of the Dutch high-voltage electricity grid are discussed in Chapter 4. The methodology and results of the scenario study are conferred in Chapter 5. The results of the bottleneck analysis, and sensitivity analysis are presented in Chapter 6. Finally, Chapter 7 concludes the study by formulating an answer to the posed research questions, and suggesting future research.

2

Background on Energy Sector Integration

In Chapter 1 the objectives set out in the National Climate Agreement are presented, which state that the Netherlands is committed to achieving both 55% reduction in greenhouse gas emissions by 2030 and climate-neutrality by 2050 [7]. The objectives are derived from the Paris Climate Agreement and the European Green Deal. The three agreements clearly outline a vision for future energy systems and are used as a backbone for this thesis. All three agreements state that further decarbonising the energy system is critical to reach the climate objectives in 2030 and 2050 [4, 7, 20]. The energy system comprises of all producers of energy carriers, the energy carriers themselves, and the end-users. Decarbonisation can be accomplished in all three parts of the energy system. The producers of energy carriers can decarbonise by deploying carbon capture systems and replacing fossil fuels with renewable energy sources where possible. The energy carriers can be decarbonised by deploying excess energy storage and conversion systems, reducing the amount of resources wasted. The end-users can decarbonise by improving energy efficiency and increasing electrification where possible.

One of the strategies proposed by the European Commission to reach the decarbonisation objectives is the European Energy System Integration Strategy. The European Commission defines energy system integration as the coordinated planning and operation of the energy system across multiple energy carriers and infrastructures [3]. The three key characteristics of an integrated energy system, in line with the decarbonisation methods mentioned above, are: (1) a more circular energy system, with energy efficiency at its core, (2) a greater direct electrification of end-use sectors, and (3) the use of renewable and low-carbon fuels for end-use applications where electrification is not feasible [27]. According to the European Energy System Integration Strategy, the benefits of energy system integration can be summarised fivefold: (1) to reduce the greenhouse gas emissions in sectors that are more difficult to decarbonise, (2) to reduce the amount of energy needed and reduce the related climate and environmental impacts, (3) to strengthen the competitiveness of the European economy, (4) to provide additional flexibility and boost storage technologies, and (5) to contribute to greater consumer empowerment, improved resilience and security of supply [27].

The National Climate Agreement envisages a Dutch energy system whose key characteristics are: (1) a reduction of energy waste streams by creating a circular energy system, (2) an increase in demand for electricity due to the electrification of end-use sectors and the conversion of electricity to other sustainable energy sources, and (3) electricity fully supplied by renewable energy sources [7]. One of the strategies posed in the National Climate Agreement as a key concept to create the envisaged energy system and to achieve climate-neutrality by 2050 is energy sector integration. The European Commission defines energy sector integration as the linking of various energy carriers (e.g., electricity, heat, cold, gas, solid and liquid fuels) with each other and with the energy end-use sectors (e.g., households, buildings, transport, and industry) [28].

It can be observed that both the European Green Deal and the National Climate Agreement propose the strategy of energy system integration and energy sector integration as key strategies to achieve climate-neutrality by 2050. The main difference between the two integration strategies is the inclusion or exclusion of the sectors physical infrastructure and regulatory markets. This chapter elaborates on the energy sector integration concept. Current research, pilot projects, and modelling and simulation attempts on energy sector integration technologies are described in Section 2.1. In Section 2.2 decarbonisation methods applicable to the energy sectors of interest for this research are explored by discussing the characteristics of those energy sectors.

2.1. Literature on Energy Sector Integration

The European Energy System Integration Strategy provides an action plan to accelerate the energy transition. One of the pillars identified by the document as part of the action plan is accelerating the electrification of energy demand [27]. The process of decoupling electricity from the power sector for use across multiple sectors is commonly referred to as Power-to-X (P2X) [10]. This thesis will focus on the electrification of end-use sectors to achieve climate-neutrality. Therefore, solely the literature on the P2X concept as part of energy sector integration is explored in the first part of this section. An overview of the available modelling frameworks with emphasis on energy system integration and examples of research performed on P2X concepts with the prevalent frameworks is presented in the second part of this section.

2.1.1. Power-to-X

There is no general definition of the term P2X. In this research the interpretation of the International Renewable Energy Agency (IRENA) is adopted to describe the process. The IRENA defines P2X as the umbrella term of processes that convert the power generated from renewable sources to different types of energy carriers for use across multiple sectors, or reconvert back into power [10]. When referring to specific P2X processes, the X is replaced by the converted energy carrier or energy end-use sector. In a review paper of thirty-two Life Cycle Assessment (LCA) studies on P2X, the prevalent P2X processes are discussed and classified. The P2X processes are divided in five categories: (1) Power-to-Gas, (2) Power-to-Liquid, (3) Power-to-Transport, (4) Power-to-Heat, and (5) Power-to-Power. The first category is subdivided, based on the converted energy carrier, into: (1a) Power-to-Hydrogen, (1b) Power-to-Methane, and (1c) Power-to-Syngas [29].

The Power-to-Hydrogen ($P2H_2$) process utilises renewable electricity to produce hydrogen through water electrolysis. Alkaline, PEM, and SOEC electrolysers are the most-discussed hydrogen production technologies applied in current P2X projects [30]. The hydrogen production process is widely considered as a key element of P2X as hydrogen is often required for further manufacturing of the other energy carriers in P2X processes [29, 31]. The IRENA summarises the contribution of $P2H_2$ to the power sector transformation as fivefold: (1) reducing renewable energy curtailment, (2) providing long-term energy storage, (3) providing grid balancing services, (4) supporting sector coupling strategies by increasing the use of renewable power in other sectors, and (5) enabling distribution of renewable power across regions and globally [26]. Review papers on Power-to-Gas projects in Europe [30], Power-to-X demonstration projects in Europe [32], and Power-to-X demonstration projects worldwide [33] underpin the importance of hydrogen for P2X processes. Authors in [30] review 128 demonstration and system integration projects and conclude that the main application for current Power-to-Gas projects is the injection of hydrogen or methane into the natural gas grid for storing electricity from variable renewable energy sources. Authors in [32] review 220 projects and conclude that the main application for current Power-to-X projects is hydrogen production and processing into methane. Authors in [33] review 192 projects and conclude that the main application of P2X processes is the production of hydrogen for deployment in a large portfolio of applications. Most of the projects reviewed by authors in [33] focus on one of the following: (1) the injection of hydrogen or methane into the natural gas grid, (2) the use of hydrogen as a fuel for transport, (3) the manufacturing of liquid fuels and syngas from hydrogen, and (4) the power storage and balancing capacities of hydrogen. The remaining projects focus on the supply of heat from hydrogen-fired boilers and the manufacturing of chemicals from hydrogen. Based on the review papers it can be observed that hydrogen forms a vital component of P2X processes and most of the processes (Power-to-Gas, Power-to-Liquid, Power-to-Transport, and Power-to-Power) revolve around its availability.

Power-to-Heat (P2H) is excluded from the above mentioned review papers and is an exception to the other P2X processes as direct conversion of power to heat is possible without the need for hydrogen. The P2H concepts can produce low-temperature thermal energy for residential and industrial applications [29]. Two main mature and most-discussed technologies for power conversion into thermal energy are heat pumps and electric boilers [34, 35]. Especially the former technology can assist the transition to a decentralised energy system with a high share of renewable energy sources [29, 36]. The IRENA summarises the contribution of P2H to the power sector transformation as fivefold: (1) reducing renewable energy curtailment, (2) increasing flexibility through load shifting, (3) storing energy on large scales, (4) providing grid services via aggregators, and (5) increasing self-consumption from local renewable-based generation [37]. Large scale P2H demonstration projects are in the minority in literature. However, studies on the potential of P2H technologies at the national level have received increasing attention. The integration of the power and heating sector is often considered to be particularly promising due to the relatively low costs associated with heat storage and generation [35]. Studies at the national level on P2H potential have been performed for several countries and regions, some of them are Finland [38, 39], Germany [40], and Europe [41]. The first study on P2H potential reviews wind integration into the energy system of Finland with a high share of nuclear power. It concludes that, on the one hand, heat pumps offer the highest efficiency in balancing excess power from Variable Renewable Energy Sources (VRES). On the other hand, it concludes that P2H technologies offer a limited capability for absorbing excess power due to a mismatch in the higher electricity production and lower heat demand in the summer, and vice versa in the winter [38]. The second study at national level in Finland reviews pathways for massive penetration of VRES with intersectoral coupling through P2X technologies. The study concludes that the intersectoral coupling with P2X technologies in general, and P2H technologies in particular, is vital for a feasible Finnish energy system [39]. The study on the potential of P2H technologies in the district heating grid in Germany concludes that a huge potential can be developed in German district heating grids with a maximum P2H market share of around 60% of the maximum thermal load in 2030 [40]. The third study on the European heat roadmap proposes a heat strategy based on district (centralised) heating with a high penetration of large scale heat pumps and decentralised heating with a large penetration of individual heat pumps, and concludes that the proposed strategy can reduce the costs for heating and cooling applications by around 15% [41]. Based on the review papers it can be observed that P2H technologies form a vital component of the energy sector integration concept, due to their high balancing efficiency, large potential market share, and significant cost reduction.

2.1.2. Modelling and Simulation of Power-to-X

An overview of the literature on mathematical modelling and simulation of P2X systems is presented in a review paper by authors in [42]. They only consider P2X processes that require hydrogen for the manufacturing of other energy carriers (liquid fuels, gaseous fuels, and chemicals) and exclude the other P2X processes (Power-to-Hydrogen and Power-to-Heat). The included P2X systems are analysed based on thermodynamic, economic, and environmental considerations. The authors state that the common method applied for performing a thermodynamic analysis is a pinch analysis, with the objective of minimising energy consumption. The prevalent software is Aspen [43]. Some studies use OpenModelica [44] or a combination of Aspen and MATLAB [45]. The economic and environmental analyses do not require modelling or simulation software.

An overview of the literature on the modelling approaches of P2H systems is presented in a review paper by authors in [35]. Most of the literature reviewed are techno-economic models of the energy sector and evolved from models for electricity sector analysis into models for combined heat-and-electricity system analysis. The prevalent objective of the reviewed models is cost minimisation. The remaining objectives include scenario assessment, and (dispatch) simulation. Most of the models apply linear programming or mixed-integer linear programming to carry out the optimisation to achieve the objective. In the review paper an overlap can be observed of the base models used in several studies. Prominent examples are the BALMOREL, TIMES, and EnergyPLAN models. The BALMOREL model is a partial equilibrium model applicable for modelling and analysing the energy sector, with an emphasis on the electricity, and combined heat and power sectors in an international perspective. An example of a study based on the BALMOREL model is a study by authors in [46], where the model is used to determine the role of district heating in the future Danish energy system based on cost optimisation. The TIMES model is a model applicable for exploring future energy sector scenarios and optimises for a least-cost energy system based on a number of user constraints. An example of a study based on the TIMES model is a study by authors in [47], where the model is used to determine the effects of improved modelling of residential heat pumps on the future Danish energy system based on cost optimisation. The EnergyPLAN model is an energy system analysis tool applicable for simulating the operation of future sustainable energy solutions, with emphasis on energy systems with high shares of renewable energy sources [48]. An example of a study based on the EnergyPLAN model is a study by authors in [49], where the model is used to perform a scenario study on the European energy system to assess the impact on primary energy supply, the environment, and the economy.

The above mentioned BALMOREL model has emphasis on the integration of the electricity, and combined heat and power sectors. The above mentioned TIMES and EnergyPLAN models have emphasis on energy system integration in general. An other modelling framework with emphasis on energy system integration is Backbone. Backbone is an energy network optimisation tool applicable for studying the design and operation of energy systems, both from investment planning and scheduling perspectives [50]. An example of a study based on the Backbone model is a study by authors in [51], where the model is used to analyse the impact of Power-to-Gas on the cost and design of the future low-carbon urban energy system.

The above mentioned modelling frameworks are subsumed under the umbrella of energy systems models. Authors in [52] define energy system models as mathematical models that are developed for the efficient energy planning, forecasting, operation, and optimisation of all energy sources. The general use of energy systems models is described by authors in [52] to be twofold: models used in an exploratory manner for elucidating the effects of, e.g., economic development and variations in energy prices on world markets, and models used to simulate policy and technology decisions that may influence future energy demand and supply. The latter including energy efficiency policies, energy sector integration policies, emission trading policies, and renewable energy technologies. It can be observed that the research performed with the above mentioned modelling frameworks is similar to the proposed research in this thesis. However, one of the drawbacks shared by the above mentioned modelling frameworks is the absence of a detailed power system model applicable for performing an electricity grid impact analysis.

2.2. Power and Heating Sector Integration

Figure 2.1 shows the energy demand per heating and cooling application. It can be observed that over 95% of the energy demand is consumed by heating applications. As cooling applications cover a small portion of the demand, the effects of power and cooling sector integration are assumed negligible. Furthermore, it can be observed that space heating consumes around 50%, and process heating around 40% of the energy demand for heating and cooling applications. According to a study published by IEA, low-temperature heat demand constitute a great portion of the space heating, and around 30% of the process heating demand [53]. As P2H technologies are ideal for electrifying low-temperature heat demand, the need for P2H integration to decarbonise the heating sector is underpinned. The effective integration of the power and heating sector partially depends on the integration of the corresponding energy systems. The power system comprises the power sector and the infrastructure necessary for linking the energy carriers with the end-users. Similarly, the heating system comprises the heating sector and the required infrastructure. Both energy systems are explored in this section.

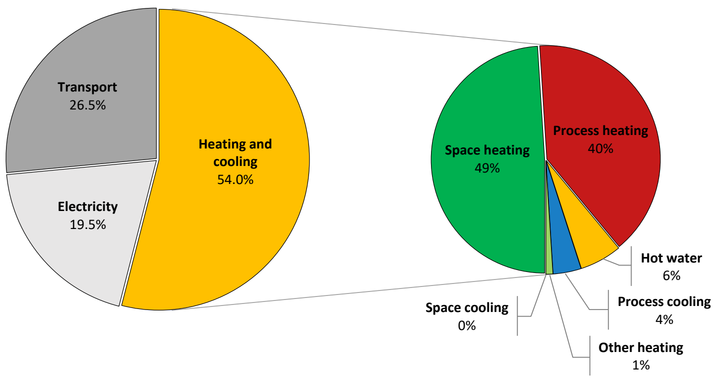

Figure 2.1: **Final energy consumption for heating and cooling applications in the Netherlands, divided by application type.**
On the left side the final energy consumption for the Netherlands is displayed and on the right side the final energy consumption for heating and cooling applications, divided by the application type. Consumption values obtained from EBN [54].

2.2.1. Power System

In an European Parliament briefing about the EU electricity market, the EU electricity system is described as a two-piece system. On the one hand, it consists of the physical infrastructure for electricity generation, transport and use, and on the other hand of an organised electricity market [12]. A schematic overview of the physical infrastructure can be seen in Figure 2.2. It comprises electricity generators, electricity transport systems, and electricity consumers. The transport systems are usually divided into systems for transmission of electricity at higher voltages over longer distances and systems for distribution of electricity at lower voltages over shorter distances to consumers. Also known as transmission and distribution systems, respectively. The electricity market consists of electricity suppliers, electricity consumers, Transmission System Operators (TSO), Distribution System Operators (DSO), and regulators [12]. The main responsibilities of the TSO and—to a lower extent—the DSO's are: ensuring overall system stability, ensuring security of electricity supply, and operating and maintaining the system assets. Furthermore, they are responsible for connecting new suppliers and consumers to the grid.

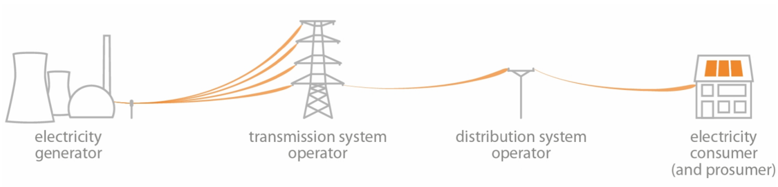

Figure 2.2: **Schematic overview of the electricity system** [12].

When electricity transmission and distribution systems were constructed, the prevalent concept of electricity grids was connecting large capacity centralised electricity generation plants to the high-voltage transmission grid and distributing the electricity to the consumers via the low-voltage distribution grid [13]. A schematic overview of such a centralised electricity grid is shown on the left side in Figure 2.3. Due to the increasing number of small-scale and local renewable electricity generation plants, the grid topology shifts to a combination of centralised and decentralised electricity generation plants. A schematic overview of such a system is shown on the right side in Figure 2.3. It can be observed that in a decentralised grid, electricity is fed into the distribution grid on all voltage levels.

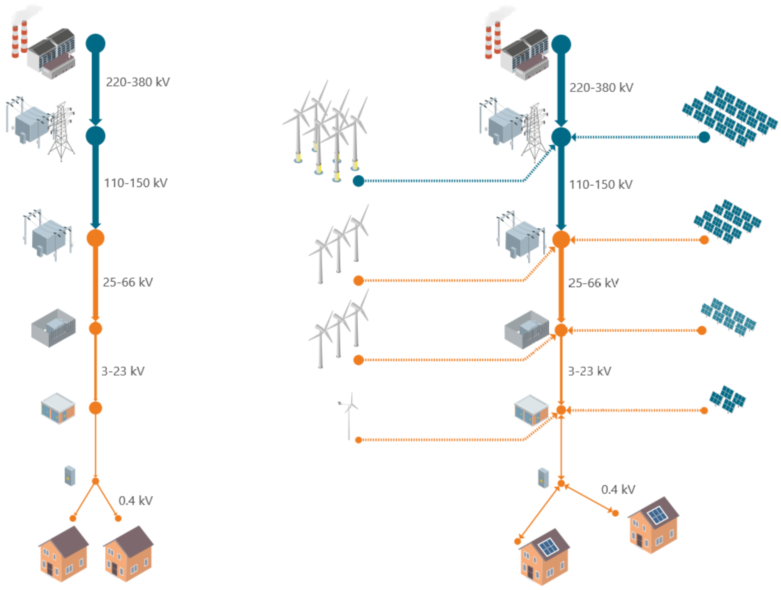

Figure 2.3: **Schematic overview of the electricity system with centralised and decentralised electricity generation** [13]. On the left side the centralised electricity generation topology can be seen and on the right side a combination of centralised and decentralised electricity generation. Dark blue lines are operated by the TSO and orange lines are operated by the DSO's.

2.2.2. Heating System

Like the power system, the heating system consists of a physical system with energy flows on the one hand and an economic system with money flows and regulating parties on the other hand. However, unlike the power system, the prevalent concept behind the heating system makes use of decentralised energy supply.

In the current power system most of the electricity is produced by converting other energy carriers into electricity at central locations and distributing the electricity to the consumers. The current heating system revolves around the idea of distributing other energy carriers to the consumers, who are responsible for producing their own heat. This approach utilises the distribution grids of other energy sectors to transport the energy carriers to the consumers. Another technology applied to a lesser extent in the heating system is district heating, where heat generated in centralised locations are distributed through an underground network of insulated pipes to consumers. The heat is often generated by cogeneration power plants, making use of the normally wasted heat produced when generating electricity. A schematic overview of such a heat network is shown in Figure 2.4.

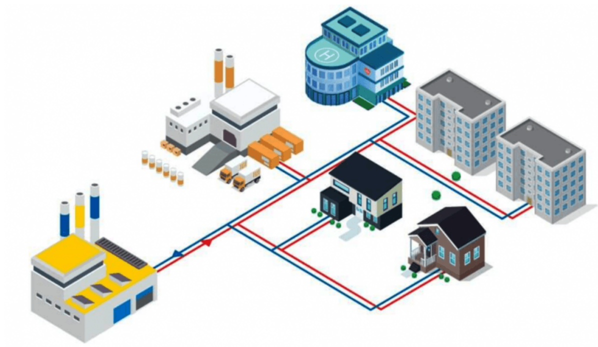

Figure 2.4: **Schematic overview of a district heating network** [14].
The red and blue lines represent heat supply pipes and cold return pipes. Households, buildings, and industry are connected to this network.

2.2.3. Energy Carriers

Naturally occurring energy carriers are referred to as primary energy carriers (e.g., crude oil, hard coal, and natural gas). The energy carriers that can be obtained from a transformation of the primary energy carriers are referred to as secondary energy carriers (e.g., petrol, electricity, and heat). The energy carriers used for electricity, and heating and cooling applications are shown in Table 2.1. It can be observed that more than three-quarters of the electricity consumption derives from fossil fuel based generation plants. Similarly, it can be observed that more than three-quarters of the energy consumption for heat and cold generation derives from fossil fuels. Furthermore, it can be observed that heating and cooling applications account for more than half of the final energy consumption in the Netherlands. Considering the objective of decarbonisation of the energy system, it is vital to invest in renewable alternatives for decarbonising these two sectors.

Renewable energies are defined as energy sources that are continually replenished by nature and derived directly from the sun, indirectly from the sun, or from other natural movements and mechanisms of the environment [55]. Examples of renewable energy sources are: solar thermal, solar PhotoVoltaic (PV), wind, hydro, geothermal, and tidal energy. Most of these sources are weather-dependent and follow seasonal patterns, leading to a variable and intermittent energy supply. The weather-dependent energy sources are also known as Variable Renewable Energy Sources (VRES). The renewable energy sources relevant to the power sector are solar PV, wind, hydro, and tidal energy. The renewable energy sources directly applicable to the heating sector are geothermal and solar thermal energy. The former collects thermal energy stored in the Earth's crust and the latter collects thermal energy from the sun. Electrification of heating applications can indirectly supply renewable energy to this sector. Electric boilers and heat pumps can be used for several end-use sectors where low-temperature heat is needed. Heat pumps can draw heat from the air, water, or ground by using electricity.

Table 2.1: **Final energy consumption for electricity, and heating and cooling applications in the Netherlands.**
The market share of the energy carriers present their contribution to the specific application. Consumption values obtained from [56].

Application	Energy carrier	Market share [%]	
Heating & Cooling		54.0%	
	Gas		62.0%
	Coal		6.0%
	Others (fossil)		17.0%
	Electricity		8.0%
	District heating		7.0%
Transport		26.5%	
Electricity		19.5%	
	Gas		51.0%
	Coal		26.5%
	Others (fossil)		9.9%
	Wind		9.2%
	Solar		3.3%
	Hydro		0.1%

3

Background on the Dutch Power System

In Section 2.2, a brief overview of the power system is given. The power system is described as a two-piece system, consisting of the physical infrastructure for electricity generation, transport and use, and an organised electricity market. This chapter will delve into the specifics of the Dutch power system by first exploring the physical infrastructure for electricity generation in Section 3.1. Section 3.2 examines the physical infrastructure for electricity transport and Section 3.3 describes the organised electricity market. The provided background on the infrastructure for electricity generation and transport, and the organised electricity market form the backbone of the power system modelling described in Chapter 4 and the scenario study presented in Chapter 5. The future plans for electricity generation, e.g., installed generator capacity and generator types, and the future plans for electricity transport are both discussed in Chapter 5.

3.1. Physical Infrastructure for Electricity Generation

The physical infrastructure of the Dutch power system comprises electricity generators, a transport system, and electricity consumers. The physical infrastructure currently in place in the Netherlands for electricity generation is explored by examining the electricity generator types, their characteristics, and connecting voltage levels.

3.1.1. Non-renewable generators

The topology of an electricity grid with centralised electricity generators, as shown on the left in Figure 2.3, is the prevalent topology for non-renewable generators, which account for around 75% of the electricity production in 2020 [57]. Three main characteristics of non-renewable generators are: (1) their size; usually large capacity power plants, (2) their location; usually centrally located, and (3) available on demand; allowing the generator to be used for balancing supply and demand. The large capacity per generator and the central location require a connection with the long-distance high-voltage transmission grid (220 kV and 380 kV lines).

The non-renewable generators can be divided by fuel type. In the Netherlands, the three common fuel types are natural gas, hard coal, and nuclear fuel [58]. The carbon dioxide emissions of the generators depend on multiple factors, among which, the fuel type and efficiency of the generators. The latter is mostly determined by the technology used for generating electricity from the energy carrier and the year of commissioning, as efficiency improvements are made over time. The non-renewable generators running on natural gas can be subdivided in Simple Cycle Gas Turbine (SCGT) generators, Combined Heat and Power (CHP) generators, and Combined Cycle Gas Turbine (CCGT)generators. The SCGT generators are the oldest operational type of gas generator in the Dutch power system. The generator operates in a simple Brayton cycle, displayed on the left side in Figure 3.1. The four stages of a simple Brayton cycle are described by authors in [59] as follows: (1-2) gas compression, (2-3) heat input, (3-4) gas expansion through a turbine, and (4-1) an open cycle heat rejection. Open cycle heat rejection consists of a continuous output of used heat and an input of new working fluid and fuel in the process. CCGT generators are based on the same theory, with the addition of a Rankine steam cycle between step 4 and 1. The Rankine steam cycle recovers the otherwise wasted heat through a heat exchanger and uses it for electricity production from the excess heat from the Brayton cycle. The four stages of a Rankine cycle are described by authors in [59] as follows: (6-7) liquid compression, (7-8) high-pressure liquid heated to dry saturated vapour, (8-9) vapour expansion through a steam turbine, (9-6) vapour condensed to liquid. The number correspond to the diagram on the right in Figure 3.1. The Brayton cycle in the combined cycle is slightly adjusted with the addition of an extra stage. Stage 4-5 in the Brayton cycle correspond to the heat exchange with the Rankine cycle in stage 7-8. Stage 5-1 in the Brayton cycle is the output of excess heat. The increase in waste heat recovery leads to a higher efficiency for the CCGT generators compared to the SCGT generators. The netto fuel efficiencies of gas generators are presented in a study published by ECN and are in the range of 45% - 59% for CCGT generators—lower to upper limit for oldest to newest CCGT generators—, and around 35% for SCGT generators [60].

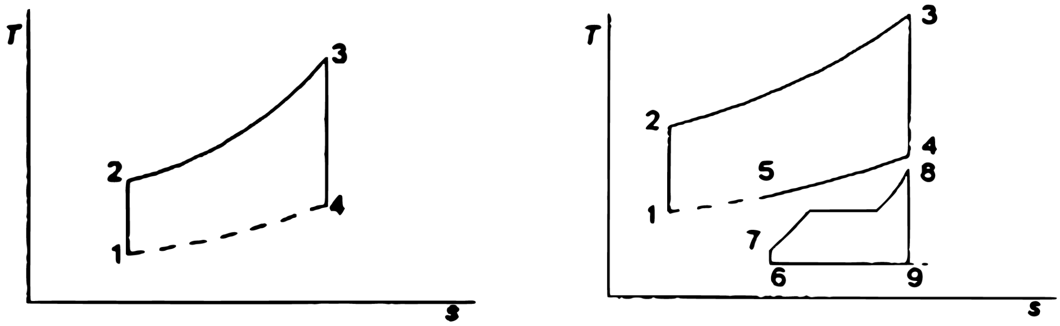

(a) Temperature-entropy diagram of simple Brayton cycle [59].

(b) Temperature-entropy diagram of combined simple Brayton cycle and Rankine cycle [59].

Figure 3.1: **Temperature-entropy diagrams of theoretical operating cycles of SCGT and CCGT generators.**

The third type of natural gas generator is the CHP generator. In the Netherlands this specific type of generator is mostly used in urban areas with connections to the thermal grids. Thereby, creating a core interdependency between the power and heating systems in the Netherlands. The CHP generator revolves around the cogeneration principle, with the purpose of recovering the waste heat from the process cycle and converting it to a heat source for district heating. The generators can be based on the steam turbine (Rankine) cycle, gas turbine (Brayton) cycle, or a combined cycle. Authors in [61] state the utilisation factor of CHP plants to be as high as 85% - 90%. With electrical efficiencies in the range of 30% - 40% and thermal efficiencies in the range of 50% - 60%.

Apart from natural gas generators, the Dutch power systems relies on hard coal generators for supplying electricity for the base load. The hard coal generators are based on the Rankine cycle, where high-pressure steam is generated by burning hard coal and used for generating electricity via a steam turbine. There are four hard coal power plants operational in the Netherlands as of 2021. However, the Dutch government ratified a treaty on the limited use of hard coal in power production, resulting in the closure of the plants in 2030. The plants may remain open if they are converted to biomass-based generators. The efficiency of the operational hard coal power plants in the Netherlands is in the range of 43% - 46% [60].

The final non-renewable generator type operational in the Dutch power system is the nuclear generator. The sole nuclear power plant is located in Borssele, Zeeland, with a net capacity of 485 MW and has been the subject of controversy since its commissioning. It is expected that the power plant remains operational up to 2034. With not a new nuclear power plant in the development pipeline before 2030, a dim future is foreseen for nuclear electricity generation in the Dutch power system.

Flexible and dispatchable generators are crucial for balancing the demand in a power system dominated by variable and intermittent energy sources. Non-renewable and several non-variable renewable generators are suited for balancing supply and demand, and supplying peak demand. The main limiting factors for these generators are their ramping rates and minimum up- and down-time. The former refers to the rate at which a generator is able to change its level of production, generally expressed in the percentage of their maximum capacity per minute [$\%P_{max}$/min]. The latter can reflect technical and cost-related constraints. Authors in [16] exemplify these constraints by suggesting a minimum down time is needed for the generator to be synchronised to the grid frequency as a technical constraint, and by imposing a minimum up time to reduce the cost of startup or shutdown as a cost-related constraint. The ramping limits and minimum up- and down-time for several generator types are presented by authors in [16] and can be seen in Table 3.1.

Table 3.1: **Overview of the technical cycling data of different generator types** [16].

	Ramping limits [%P_{max}/min]	Minimum up-time [h]	Minimum down-time [h]
Nuclear	0.25% – 5.0%	0.25 – 24	24
Hard coal	0.66% – 4.0%	0.25 – 10	3 – 10
Gas CCGT	0.83% – 10.0%	0.25 – 6	0.5 – 6
Gas SCGT	0.83% – 25.0%	0.25 – 1	0.25 – 1

3.1.2. Non-Variable Renewable Generators

Similar to the non-renewable generators, the topology of an electricity grid with centralised electricity generators is the prevalent topology for non-variable renewable generators, which account for around 7% of the electricity production in 2020 [57]. The renewable generators operational in the Dutch power system are based on biomass as input fuel, mostly comprising wood waste and manure.

Non-variable renewable generators are critical for providing the flexibility and dispatchability of generation capacity in the future power system and are expected to replace the non-renewable generators. Biomass is often referred to as a carbon-neutral fuel due to the circularity of carbon dioxide being absorbed during the products lifetime and emitted during combustion. However, processing and transporting the biomass induce extra harmful emissions that are not compensated for. Therefore, biomass is considered to be a transition fuel and must be replaced by other energy sources. One of the proposed energy sources is hydrogen, which can be produced by electrolysis. Electrolysis is a technique that uses electricity to drive a non-spontaneous chemical reaction in water, essentially splitting the water into hydrogen and oxygen. This process can function as a flexibility provider in a power system with high variable supply. The excess renewable electricity can be used to create hydrogen, which in turn can be stored for future use. The processes described for the non-renewable SCGT and CCGT generators can also accommodate hydrogen as primary fuel. The balancing capacities of non-variable renewable power plants and their size require a connection with the long-distance high-voltage transmission grid (220 kV and 380 kV lines).

3.1.3. Variable Renewable Generators

The topology of an electricity grid with decentralised electricity generators, as shown on the right in Figure 2.3, is the prevalent topology applied to variable renewable generators, which account for 19% of the electricity production in 2020 [57]. Solar and wind are the two primary energy sources for renewable electricity generators in the Dutch power system. Generators based on hydro and tidal energy are operational on a small scale, but are negligible in size and installed capacity compared to the renewable generators based on solar and wind energy. The main characteristics of these renewable generators are their weather-dependency and seasonal variation, leading to a variable, uncertain, and uncontrollable electricity supply.

The renewable generators that directly convert sunlight into electricity are known as solar Photovoltaic (PV) panels. Generally, a PV panel consists of 60 - 120 individual solar PV cells. The individual cells convert the sunlight to electricity by first absorbing the energy from the light in the cell, which causes electrons to break free from their bonds. The freed electrons flow through the cell material creating a direct current flow. The current flow is gathered by the conductors on the individual cells and merged per panel. A typical solar PV panel has a capacity of 0.15 - 0.2 kWp per square meter surface area. A division is often made in studies on the future power sector based on the total installed capacity per location. Solar PV systems smaller than 15 kWp are referred to as small scale systems and are usually installed on residential roofs. Systems with a capacity larger than 15 kWp are referred to as large scale systems and are usually located on roofs of non-residential buildings and in more rural areas on large fields. In the Netherlands an average of 1,000 full-load hours can be achieved with solar PV panels.

The renewable generators that convert wind into electricity are known as wind turbines. A wind turbine harvests the wind's kinetic energy by using blades that generate lift, which causes the blades to turn. An electric generator is connected to the blades via a drive shaft. The electric generator produces electricity in alternating current. The height of the turbine and the diameter of the blades strongly influence the capacity of a wind turbine. According to a study published by Wind Europe [62], the average capacity of onshore turbines installed in 2019 was 3.1 MW and the average installed capacity of offshore turbines was 7.2 MW. The study presents an European average of 2,100 full-load hours and 3,300 full-load hours for onshore and offshore wind turbines, respectively. According to a study published by IEA [63], the full-load hours for onshore and offshore wind turbines in the Netherlands are expected to increase to 2,860 full-loads hours and 3,960 full-load hours, respectively.

In Figure 3.2 a similar schematic diagram can be seen as shown in Figure 2.3, with the addition of installed capacity and their connecting voltage levels. It can be observed that the solar PV systems and the onshore and offshore wind turbines are connected at all possible voltage levels depending in the system capacity.

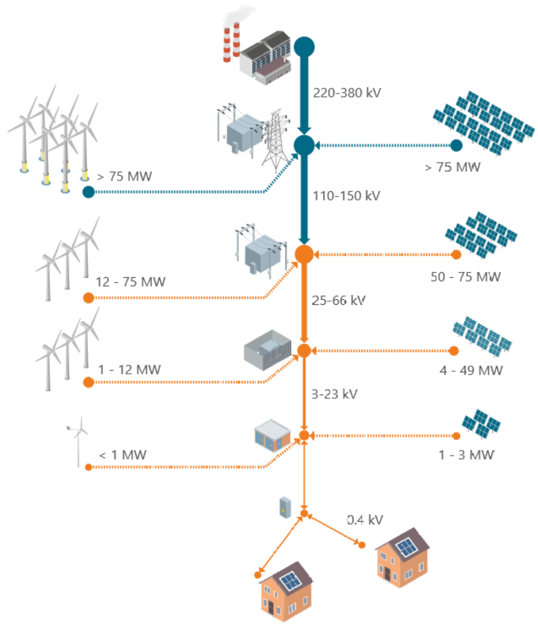

Figure 3.2: **Schematic overview of the electricity system with decentralised electricity generation** [13].

3.2. Physical Infrastructure for Electricity Transport

The Dutch electricity transport system is divided in an electricity transmission system and an electricity distribution system. All high-voltage assets of 110 kV and up are considered to be part of the transmission system and are maintained and operated by TenneT TSO B.V.. All electricity transmission assets operating at lower voltages are part of the distribution system. The Dutch high-voltage grid consists of around 340 high-voltage stations, around 10,000 kilometres of high-voltage lines, around 25 transformers, and generators and loads. The high-voltage grid operates at a frequency of 50 Hz alternating current, in line with the European standards.

3.2.1. High-Voltage Stations

Authors in [8] simplify the power system as a collection of nodes, representing the high-voltage stations, that are connected by power carriers (e.g., overhead and underground lines). Generators can be connected to an individual node, that subsequently divides the power over the connected lines and distributes it to the consumers. Transformers can be installed at the nodes to interconnect different voltage levels in the system. Protection, control and data acquisition equipment is installed at these stations as well.

3.2.2. Transformers

Transformers are located at high-voltage stations and are crucial for the efficient and reliable operation of the transmission and distribution grids. Transformers are components in the AC power system that enable power generation at relatively low-voltage levels (10 - 25 kV, limited by the insulation of the generator), transportation at high-voltage levels (110 - 380 kV, reducing transportation losses), and consumption at a safe low voltage level of around 0.4 kV [8]. Schavemaker and Van der Sluis state that three high-voltage stations transform 380 kV to 220 kV and around 20 high-voltage station transform 380 kV or 220 kV to 150 kV or 110 kV [8]. The capacity of the installed transformers at these high-voltage stations range between 200 MVA - 750 MVA and the number of transformers per location range between 1 - 4. Figure 3.3 shows a schematic overview of the voltage levels and transformation steps in the Dutch power system.

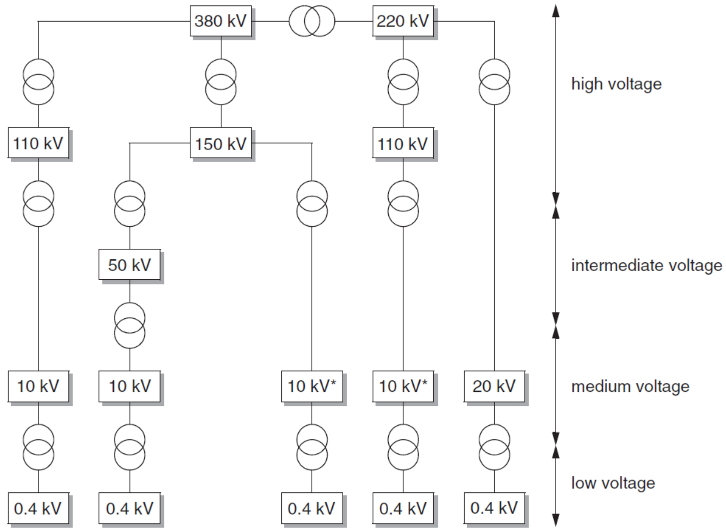

Figure 3.3: **Voltage levels and transformation steps in the Dutch power system** [8].
*this voltage level can be 20 kV.

3.2.3. High-Voltage Lines

There are two main types of high-voltage lines: (1) overhead transmission lines and (2) underground cables. Authors in [8] describe the advantages of the former as natural cooling and insulation provided by the surrounding air, as well as the lower investment costs. The authors describe the advantages of the latter as more reliable due to less exposure to wind and lightning, and a lower need for preventive maintenance. Most of the high-voltage lines in the Dutch power system transport electricity in three-phase AC. The exceptions are European interconnection lines and lines connecting wind parks located far offshore, they transport electricity in DC. The transmission and distribution of DC electricity requires a conversion step to AC performed by converter stations.

3.2.4. Converter Stations

A special type of high-voltage stations are the converter stations, where direct current is converted to alternating current and vice versa. Electricity transport over longer distances and at higher voltages often uses DC, resulting in lower power losses. These stations must be located on both ends of a High-Voltage Direct Current (HVDC) transmission line. The use of HVDC transmission lines and converter stations are considered key for landing large offshore wind farms. As it is expected that the future large offshore wind farms in the Netherlands will be located further offshore, an offshore converter station will collect and convert the power produced by the offshore wind farms (AC to DC conversion) and transport it to land via HVDC transmission lines. At the grid landing locations, the HVDC transmission line will be connected to a high-voltage station converting the power to AC before feeding it in to the electricity grid.

3.2.5. European Interconnection

Authors in [8] the main advantages of interconnected power systems as the following: (1) improved system reliability, (2) better overall system efficiency, and (3) bigger geographical area covered. The geographical coverage leads to a spread in peak load due to a span over multiple time zones, and a reduced variability of renewable generators due to the large geographical spread (e.g., clouds in the Netherlands can be compensated by blue skies in Germany). The improved system reliability and efficiency are mainly the result of the increase in the generation pool size.

The European TSO's are working together on maintaining and expanding interconnection lines within the European Union. TenneT's objective for 2025 is to have an operational interconnection capacity of 10.8 GW with five different countries. The capacity of the DC interconnection line with Britain—referred to as the BritNed cable—is 1 GW. The DC interconnection lines with Norway and Denmark—NorNed and COBRA cables—both have a capacity of 0.7 GW. The capacity of interconnection with Germany is 5 GW and the interconnection capacity with Belgium is 3.4 GW [64, 65].

3.3. Organised Electricity Market

The electricity market can be compared to any other economic market where buyers and sellers must agree on a price. One big difference is the inability of storing electricity in large quantities. This leads to the constantly varying cost conditions of electricity supply influenced by the continuously changing electricity demand and intermittent availability of generation capacity [8]. The electricity market consists of electricity suppliers, electricity consumers, Transmission System Operators (TSO), Distribution System Operators (DSO), and regulators [12]. The main responsibilities of the TSO and—to a lower extent—the DSO's are: ensuring overall system stability, ensuring security of electricity supply, and operating and maintaining the system assets. Furthermore, they are responsible for connecting new suppliers and consumers to the grid. In the case of the Netherlands, the responsible parties are: the TSO TenneT, and the DSO's Rendo, Coteq, Liander, Enexis, Stedin, Westland Infra, and Enduris. As the electricity market comprises all market aspects from production and import to consumption and export of electricity, only the aspects of interest for this research are further explored. The main area of interest is the electricity market clearing: the two-sided auction model where both supply and demand bids are made. The point where the aggregated supply and aggregated demand meet is referred to as market clearing. The intersection represent the Market Clearing Price (MCP) and the Market Clearing Volume (MCV). The electricity supply bid is based on the merit order and ranks the available electricity generation sources based on the ascending order of marginal costs of electricity production. The marginal cost of a generator is often based on the costs associated to the production of one extra unit of electricity. This entails the fuel costs and CO_2 emissions costs of the individual generator. An example of market clearing can be seen in Figure 3.4.

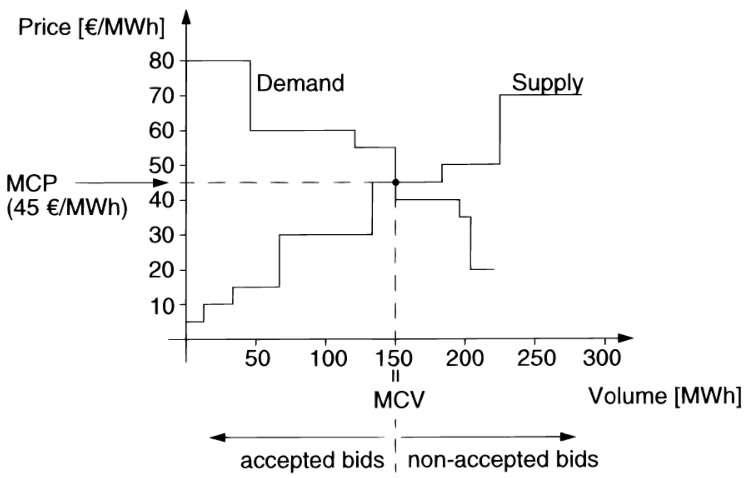

Figure 3.4: **Market clearing example** [8].

In the Netherlands, the electricity is mainly bought or sold by traders via one of two ways: (1) directly from producers or energy suppliers, or (2) on the Amsterdam Power Exchange (APX). An example of the former is a data centre buying all electricity produced by an offshore wind farm directly from the wind farm operator. For this thesis, the latter is of importance as it is assumed that all electricity is traded and cleared via the above described market clearing model. The APX is part of the EPEX SPOT market, a pan-European electricity market. The exchanges are online trading platforms for electricity, where electricity supply and demand are brought together. In the case of the Netherlands, the electricity traders on the exchanges mostly comprise energy companies, e.g. Eneco, Vandebron, Vattefall, and Essent. In turn, the electricity consumers buy their electricity from the energy companies.

4 Modelling and Validation

The research objective for this thesis is twofold, as stated in Section 1.3. The first objective is to develop a representative model of the Dutch high-voltage electricity grid, and the second objective is to analyse the effects of heating sector electrification scenarios on the electricity grid. This chapter will present the methodological approach in fulfilling the first objective. In Section 4.1, the modelling approach for the current electricity grid is presented. Section 4.2 discusses the validation of the created power system model.

4.1. Modelling

For creating a representative model of the Dutch high-voltage electricity grid, the pandapower package [66] for Python [67] is used. This package is applicable to several use cases, one of them is running an optimal power flow for electricity grids. This section explores the available literature on power system modelling and classifies the desired power system model for this research. Then, the available open data and modelling approach are presented, followed by establishing the limitations of the available open data. The steps taken for model aggregation are stated and finally, the load and generation mapping is discussed.

4.1.1. Scope of the Desired Power System Model

The general definition of the umbrella term of energy system models is presented in Section 2.1. The prevalent usage and categorisation of energy system models in the UK is presented by authors in [68]. The authors propose a classification schema based on review papers on energy system models [69], utilised computer tools for energy system modelling [70], and classification methodology for energy system models [71]. The aim of the classification schema proposed by authors in [68] is to make the future literature on energy system modelling more transparent. The need for classification of energy system models is described by author in [71] as they can provide insights in similarities between existing energy models and can facilitate the selection of a suitable energy model. This section classifies the desired power system model for this research and explores the common types of power system models and modelling frameworks.

Classification of the Desired Power System Model

The model classification is important for this thesis, because its defines the scope of the desired power system model and contributes to transparency in literature on energy system modelling. The desired power system model for this thesis is classified based on the classification schema proposed by authors in [68] and classification methodology presented by author in [71]. The authors divide the classification schema in three main parts: (1) the model purpose and structure, (2) the technological detail, and (3) the mathematical description.

The second research objective described in Section 1.3 is to analyse the impact of heat electrification scenarios in 2050 on the Dutch high-voltage electricity grid by identifying the bottlenecks and evaluating grid investment decisions. The purpose of the model is to balance power demand and supply on an hourly basis throughout the entire year, in order to identify the bottlenecks. The purpose can be decomposed to define a general purpose of the model. In general, the model must be able to explore the future by performing scenario analysis. More specifically, the model must focus on balancing power demand and supply, and assessing the impact of policy and technology decisions. The characterisations are ranked in the range 'more' or 'less'. The characterisations are (1) the degree of endogenisation—ratio between endogenous and exogenous model parameters—, (2) the extent of description of non-energy sector components, (3) the extent of description of energy end-users, and (4) the extent of description of energy supply technologies. The description of energy end-users and energy supply technologies are imperative to the model objective. The endogenisation of model parameters and description of non-energy sector components are of less importance for analysing energy sector integration and thus for the desired model. The desired model has national geographical coverage and can be applied to a specific energy sector. The scenario analysis will be performed for the year 2050, setting the time horizon to long term analysis. The preferred time step for the desired model is one hour, based on data availability and simulation simplicity. An overview of the purpose and structure of the desired power system model is given in Table 4.1.

Table 4.1: **Classification of the desired power system model - purpose and structure.**
Based on the classification schema proposed by authors in [68] and classification methodology proposed by author in [71].

1. Purpose of the model	**In general**	Exploring future scenarios
	More specific	Energy demand–supply analysis
		Impact analysis
2. Structure of the model	Less degree of endogenisation	
	Less detailed description of non-energy sectors	
	More detailed description of end-users	
	More detailed description of supply technologies	
3. Geographical coverage	National	
4. Sectoral coverage	Power sector	
5. Time horizon	Long term	
6. Time step	Hourly	

The second part of the schema concerns the technological detail of the model. It is split in four sections: renewable technologies inclusion, storage technologies inclusion, demand characteristics inclusion, and costs inclusion. The desired model must perform a scenario analysis based on the energy sector outlook presented in Chapter 5. The scenarios involve electrification of different energy end-use sectors and an increasing penetration of variable renewable technologies. All renewable technologies discussed in Chapter 5 and all electricity demand sectors must be included in the model. The possibility of modelling non-renewable power plants in the model is desired, therefore the model must allow for modelling of fuel prices and CO_2 costs. In Table 4.2 an overview of the technological detail of the desired power system model is presented.

Table 4.2: **Classification of the desired power system model - technological detail.**
Based on the classification schema proposed by authors in [68] and classification methodology proposed by author in [71].

7. Renewable technology inclusion	Solar PV
	Wind
8. Storage technology inclusion	-
9. Demand characteristics inclusion	Households demand
	Buildings demand
	Transport demand
	Agriculture demand
	Industry demand
10. Cost inclusion	Fuel prices
	CO_2 costs

A distinction is made in the analytical approach of models between top-down, bottom-up, or hybrid energy models. In general, top-down energy models are used by economists to assess financial effects of, e.g., energy policies. The bottom-up models are often used by scientist to assess system effects of, e.g., technical opportunities. Hybrid models are a combination of existing top-down and bottom-up models. The analytical approach applicable to the objective for this thesis is a bottom-up approach. The underlying methodology applicable to balancing supply and demand in an energy system, given certain system constraints, is an optimisation model. The input of an optimisation model is an objective function to be minimised. The function depends on the desired output of the model. In the case of power system modelling, fuel cost minimisation and least line resistance are most likely used as objectives. The programming approach preferably taken by the desired model is defined by the mathematical approach stated in Table 4.3. It depends on the software used for creating the model and can be a combination of the stated approaches. The data requirement for the model is quantitative and aggregated based on the available data and its spatial resolution. An overview of the mathematical description of the desired power system model is given in Table 4.3.

Table 4.3: **Classification of the desired power system model - mathematical description.**
Based on the classification schema proposed by authors in [68] and classification methodology proposed by author in [71].

11. Analytical approach	Bottom-up
12. Underlying methodology	Operation optimisation
	Cost optimisation
13. Mathematical approach	Linear programming
	Mixed-integer programming
	Dynamic programming
14. Data requirements	Quantitative
	Aggregated

The characteristics of the desired power system model are described in Tables 4.1, 4.2, and 4.3. The energy sectors that are covered by the scenario study are the power and heating sector. The former is the sole sector of interest for the desired power system model as the objective is to analyse the effects on the electricity grid. Therefore, a power system model with the above mentioned characteristics is desired.

Power System Modelling

Power system modelling can be distinguished from energy system modelling by its clear focus on electricity and the utilisation of a more detailed power grid. The modelling of the technical and physical behaviour of the underlying power grid is often combined with modelling of the electricity market mechanisms.

Authors in [72] classify the technical and physical behaviour of a power grid in four different types of grid models, ranging from an unconstrained electrical grid to a fully constrained AC electrical grid. The different types of grid models described by the authors in [72] are used in this thesis to define the type of grid model and corresponding level of detail of the desired power system model. The authors in [72] describe the simplest model as the single-node model, representing an unconstrained electrical grid with all power system components aggregated into one virtual point, or node. The second type described by the authors is the transshipment model consisting of multiple nodes that are able to mutually exchange power, solely constrained by net transfer capacity. The authors in [72] describe the third type of grid model as the DC model, comprising several nodes and power lines, which are constrained by the resistance and maximal capacity of the power lines. The DC model allows for active power flows to be determined. The fourth type of grid model described by the authors in [72] is an AC power flow model, essentially consisting of the DC model with added constraints, e.g., reactance, capacitance and inductance. This allows for active and reactive power flow calculations. It can be observed from the research by authors in [72] that an increase of detail in the grid model is accompanied with extra input data requirements. For the AC power flow model reactive power and voltage must be defined for each node, and reactance, capacitance and inductance must be defined for all power lines. Data unavailability led to the decision of utilising the DC power flow grid model type as basis.

Generally, the electricity market models are categorised in Unit Commitment Models (UCM) and Generation Expansion Planning (GEP) models. UCM are based on an optimisation problem used to determine the optimal operation schedule of generating units at every time step to balance the varying power demand. Operational power plant capacity, grid data, and fuel cost are used to determine the dispatch order of the power plants. GEP models are used to determine capacity expansion needs for several components of a power system, such as power plants and power lines. Apart from their general purpose, authors in [73] differentiate UCM and GEP models based on the number of time steps used for analysis. Namely, an UCM often simulates each hour of the year, and a GEP model each day or week of the year. The electricity market model of interest for the research objective in this thesis is the UCM.

The desired power system model or modelling frameworks must be capable of creating a grid model based on the DC power flow type and representing the electricity market based on the UCM type. Another criteria for the desired power system model is for it to be based on open data and software. The importance of open data and software for this thesis is underpinned by the aim that researchers across universities in the Netherlands will use this open source representative model of the Dutch high voltage electricity grid for various applications, such as scenario analysis on electrification and decarbonisation of end-use sectors. The representative model will enable interdisciplinary research on policy making and investment decisions specific to the Netherlands. Open-source models and frameworks applicable to energy system modelling and, more specifically, to power system modelling are listed by authors in [74]. The listed open-source power system frameworks based on the Python programming language are GridCal, pandapower, PyPSA, and PYPOWER. In contrast to other open-source power system frameworks (e.g., GridCal, PyPSA, PYPOWER), pandapower claims that all pandapower element behaviour is tested against commercial tools, such as DIgSILENT PowerFactory or PSS Sincal. Therefore, the pandapower package for Python is used for creating the desired power system model.

4.1.2. Available Open Data and Modelling Approach

ArcGIS was an important source for obtaining open data on assets in the Dutch high-voltage electricity grid as TenneT TSO B.V. maintains a map comprising all high-voltage assets [75]. The ArcGIS map includes data on all high-voltage stations, transformers, and lines. The data of significance for modelling for this thesis are: geodata, voltage level, object ID, connection ID's, and shape length. Geodata is used for visualising the grid assets and results. The voltage level is used to group all assets and for load and generation mapping. The object ID and connection ID's are used for defining the name of each bus and subsequently defining the connection points of all lines to the correct buses. The shape length is used to define the line length in the pandapower model. The Dutch high-voltage electricity grid obtained from the ArcGIS data is shown in Figure 4.1.

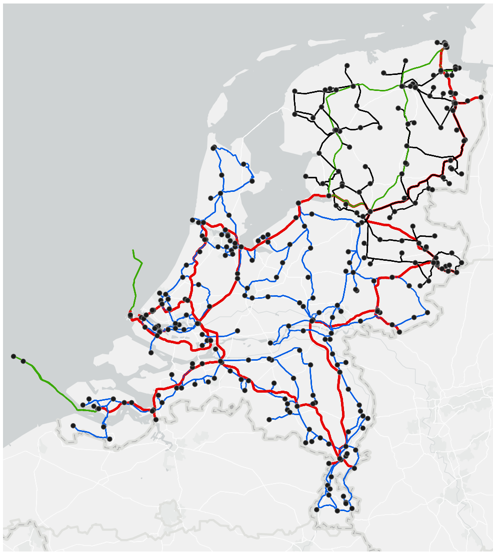

Figure 4.1: **Dutch high-voltage grid in 2021.**
Black dots represent high-voltage stations. Black, blue, green, and red lines represent 110 kV, 150 kV, 220 kV, and 380 kV lines, respectively. Map data obtained from TenneT's ArcGIS map [75]. Basemap obtained from Esri [76]

High-Voltage Stations

High-voltage stations are modelled as buses in the pandapower package. The buses are the nodes of the model that all other elements can connect to. Each bus is given a name, voltage level, and geodata corresponding to the asset data obtained from TenneT's ArcGIS map [75]. Any missing geodata is manually added to the buses from Google Maps. The name, voltage level, and total number of high-voltage stations are verified with a grid diagram published by TenneT TSO B.V. [77], and a grid diagram and interactive map published by HoogspanningsNet [78, 79]. For modelling a bus in pandapower, the maximum and minimum bus voltages in p.u. are required. The bus voltages are set to 1.05 and 0.95, respectively.

External Grids

All European interconnection lines are modelled as high-voltage lines originating from one of the buses near the Dutch border and ending at one of the external grid nodes. The external grid nodes are modelled as buses on the location where the interconnection lines cross the border. To each external grid node a generator is mapped. The generator can act as a source or sink of electricity. The limits of each generator are set to the maximum transport capacity of the corresponding interconnection line.

The external grid connections are obtained from the ArcGIS data [75]. The name and location of the bus connecting the external grid to the Dutch grid is verified with the grid diagram published by TenneT TSO B.V. and HoogspanningsNet [75, 78]. A document published by TenneT TSO B.V. provides specifications of the 220 and 380 kV grid. The technical data in that document is used for this thesis to obtain the capacity of the interconnection lines with the external grids in Germany and Belgium [80]. The capacity of interconnection lines to other countries was acquired from the information page on the TenneT TSO B.V. website [81].

Transformers

Transformer stations create a connection between two different voltage levels. The location of the transformers and the connecting high- and low-voltage buses are obtained from the ArcGIS map and are verified with the topology of the Dutch grid [75, 77]. The capacity and other parameters of each transformer are obtained from the quality and capacity plans published by TenneT TSO B.V. [82, 83]. For modelling a transformer in pandapower, the short circuit voltages and losses in the transformer need to be defined. For these parameters, the standard transformer type values are used.

High-Voltage Lines

High-voltage lines create a connection between two high-voltage stations at the same voltage level. The connecting buses, voltage levels and length of these lines are obtained from the ArcGIS map [75]. For the 220 and 380 kV lines, the length can be verified with the technical document used for finding the capacity of the interconnection lines [80]. The parameters of the lines (e.g., resistance, reactance, and maximum current) are obtained from the same technical document. For the 110 and 150 kV lines, no specifications were found on length or other parameters. As the ArcGIS data for the length of the 220 and 380 kV lines matched the length specified in the specifications document published by TenneT TSO B.V., it is assumed that the length for the 110 and 150 kV lines is reasonably accurate. For the other parameters of the 110 and 150 kV lines, standard line types provided by the pandapower package are used. A summary of the pandapower network comprising the stations, external grids, transformers, and lines is given in Table 4.4 and is visualised in Figure 4.2.

Table 4.4: **Overview of pandapower network.**

Buses	
Number of 110 kV buses	106
Number of 150 kV buses	194
Number of 220 kV buses	17
Number of 380 kV buses (excluding external grid buses)	37
External grid buses	10
Lines	
Number of lines	724
Length of lines [km]	10,365
Transformers	
Number of transformers	33

Generators

Generators can be modelled based on two principles, the first type of generator is a voltage controlled generator and requires active power and a voltage set point as input parameters. The second type of generator represents a generator with constant generation without voltage control, referred to as a static generator. The difference mainly depends on the generation type of the generator. Renewable energy sources, such as wind and solar systems, will be modelled as static generators. Fossil power plants are able to be voltage controlled to reactive power capabilities and are modelled as the first type of generator. All generators are modelled as flexible generation plants. The nominal power of the non-renewable plants limits the generation capacity of those plants. The maximum generation capacity per time step obtained from the capacity factor profiles for renewable plants limits their generation capacity.

The non-renewable generation capacity is divided by fuel type (e.g., hard coal, natural gas, nuclear, and waste) and plant technology (e.g. natural gas can be used in CCGT and combi power plants). The total non-renewable capacity in the Netherlands is determined by comparing the open data obtained from the transparency platform of ENTSO-E [84], the system and transmission data platform of TenneT TSO B.V. [85] and a report published by ECN about the fuel mix in the electricity sector in 2020 [60]. The operational status of

Figure 4.2: **Dutch high-voltage grid in 2021 as modelled in pandapower.**
Black, blue, green, and red dots and lines represent the 110 kV, 150 kV, 220 kV, and 380 kV level, respectively. Prints use map data from Mapbox and OpenStreetMap and their data sources.

the large power plants is verified with information obtained from web pages of the power plant owners and operators. Mothballed power plants are modelled in the pandapower network, but are out-of-service.

Renewable generation capacity is determined based on statistics published by CBS on installed wind and solar power in the Netherlands [86, 87]. As renewable energy sources are weather-dependent and can not operate at full capacity throughout the year, hourly capacity factor profiles for solar and wind power are used to determine the maximum generation capacity per time step. The capacity factor is a measure of how often an electricity generator runs for a specific period of time. The capacity factor is expressed as a percentage and calculated by dividing the actual electricity output by the maximum possible output. Hourly capacity factors for solar and wind power are obtained from Renewables.ninja [88, 89]. To give an idea of the general trend throughout the year, the capacity factors are averaged per day and are shown in Figures 4.3 and 4.4.

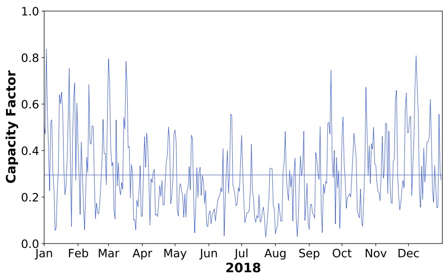

(a) Onshore wind.

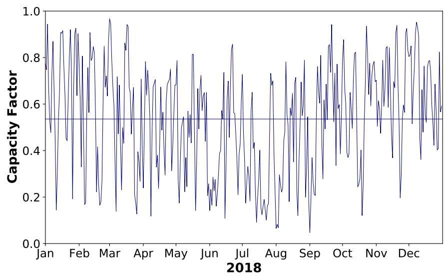

(b) Offshore wind.

Figure 4.3: **Averaged daily capacity factor profile for wind in 2018.**

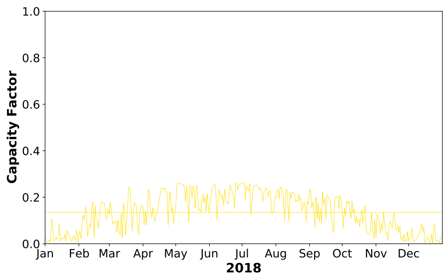

Figure 4.4: **Averaged daily capacity factor profile for solar in 2018.**

Loads

In pandapower, the loads can be modelled as either controllable/curtailable loads or uncontrollable loads. The former requires the active and reactive power of the load to be defined for each load. The latter requires solely the active power of the load to be defined. In the power system model developed in this research, all loads are modelled as uncontrollable loads. The total load can be divided by load per energy end-use sectors. Seven energy end-use sectors are defined in this research and are segregated based on characteristics and load profiles. The different energy end-use sectors as specified by the Energy Transition Model will be used, with an additional subdivision in the industry sector. This sector will be subdivided in:

- **ICT** - flat load profile. Expected to grow enormously in the future and may be interesting for load mapping in future scenarios.
- **Paper, Food, and Other (PFO)** - same load profile as the ICT sector, different from the rest of the industrial load. The 'Other' in PFO refers to all uncategorised residual insdustrial load.
- **All Other** - flat load profile. Consists of all industrial sectors apart from the four mentioned above.

The load profiles for end-use sectors are defined by the documentation of the Energy Transition Model [90] in terms of electricity demand profiles defined by NEDU [91]. The profiles per end-use sector are shown in Figure 4.5. The total load in a year for each end-use sector is obtained from the Klimaatmonitor database [92].

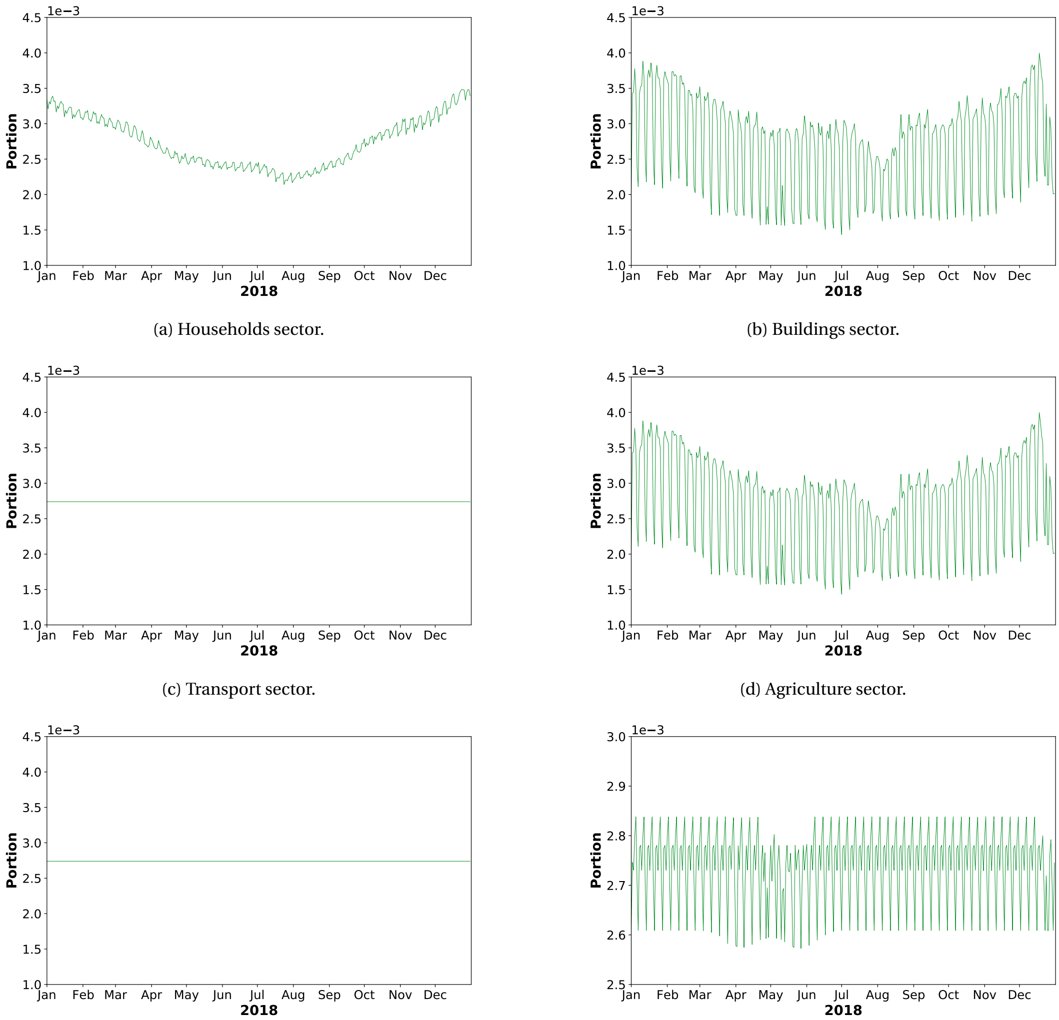

(a) Households sector.

(b) Buildings sector.

(c) Transport sector.

(d) Agriculture sector.

(e) Industry - Other sector.

(f) Industry - PFO sector.

Figure 4.5: **Load profiles for all end-use sectors in 2018.**

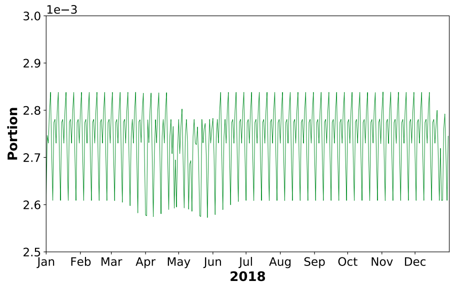

(g) Industry - ICT sector.

Figure 4.5: **Load profiles for all end-use sectors in 2018.**

Marginal costs

For running an optimal power flow, the merit order of the generation capacity needs to be determined. The merit order is based on the marginal cost (e.g., fuel cost and CO_2 emission cost) for running the power plant. The fuel cost per plant type is determined by a combination of the fuel efficiency of the generator, the CO_2 Emission Factor (EF) of that specific fuel type, the CO_2 Emmissions Trading System (ETS) price, and the fuel price. The fuel efficiencies of most of the plant types are obtained from a study published by ECN on the electricity fuel mix [60]. The fuel efficiency for waste plants is based on data presented by AEB—a waste management company in Amsterdam [93]. The CO_2 EF per fuel type are obtained from a report of the Netherlands Enterprise Agency [94]. The CO_2 ETS, natural gas, and coal prices can be found on financial data platforms, such as Market Insider and Yahoo! Finance [95–97]. The fuel cost for biomass, waste, and blast furnace gasses are assumed zero. Biomass and waste due to the fuel subsidies and blast furnace gasses due to it being a waste product. The marginal cost for these fuel types is based solely on their CO_2 emissions. The marginal cost for a nuclear power plant is based on values given in the Energy Transition Model [90]. The marginal costs for the renewable power plants are equal to zero, as they do not emit CO_2 and rely on natural resources.

4.1.3. Model Aggregation

The focus lies on creating a model of the Dutch high-voltage electricity grid and analysing effects of nationwide energy demand transformation. The main component of the electricity grid responsible for nationwide security of supply is the transmission grid. In the Netherlands, the transmission grid consists of the high-voltage buses and lines of 220 kV and up. The high-voltage buses and lines of 150 kV and down are mostly used for distributing the electricity to and within cities, municipalities, and rural areas. Therefore, the network model is restricted to 220 kV and 380 kV buses, lines and transformers.

The number of buses, lines, transformers, loads and generators highly influence the model simulation times. Thus, the number of buses and lines is further reduced based on their location and the number of connected consumers. The 220 kV network is mainly located in Friesland, Groningen, Drenthe, and Overijssel, where the loads are lower than in the Randstad area. The decision is made to aggregate the loads and nodes per province, thereby reducing the number of 220 kV buses from 16 to 10. The number of 380 kV buses is reduced from 35 to 25 by looking at the location of each bus and the number of connected producers and consumers. Buses that are located close to each other are aggregated. Buses with few external connections are removed and loads are moved to the closest remaining bus. A summary of the aggregated pandapower network is given in Table 4.5 and is visualised in Figure 4.6.

Table 4.5: **Overview of aggregated pandapower network.**

Buses	
Number of 220 kV buses	10
Number of 380 kV buses (excluding external grid buses)	25
External grid buses	10
Lines	
Number of lines	92
Length of lines [km]	3,039
Transformers	
Number of transformers	3

(a) Aggregated Dutch high-voltage grid in 2021. Black dots represent high-voltage stations. Green and red lines represent 220 kV and 380 kV lines, respectively. Map data obtained from TenneT's ArcGIS assets [75]. Basemap obtained from Esri [76]

(b) Aggregated Dutch high-voltage grid in 2021 as modelled in pandapower. Black dots represent high-voltage stations. Green and red lines represent 220 kV and 380 kV lines, respectively. Prints use map data from Mapbox and OpenStreetMap and their data sources.

Figure 4.6: **Aggregated Dutch high-voltage grid in 2021.**

4.1.4. Generation and Load Mapping

One of the major limitations of the available open data evolves around load and generation mapping. Apart from the locations of large non-renewable power plants and large offshore and onshore wind farms, the spatial electricity generation throughout the rest of the Netherlands is hard to find. Additionally, the bus connecting the power plants to the high-voltage electricity grid is often not explicitly mentioned. Therefore, assumptions must be made for the mapping of generators to the network model. The same holds true for load mapping. Even though the spatial electricity demand is better established on pages like the Klimaatmonitor from Rijkswaterstaat or StatLine from CBS, assumptions must be made for mapping the municipal demand to the buses of the network model.

For modelling simplicity only non-renewable power plants with a generation capacity of more than 25 MW and renewable power plants with a generation capacity of more than 50 MW are mapped onto separate nodes. The locations for mapping the power plants are determined by checking the closest connecting node to the high-voltage grid. In the installed capacity document published by TenneT TSO B.V. [85], most of the locations of non-renewable power plants are included. The missing locations are obtained for this thesis from the web pages of the power plants owners and operators. The locations of the renewable power plants are retrieved from the web pages of Bosch & van Rijn and Windenergie Nieuws [98, 99]. The locations are overlayed on the ArcGIS map to find the closest connecting node for each power plant. The remaining renewable generation capacity is aggregated per province and mapped onto the node which is at the heart of the local distribution grid. This is determined by looking at the high-voltage lines of 150 kV and down in the ArcGIS map [75].

The mapping of the loads differ per energy end-use sector and depend on multiple variables. A summary of the aggregated generation and load is given in Table 4.6. The mapping of the aggregated generation and load is visualised in Figure 4.7. The mapping and aggregation of the loads are based on:

- **Households** – the households sector load is divided in two: the load of the four largest cities and the remaining load.
  - Amsterdam, Rotterdam, The Hague, and Utrecht are mapped on the closest node connecting them to the Dutch grid. This is determined by looking for the node connecting the lower high-voltage lines of the city's distribution grid to the high-voltage grid.
  - All other household loads are aggregated per province and mapped onto the node which is at the heart of the local distribution grid.

- **Buildings** – the buildings sector load is aggregated per province and mapped onto the node which is at the heart of the local distribution grid.
- **Transport** – the transport sector load is aggregated per province and mapped onto the node which is at the heart of the local distribution grid.
- **Agriculture** – the agriculture sector load is aggregated per province and mapped onto the node which is at the heart of the local distribution grid.
- **Industry** – as the industrial sector load is generally more clustered in rural locations, other nodes are used for mapping the load. CBS published a document containing the total annual load of all middle- and large-consumers of electricity over all municipalities in the Netherlands [100]. This document is used for this thesis to determine the closest node connecting the largest electricity-consuming municipalities via the local distribution grid to the high-voltage grid. The node is determined by first grouping the municipalities per province, and then selecting the largest electricity-consuming municipalities per province.

Table 4.6: **Overview of aggregated generation and load.**

Generation	
Total number of generators	121
Non-renewable generators (e.g., gas, coal, and nuclear)	78
Renewable generators (e.g., solar and wind)	43
Number of buses mapped with a generator	27
Load	
Number of loads	132
Number of buses mapped with a load	28

(a) Total demand mapped per node. The larger the circle the larger the total yearly demand. Basemap obtained from Esri [76]

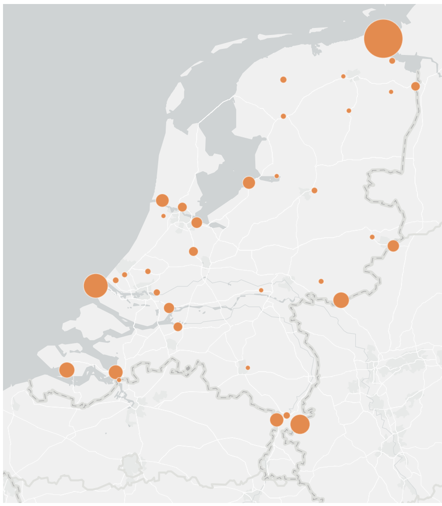

(b) Total generation capacity mapped per node. The larger the circle the larger the total yearly demand. Basemap obtained from Esri [76]

Figure 4.7: **Spatial demand and generation.**

4.1.5. Assumptions and Limitations of the Power System Model

The internal parameters of the pandapower model are mostly based on reports and documents published by TenneT TSO B.V.. Some assumptions are made as a result of the unavailability of open data or the limitations of the pandapower package. The assumptions made on the internal parameters are discussed below.

- **Ramping constraints:** Assumed zero due to limitations of the pandapower package. Explained in more detail in Section 3.1. Refers to the rate at which a generator is able to change its level of production. The importance of ramping constraints depend on the generation pool simulated. Nuclear and hard coal generators tend not to be able to fully ramp up or down within an hour. Natural gas generators tend to be able to fully ramp up or down within an hour. As the optimal power flow is calculated for hourly time steps and the future generation pool excludes nuclear and hard coal generators, the ramping constraints become less important.

- **Minimum up- and down-time:** Assumed zero due to limitations of the pandapower package. Explained in more detail in Section 3.1. Refers to the minimum amount of time that a generators should be up or down. The minimum up- and down-times of generators are usually of more importance than the ramping constraints when looking at hourly simulations. However, as these constraints are imposed by the power plants owner, they can differ per plant of the same generation type.
- **Dynamic line loading:** Assumed constant. Dynamic line loading data is available for the 220 kV and 380 kV high-voltage lines in the Dutch high-voltage grid. The line loading capacities mainly depend on the outside temperatures and are higher for winter and lower for summer season. As the dynamic line loading is weather-dependent, an extra controller per high-voltage line should be added to the model to accurately depict change in line loading. Due to an increase in complexity of the model, the line loading capacities are assumed to be constant. The capacity value for summer season is assumed.
- **Slack node:** Assumed the external grid node with the highest balancing capacity. It is common practice to define the slack node for power flow calculations as the node with highest balancing capacity.

The input of the model is based on the output of other models or data sets. Generally, the output is in the form of a total load or total generation value per time step. Assumptions are made for mapping the loads and generation capacities on the pandapower model. The assumptions related to the input and behaviour of the model are discussed below.

- **Planned and unplanned maintenance:** The planned and unplanned maintenance of high-voltage assets and power plants are not considered in the model.
- **External grids/Interconnectors:** The interconnection capacity is assumed to be available at full capacity throughout the year. Apart from a capacity decrease due to planned and unplanned maintenance, the capacity can also decrease as a result of scarce generation capacity available in neighbouring countries. As the interconnection lines are rarely operational at full capacity in reality, the balancing power provided as a result of this assumption is inaccurate.
- **Cost of interconnection:** The cost of electricity import and export are unknown and vary through time. As the marginal cost of an asset determines the unit commitment and thus the power flows in the model. An assumption needs to be made on the cost of the interconnection capacity. The cost are adjusted in a way that export and import of electricity ends up at the top of the merit order and therefore are solely used for peak balancing or renewable export. This assumption is based on an assumption made by TenneT TSO B.V. to create a similar model for sector integration analysis [23].

4.2. Validation

For determining the degree of confidence in the power system model, validation must be performed. This section explores the methods applicable to the validation of simulation models found in literature. The methods suited for validation of the developed power system model are identified and applied. The results of the validation, and the degree of confidence obtained are presented.

4.2.1. Methods for the Validation of Simulation Models

Every modelling approach differs from reality as a result of aggregation, past trends and other assumptions. They provide a good approximation of the power system at best. However, they are crucial for analysing policy and technology decisions, and their effects on the power system. Therefore, the level of accuracy of the model's output must be established by verifying and validating the power system model. As both model validation, and model verification methods are described in literature, it is important to first distinguish the two terms. Definitions of verification and validation adopted by the American Institute of Aeronautics and Astronautics (AIAA) are as follows [101]:

Verification: "The process of determining that a model implementation accurately represents the developer's conceptual description of the model and the solution to the model."

Validation: "The process of determining the degree to which a model is an accurate representation of the real world from the perspective of the intended uses of the model."

Author in [17] describes the validation processes on the basis of the schematic shown in Figure 4.8. The problem entity is described by the author as the system, idea, situation, policy, or phenomena to be modelled. The conceptual model is the mathematical representation of the problem entity, and the computerised model is the conceptual model implemented on a computer. The validation processes are shown as the connections between the processes. Author in [17] defines data validity as ensuring that the data used for conceptualising, testing and running the model is reasonable and correct. Conceptual model validation is defined by the author as ensuring that the underlying assumptions and theories for the conceptual model are accurate, and the problem is properly depicted for the intended use of the model. Computerised model verification is defined by the author as assuring that the conceptual model is correctly programmed and implemented. Finally, operational validation is defined by author in [17] as determining if the accuracy of the model's output behaviour is sufficient for the intended purpose of the model. Data validity is often not included in model validation and will therefore not be discussed. The remaining three model verification and validation steps are discussed below. The methods applicable to the validation and verification of the power system model are identified and applied later on in this section.

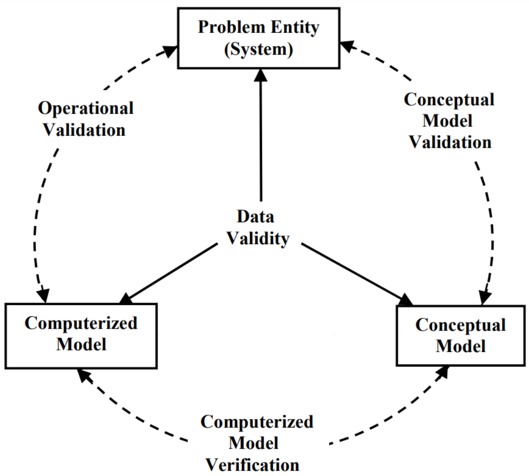

Figure 4.8: **Simplified version of the validation processes**
Based on the process by author in [17].

Conceptual Model Validation
Author in [17] states that the fundamental techniques used for conceptual model validation are face validation and traces. The former requires experts on the problem entity to evaluate the conceptual model by examining the modelling principles, and the latter requires component tracking through the entire model to examine the modelling philosophy.

Computerised Model Verification
In general, simulation languages are verified and validated against other software, and therefore assumed to be error free. However, errors can still originate from invalid data or errors in the model itself. Author in [17] states that the commonly used techniques for determining computerised model verification are structured walk-throughs and traces.

Operational Validation
Author in [17] classifies operational validation based on two types of systems, relating to whether it is possible to obtain data on the operational behaviour of the problem entity or power system itself. If data is available on system operations, the problem entity is described as observable. The operational validation techniques

suited to each system are represented in Table 4.7. The author states that if a system is not observable, it is generally not possible to obtain a high degree of confidence in the model. In the validation of these non-observable system, the author advises a thorough analysis of the model output behaviour and comparisons with other valid models if possible [17]. The author presents several options for analysing the model output behaviour, among which operational graphics, and a parameter variability/sensitivity analysis. Operational graphics relate to the graphical display of performance indicators of the model as the simulation runs through time to ensure their correct behaviour. Parameter variability/sensitivity analysis relates to analysing the effect on the model's behaviour or output by changing values of input or internal parameters. The accuracy of the parameters that are sensitive and cause substantial change in the model's output, determine the accuracy of the model itself.

Table 4.7: **Classification of operational validity** [17].

	Observable system	**Non-observable system**
Subjective approach	Comparison using graphical displays Explore model behaviour	Explore model behaviour Comparison to other models
Objective approach	Comparison using statistical tests and procedures	Comparison to other models using statistical tests

4.2.2. Validation of Power System Model

Some of the validation techniques proposed by author in [17] depend on the availability of power system data. However, no open transmission grid data can be found for the level of detail needed to validate the model. Non-renewable operational generation capacity, historical solar and wind profiles, and historical fuel prices are obtained for the unit commitment side of the power system model for the year 2018. This is used as input data for the aggregated power system model described above. The model is validated following the three verification and validation steps proposed discussed in Section 4.2.1. The validation techniques used for validating the power system model are presented in Table 4.8.

Table 4.8: **Validation techniques applied to the power system model**.

	Performed
Conceptual model validation	Traces
Computerised model verification	Structured walk-throughs Traces
Operational validation	Operational graphics Historical data validation Sensitivity analysis

Conceptual Model Validation

The theory of conceptual model validation is defined in Section 4.2.1 and the use of traces is proposed. This entails the tracking of entities through the entire model to examine the modelling philosophy and to determine if the necessary accuracy is achieved.

The underlying assumptions and theories for the conceptual model are compared to the infrastructure framework presented by TenneT TSO B.V. for creating the Infrastructure Outlook 2050 document published in cooperation with N.V. Nederlandse Gasunie [23]. TenneT TSO B.V. essentially is an expert on the problem entity of this thesis and therefore their model can be considered as an accurate comparison for validation purposes. The intended use of the infrastructure framework presented in that document is to analyse congestion caused by sector integration in 2050. The objective of the developed framework is inline with the objective of the model created by the author of this thesis. The modelling approach and assumptions taken in the Infrastructure Outlook are: (1) create hourly values for demand and supply, based on historical weather data to quantify the weather-dependent behaviour of solar and wind power, (2) import/export of power is the models last option for balancing the electricity system, (3) regionalisation of the national supply and demand data for localising bottleneck in the grid, (4) create a model based on a linear programming algorithm that calculates the optimised network flow pattern, (5) assume that the location of the conventional power plants in 2050 will not change, and (6) each line is assumed to have a (bidirectional) transport capacity expressed as a maximum possible energy flow in MW. The model incorporates the 380 kV and 220 kV high-voltage assets, including the expansions up to 2030. The hourly demand data was mapped to municipalities and are linked to the closest high-voltage station of the electricity grid. All underlying assumptions and the modelling approach are similar to the assumptions and approach used by TenneT TSO B.V. One big difference is the spatial detail of demand data in the models. The basic aggregation method is similar, however, most of the data is mapped per province or RES region instead of municipalities due to the unavailability of spatial demand data.

The tracking of entities in the conceptual model is performed in several steps, among which: (1) cross-checking the aggregation of demand data per province or region against the total demand data, (2) cross-checking the capacity factor of solar and wind profiles used against expected capacity factors, (3) crosschecking the location of generators against the location specified by the plant owners, and (4) crosschecking the marginal cost of power plants against the expected merit order of the system.

Computerised Model Verification

The theory of computerised model verification is defined in Section 4.2.1 and the use of structured walk-throughs and the use of traces is proposed. The former refers to a technique where the technical aspects of the software development process are reviewed and discussed in an organised manner to find defects. The latter refers to the tracking of entities through the entire model to examine the modelling accuracy.

In the pandapower package a diagnostic tool is programmed for verifying the correct modelling of a network. The tool automatically checks the network for the most common issues leading to errors, among which: (1) invalid values, (2) existence of only one external grid, (3) inconsistent voltages, and (4) disconnected elements. The diagnostic tool is used to further verify the model for coding errors, after the model is finished. Structured walk-throughs of the model were performed during the primary coding of the model and during each coding session for expanding the model. The primary coding session consisted of gradually building up the model with the open data gathered and was based on the assumptions and approach validated during the conceptual model validation.

As pandapower is a plug-and-play simulation language, the model's structure and the mathematical relationships are already coded and are not easily verifiable by structured walk-throughs. Therefore, modelling entities are tracked from input to output for the correct mathematical relationships. Several steps and entities are tracked, among which: (1) the mapping of demand per node—relates to the model mapping the correct demand per time step on the corresponding node and the model adding up the multiple demands per node—, (2) the maximum available generation capacity for solar and wind energy sources per time step—relates to the model multiplying the capacity factor per time step with the generation capacity—, (3) the merit order per time step—relates to the unit commitment of the model and thus the overall capacity factors of all generators in the system—, and (4) the model operates within limits—relates to the model correctly applying load, generation, and voltage limits.

Operational Validation

The theory of operational validation is defined in Section 4.2.1 and the use operational graphics and the use of a parameter variability/sensitivity analysis is proposed. The former relates to the graphical display of performance indicators of the model as the simulation runs through time. The latter relates to analysing the effect on the model's behaviour or output by changing values of input or internal parameters.

The first step is to operationally validate the model by graphically displaying the performance indicators of the model. The operational generation capacity, historical solar and wind profiles, and historical fuel prices are obtained for the year 2018. This is used as input data for the aggregated power system model described in Section 4.1. An hourly DC optimal power flow is executed for the year 2018 and the next performance indicators are depicted per time step: (1) capacity factor per generator type, (2) marginal cost per generator type—combination of the fuel and CO_2 emission costs—, (3) ramping rates per generator type, (4) load profiles per end-use sector. Furthermore, the minimum, mean, and maximum line and transformer loading percentages are calculated and displayed. All graphs are compared to common knowledge and expectations for the Dutch power system, and the graphs depicted in the Annual Market Update document for 2018 published by TenneT TSO B.V. [102].

The degree of confidence for the intended use of the model is high enough for it to be used as base model for the scenario study. Afterwards, a sensitivity analysis is performed on the expected sensitive parameters to determine the level of overall accuracy of the model. The sensitivity analysis is discussed in Section 6.2.

5
Scenario Study

The research objective for this thesis is twofold, as stated in Section 1.3. The first objective is to develop a representative model of the Dutch high-voltage electricity grid, and the second objective is to analyse the effects of heating sector electrification scenarios on the electricity grid. This chapter presents the methodological approach in fulfilling the second objective. Section 5.1 explores the available literature and reports to establish the power and heating sector outlook for the Dutch energy system in 2050. Section 5.2 translates the national energy sector outlooks to three generation and three load scenarios based on the level of penetration of Variable Renewable Energy Sources (VRES) in the power sector and the level of electrification in the heating sector. Finally, Section 5.3 builds on the validated model of the current high-voltage electricity grid presented in Section 4.1 and describes the steps taken to arrive at the fundamental model of the future electricity grid.

5.1. Literature on Energy Sector Outlook 2050

Figure 5.1 shows the structure of the ratified agreements and the corresponding areas of influence. The National Climate Agreement and the European Green Deal are both strategy documents based on the objectives agreed upon in the Paris Climate Agreement. Within the National Climate Agreement sector-specific commitments are presented. It states that targets for the built environment and electricity sectors must be elaborated on a regional level [7]. The Dutch government divided the Netherlands in 30 regions responsible for their own regional energy strategy. As a fundamental part of the strategy documents, studies are commissioned by the signing parties on the feasibility of the proposed policies and pathways. These studies provide insights on the power and heating sector outlook from a continental to a regional level of detail and form the basis for the scenario study.

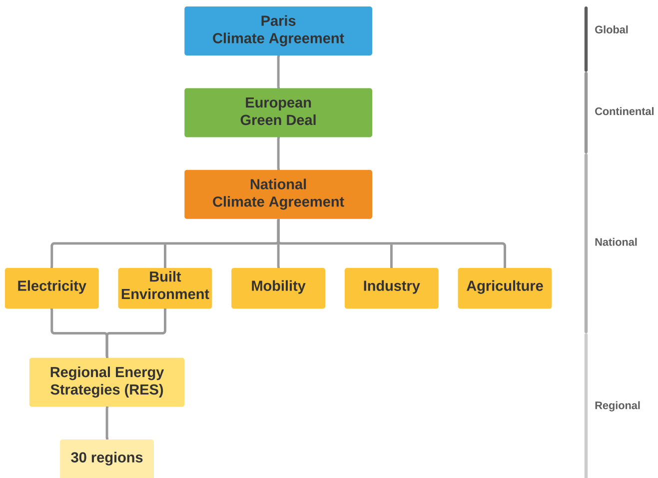

Figure 5.1: **Structure of agreements.**

5.1.1. Power Sector Outlook 2050

The power sector outlook for 2050 is based on studies commissioned by the Ministry of Economic Affairs and Climate Policy [7, 103, 104], strategy documents published by the RES regions [18, 105–133], and a 2050 scenario study published by Berenschot and Kalavasta [134]. These studies and documents provide insights in the national and regional objectives set for 2030 onwards. Documents published by TenneT TSO B.V. [64, 82, 83, 135], and the strategy documents published by the RES regions [18, 105–133] envisage the power sector for 2030. Studies commissioned by the Government [7, 103, 104], and the scenario study published by Berenschot and Kalavasta [134] envisage the power sector for 2050. The detailed analysis in the 2030 documents is combined with the vision sketched in the 2050 documents to arrive at a fairly detailed power sector outlook for 2050. The documents focus on different components of the power sector. A division is made between the renewable and non-renewable generation, with the renewable generation being subdivided in variable renewable and non-variable renewable generation.

Renewable Generation

The National Climate Agreement foresees a high penetration of variable renewable energy sources in the power sector in the Netherlands. The focus lies on offshore wind, solar PV and a hydrogen-based energy sector in general. One of the studies commissioned by the Government is a scenario study published by the Netherlands Environmental Assessment Agency on the future of wind generation in the North Sea [103]. This study explores four scenarios ranging from a business as usual scenario to a scenario fully focused on climate-neutrality. They foresee an installed offshore wind capacity in 2050 ranging from 12 - 60 GW. Another study commissioned by the Government is a more recent and scientifically sound study published by DNV GL on the North Sea Outlook for 2050 [104]. This study forms the basis for the offshore wind generation capacity assumed in the scenario study by Berenschot and Kalavasta [134], as well as the basis for the latest studies on the power sector outlook for 2050. Two scenarios are discussed in the study by DNV GL, the first scenario is based on an import-dependent power sector with an offshore wind capacity of 38 GW and the second is based on a self-sufficient power sector with an offshore wind capacity of 72 GW.

The future onshore wind capacity for 2030 and the generator locations are thoroughly researched in the RES 1.0 documents published by the individual RES regions [18, 105–133]. The RES 1.0 documents state the objective of 7 GW of operational onshore wind capacity in 2030. In the 2050 scenario study published by Berenschot and Kalavasta, four scenarios are presented differentiated by the level of cooperation between regions, nations, and continents [134]. The onshore wind capacity in the scenarios focusing on a self-sufficient regional and national power sector is estimated to be 20 GW. The scenarios focused on international cooperation to achieve the climate objective, estimate an onshore wind capacity of 10 GW [134].

The last variable renewable energy source of interest for the Netherlands is solar PV. The National Climate Agreement separates the objectives for this resource in two, based on installed capacity. Solar PV installations with a peak capacity of 15 kW and up are regarded as large scale and are considered to be the responsibility of the individual RES regions. Installations with a peak capacity lower than 15 kW are regarded as small scale and are considered to be public responsibility. The objectives set for the small scale solar depend heavily on the financial policies set by the Government. The RES regions specify a large scale solar PV capacity of 28 GW in 2030. The National Climate Agreement set the goal for small scale solar PV capacity at 7 GW in 2030 [7]. The scenario study published by Berenschot and Kalavasta presents a large scale solar PV capacity in the range of 34 - 58 GW and a small scale capacity in the range of 13 - 35 GW [134].

The non-variable renewable energy sources in the future power sector mainly comprise hydrogen-based generators. The CCGT and SCGT generators can be repurposed to run on hydrogen as primary fuel. Berenschot and Kalavasta foresee a hydrogen generation capacity ranging between 0 - 17 GW for hydrogen burned in SCGT and 0 - 18 GW for hydrogen burned in CCGT generators [134]. In Table 5.1 an overview of the 2050 outlook on renewable generation in the power sector is shown.

Non-Renewable Generation

None of the documents and studies foresee a bright future for non-renewable energy sources. The 2050 climate-neutral scenario study predicts the use of biogas in combination with Carbon Capture and Storage (CCS) as balancing and peak load electricity generators. The total installed capacity of non-renewable generators is estimated to be in the range of 0.4 - 6 GW [134].

Table 5.1: **Overview of the renewable power sector outlook for 2050.**

	Installed Capacity
Wind turbines [GW]	19 - 92
Onshore [GW]	7 - 20
Offshore [GW]	12 - 72
Solar PV [GW]	35 - 93
Large scale (> 15 kWp) [GW]	28 - 58
Small scale (< 15 kWp) [GW]	7 - 35
Hydrogen plant [GW]	0 - 35
Hydrogen CCGT [GW]	0 - 17
Hydrogen SCGT [GW]	0 - 18

5.1.2. Heating Sector Outlook 2050

The heating sector outlook for 2050 is based on a study commissioned by the Ministry of Economic Affairs and Climate Policy [136], a strategy document on the European heat roadmap [25], and a 2050 scenario study published by Berenschot and Kalavasta [134]. Energy policies and proposals presented by the Dutch government related to the future heating sector can be categorised in two objectives, the first is the reduction of heat demand and the second is the stimulation of low-carbon heat generation. The latter is the subject of a study published by Aalborg University on the quantification of the impact of low-carbon heat generation as a part of the European Heat Roadmap series [25]. The study presents four fundamental technologies/proposals that contribute to the efficiency, decarbonisation, and affordability of the future heating sector. The first proposal is the expansion of the thermal grids—the physical infrastructure for district heating—, which is crucial to enable better integration of renewable energy and excess heat sources. It estimates a market share of district heating of the total heating demand in the range of 47% - 76%. The second proposal is excess heat recovery from the industrial sector, which can account for at least 21% of the district heating demand. The third technology regards the short-term storage units for district heating. Short-term thermal storage units should be integrated in the thermal grids to increase the use of renewable energy sources and large scale heat pumps. The fourth and final technology presented are individual heat pumps, which enable electrification of heating demand in areas where district heating is not viable. It is estimated that individual heat pumps can provide up to 24% of the heat demand for the households and buildings sector.

The 2050 scenario study published by Berenschot and Kalavasta estimates around 40% - 60% of the heating demand in the agricultural sector to be covered by geothermal heat sources [134]. The study presents the predicted demand growth for the different energy end-use sectors based on research performed by PBL. The predicted growth is assumed to be equal for all scenarios, the varying parameters are the parameters related to heat supply sources.

District Heating

In the study published by Aalborg University a district heating market share of 47% - 76% of the low-temperature heating demand in the year 2050 is presented [25]. The Netherlands Environmental Assessment Agency published a study on the outlook of climate-neutral thermal grids in the Netherlands for 2050. They envisage a district heating market share of 60% - 75% for low-temperature thermal grids [136]. According to a report published by IEA on heat pumps in district heating systems, large scale heat pumps in combination with storage systems have the potential to become a key technology in future district heating systems. The technology can increase the flexibility of the heating systems and can balance an electricity grid with variable renewable energy sources. The study estimates that large scale heat pumps can supply around 25% of the low-temperature district heating demand [137].

The report on the outlook of climate-neutral thermal grids explores the potential of geothermal heat supply. They estimate the potential of geothermal heat to be in the range of 85 - 1000 PJ per year depending on the proposed investment policies [136]. The total low-temperature heat demand for 2050 is estimated to be around 350 PJ, of which at least 25% can be covered by geothermal heat. The low-temperature heat demand for the industrial sector can be covered by district heating sources. IEA estimates the low-temperature heat demand to account for 30% of the total industrial heat demand [53]. Medium- and high-temperature heat demand must be covered by other renewable sources, such as hydrogen-fired boilers. Table 5.2 presents an overview of the renewable heating supply outlook.

Table 5.2: **Overview of the renewable heating sector outlook for 2050.**

	Market share [%]
Households & Buildings	
Individual heat pumps	0% - 24%
District heating	47% - 76%
Large scale heat pumps with thermal storage	0% - 25%
Geothermal heat	at least 25%
Agriculture	
Large scale heat pumps with thermal storage	0% - 50%
Geothermal heat	40% - 60%
Industry	
District heating	0% - 30%
Geothermal heat	0% - 100%

5.2. Scenario Study

Five scenarios will be studied: one base case and four energy sector integration scenarios. The four integration scenarios are build upon the base case and differ based on two main components: the level of electrification of the heating sector and the level of VRES penetration in the generation sector. The load profiles are obtained from the Energy Transition Model [90]. General parameters are maintained the same for all load scenarios, e.g., demand growth, prosperity changes, behavioural changes, weather scenarios. Solely parameters involving electrification of heating demand are adjusted for obtaining the profiles. This section first presents the basic assumptions made for each individual scenario. Then, the load profiles and the generation pool obtained from the scenario study are described.

5.2.1. Overview of Scenarios

Table 5.3 provides a summary of the scenarios based on the electrification of the heating sector, the operational generation pool, and the height of the investments necessary to achieve the CO_2 emission targets.

Table 5.3: **Overview of the scenarios.**

	Load	**Generation pool**	**Emission target**
Base case	Business as usual	Business as usual	Very high
Scenario 1	Business as usual for heat supply of industry Low electrification of heat supply of households, buildings, and agriculture	Low VRES penetration Hydrogen plants Natural gas plants	High
Scenario 2	Business as usual for heat supply of industry Low electrification of heat supply of households, buildings, and agriculture	High VRES penetration Hydrogen plants	Medium
Scenario 3	High electrification of heat supply of industry High electrification of heat supply of households, buildings, and agriculture	Low VRES penetration Hydrogen plants Natural gas plants	Medium
Scenario 4	High electrification of heat supply of industry High electrification of heat supply of households, buildings, and agriculture	High VRES penetration Hydrogen plants	Low

Base Case

The base case is based on the 2030 target scenario presented in the study published by Berenschot and Kalavas-ta [134]. All the data used in the study are derived from the Climate Agreement and are checked for feasibility by the authors of the study. Similar to the grid improvements, 2030 is used as the reference year in this thesis. From there on the base case assumes business as usual. The CO_2 emission target can be achieved by investing heavily in CCS technologies.

Scenario 1 - Low Electrification and Low VRES Penetration

The first scenario is most similar to the base case and consists of a low level of electrification of the heating sector combined with a low level of VRES penetration. District heating penetration in the households and buildings sector are assumed to be equal in both the low and high electrification scenarios, the big difference between the two is the technology used for the supply of heat. This scenario assumes low electrification of the district heating sources and other non-industrial heat demand. The industrial heat demand and large parts of the electricity demand are supplied by generation technologies running on hydrogen. The remaining electricity generation pool consists of a low level of VRES penetration capacity—based on the lower limits stated in the power sector outlook studies—and a small dispatchable pool of SCGT and CCGT generators running on natural gas. The CO_2 emission targets can be achieved by making substantial investments in CCS technologies for the non-renewable generation pool and non-electrified heating supply.

Scenario 2 - Low Electrification and High VRES Penetration
The second scenario consists of a low level of electrification of the heating sector combined with a high level of VRES penetration. The load profiles based on low electrification of the heating sector obtained for the first scenario are also used for analysing the second scenario. The available generation pool is solely based on renewable electricity generators. Hydrogen-fired SCGT and CCGT generators are used for balancing supply and demand, and as fast-responding generators for providing electricity during peak loads. The base electricity generation pool consists of a high level of VRES penetration, based on the upper limits stated in the power sector outlook studies. The CO_2 emission targets can be achieved by making substantial investments in CCS technologies for the non-electrified heating supply.

Scenario 3 - High Electrification and Low VRES Penetration
The third scenario consists of a high level of electrification of the heating sector combined with a low level of VRES penetration. High electrification of the heating sector assumes a high electrification of technologies used for the supply of heat in the district heating sector, the non-industrial sector, and the industrial sector. The upper limits of electrified heating sources in the heating sector are implemented for this scenario and are based on the heating sector outlook. The limiting factor for the electrification of heating sources mostly originates from the temperature range of the heat demand. The high-temperature heat required for industrial processes is difficult to generate without using combustion-based generators. In this scenario, the high-temperature heat demand is supplied by hydrogen-fired generators. The electricity generation pool is similar to the pool described in the first scenario. The CO_2 emission targets can be achieved by making substantial investments in CCS technologies for the non-renewable generation pool.

Scenario 4 - High Electrification and High VRES Penetration
The fourth scenario consists of a high level of electrification of the heating sector combined with a high level of VRES penetration. The load profiles based on high electrification of the heating sector obtained for the third scenario are also used for analysing the fourth scenario. The electricity generation pool is similar to the pool described in the second scenario. The CO_2 emission targets can be achieved without substantial investments in CCS technologies.

5.2.2. Load Scenarios
Three different load scenarios are studied: (a) base case, (b) low electrification of the heating sector, and (c) high electrification of the heating sector. The base case revolves around business as usual from 2030 onwards. The year 2030 is chosen as basis due to the reasonably accurate representation of the actual heat generation pool, similarly to the generation scenarios. The three load scenarios comprise electricity demand for all applications in all energy end-use sectors. The big difference between them is the level of electrification of the heating sector and the resulting change in the overall electricity load and load profiles. The non-electrified heating sources are mentioned, but are outside the scope for this research. The heat generation pool is based on the heating sector outlook presented in Section 5.1. The overall load profiles are created by adjusting parameters relevant for the electrification of heating demand in the Energy Transition Model of Quintel Intelligence [90]. To give an idea of the general trend throughout the year, the hourly load profiles are averaged per day and presented per end-use sector. The total monthly electricity demand of all end-use sectors is shown in Figure 5.2. The scenarios created in the Energy Transition Model are saved and can be explored at:

- **Base case** - `https://pro.energytransitionmodel.com/saved_scenarios/11260`
- **Low electrification** - `https://pro.energytransitionmodel.com/saved_scenarios/11264`
- **High electrification** - `https://pro.energytransitionmodel.com/saved_scenarios/11262`

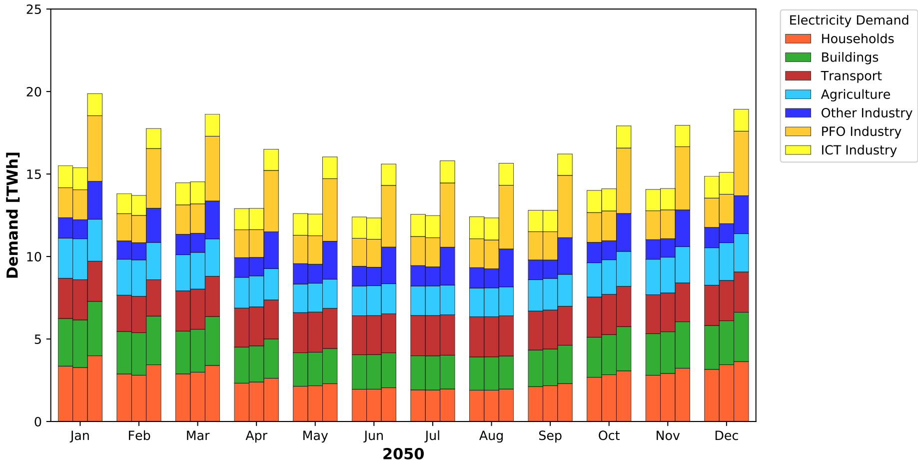

Figure 5.2: **Monthly electricity demand for all demand scenarios.**
From left to right: base case, low electrification, and high electrification.

Households Sector

The heat generation pool for the households sector comprises all-electric heat pumps, hybrid heat pumps, electric and gas-fired heaters, gas-fired combi boilers, wood pellet boilers, and geothermal heat supply. The heat pumps and electric boilers are suitable technologies for electrifying the households sector. Geothermal heat is a renewable technology that can partially be referred to as an electrified heating source, due to the electricity needed for circulating the working fluid. Geothermal heat and large scale/collective heat pumps can supply heat to the district heating networks.

According to a study on climate-neutral thermal grids in the Netherlands, the potential heat demand in the households sector of low-temperature heat supplied by district heating networks is 165 PJ per year [136]. In the scenarios developed for this thesis, this amounts to 69% of the total heating demand in the households sector. The market share of district heating is maintained the same for the low and high electrification scenarios. The all-electric heat pumps in the base case heat generation pool generate heat from drawing ambient heat from the air or ground. 60% of the all-electric heat pumps are heat pumps that draw ambient heat from the air. This amounts to 7% of the total heating demand to be supplied by all-electric air heat pumps. The market share of all-electric air heat pumps in the base case is maintained for the low electrification scenario. The remaining share of heat generation technologies in the low electrification scenario is based on the scenario study by Berenschot and Kalavasta. The study states that the heat generation pool in the households sector only consists of district heating, heat pumps and hybrid heat pumps [134]. For this thesis, this translates to hybrid heat pumps completing the heat generation pool for the low electrification scenario.

The heat generation pool for the high electrification scenario mostly consists of district heating and all-electric heat pumps. The scenario study by Berenschot and Kalavasta mentions that a small percentage of heat supply will probably be supplied by hybrid heat pumps, as they are favourable for less-insulated residential buildings due to higher heating capacities per system [134]. For this thesis, this translates to hybrid heat pumps completing the heat generation pool for the high electrification scenario with a market share of 5%. Table 5.4 shows an overview of the market share per heat generation technology in the households sector for all three scenarios.

Table 5.4: **Overview of heat generation technologies in the households sector per scenario. ETM parameters.**

	Base case	Low electrification	High electrification
District heating	16%	69%	69%
Electrified heating	12% all-electric heat pump 5% hybrid heat pump (gas) 2% electric heater	7% all-electric heat pump 24% hybrid heat pump (hydrogen)	26% all-electric heat pump 5% hybrid heat pump (hydrogen)
Non-electrified heating	58% gas-fired combi boiler 5% wood pellet boiler 2% gas-fired heater	-	-

The load profiles resulting from loading the parameters from Table 5.4 in the Energy Transition Model are obtained. Figure 5.3 shows the load profiles for all three scenarios divided by electricity for heating, electricity for cooling, and electricity for other applications. The load profiles are presented as portions of the total load size for the individual applications. It can be observed that the cooling and other electricity profiles are similar in all three scenarios. The electricity load for heating applications differs per scenarios. The significant change in load profiles originate from the technologies used for heating, specifically the amount of heat supplied by hybrid heat pumps. The hybrid heat pumps switch between electricity and gas/hydrogen for heat generation, the latter being the main source of supply during electricity peak loads and high heat demand. Therefore, the higher market share of hybrid heat pumps in the low electrification scenario result in a significant change in load profile during the winter months.

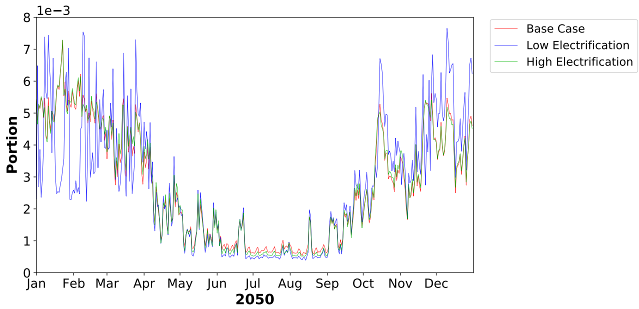

(a) Electricity demand for heating applications in the household sector for all demand scenarios. The load profile is shown as a portion per time step of the total load in a year, and is calculated by dividing the load per day by the total load in a year.

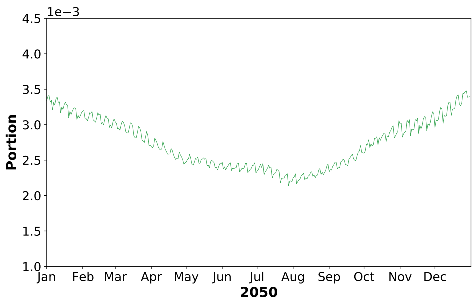

(b) Electricity demand for cooling applications in the household sector for all demand scenarios. The load profile is shown as a portion per time step of the total load in a year, and is calculated by dividing the load per day by the total load in a year.

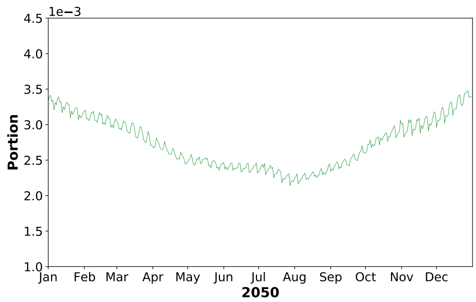

(c) Electricity demand for other applications in the household sector for all demand scenarios. The load profile is shown as a portion per time step of the total load in a year, and is calculated by dividing the load per day by the total load in a year.

Figure 5.3: **Electricity demand profiles in the households sector for all demand scenarios.**

It can be observed that the load profile of electricity used for cooling applications is similar to the other electricity demand and is lower during summer months and higher during winter months. According to Quintel Intelligence, they tested the ETM for various cooling curves and concluded that all of the available curves results in an electricity demand curve very different from the measured total demand curve. In combination with a negligible electricity demand for cooling applications, the ETM adopts the load profile shown for other electricity applications for creating the load profile for cooling applications. For this thesis, this translated to the effects of power and cooling sector integration to be neglected. The varying levels of electrification of the heating sector result in a varying total electricity demand in the households sector. The monthly electricity demand per application and per scenario is shown in Figure 5.4.

The thermal grids used for district heating supply of the households and buildings sector and the corresponding heat generation pool are combined in the ETM. The pool for the low electrification scenario is based on the lowest penetration of renewable heat generation technologies presented in the scenario study by Berenschot and Kalavasta [134]. The heat generation pool for the high electrification scenario is based on a report published by IEA [137] that states that collective heat pumps can supply up to 25% of the low-temperature district heating demand and a report published by PBL [136] that states that geothermal heat

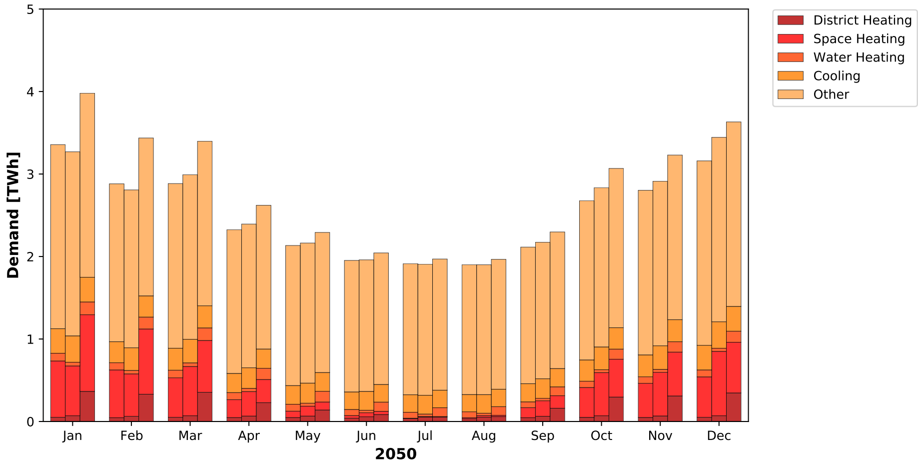

Figure 5.4: **Monthly electricity demand in the households sector for all demand scenarios.** From left to right: base case, low electrification, and high electrification

can supply at least 25% of the district heating demand. For this thesis, this translates to the capacities of the renewable technologies shown in Table 5.5. The capacities are calculated based on the predicted market share per technology. Table 5.5 gives an overview of the renewable technologies in the generation pool for the three scenarios.

Table 5.5: **Overview of heat generation technologies for district heating in the households and buildings sectors per scenario. ETM parameters.**

	Base case	Low electrification	High electrification
Electrified heating	615 MW collective heat pump with thermal storage	750 MW collective heat pump with thermal storage	3950 MW collective heat pump with thermal storage
Non-electrified heating	-	700 MW geothermal	3900 MW geothermal

Buildings Sector

The heat generation pool for the buildings sector comprises all-electric heat pumps, biomass- and gas-fired heaters, hydrogen- and gas-fired combi boilers, and geothermal heat supply. The heat pumps are a suitable technology for electrifying the buildings sector. Due to the size of individual heat pump installations needed for electrifying the buildings heat demand, they are often installed with thermal storage capacity for providing flexibility to the grid. Geothermal heat is a renewable technology that can partially be referred to as an electrified heating source, due to the electricity needed for circulating the working fluid. Geothermal heat and large scale/collective heat pumps can supply heat to the district heating networks. As the buildings sector mostly encompasses non-residential buildings in residential/urban areas, the district heating networks for the households and buildings sector are shared.

According to the study on climate-neutral thermal grids in the Netherlands, the potential heat demand in the buildings sector of low-temperature heat supplied by district heating networks is 105 PJ per year [136]. In the scenarios developed for this thesis, the predicted energy demand in the ETM for the buildings sector is lower than 80 PJ in 2050. The market share of district heating networks in the households sector is adopted for the buildings sector. Thus 69% of the total heating demand in the buildings sector is supplied by district heating network and is maintained the same for the low and high electrification scenarios. The market share of all-electric heat pumps in the base case is maintained for the low electrification scenario. The remaining share of heat generation technologies in the low electrification scenario is based on the scenario study by Berenschot and Kalavasta, which states that the heat generation pool in the buildings sector only consists of district heating, heat pumps and hybrid heat pumps [134]. For this thesis, this translates to hybrid heat pumps completing the heat generation pool for the low electrification scenario.

The heat generation pool for the high electrification scenario consists of district heating and all-electric heat pumps. Table 5.6 shows an overview of the market share per heat generation technology in the buildings sector for all three scenarios.

Table 5.6: **Overview of heat generation technologies in the buildings sector per scenario. ETM parameters.**

	Base case	**Low electrification**	**High electrification**
District heating	5%	69%	69%
Electrified heating	12% all-electric heat pump with thermal storage	12% all-electric heat pump with thermal storage	31% all-electric heat pump with thermal storage
Non-electrified heating	80% gas-fired combi boiler 3% biomass-fired heater 2% gas-fired heater	19% hydrogen-fired combi boiler	-

The load profiles resulting from loading the parameters from Table 5.6 in the Energy Transition Model are obtained. Figure 5.5 shows the load profiles for all three scenarios divided by electricity for heating, electricity for cooling, and electricity for other applications. The load profiles are presented as portions of the total load size for the individual applications. It can be observed that the cooling and other electricity profiles are similar in all three scenarios. The electricity load for heating applications differs per scenarios. The significant change in load profiles originate from the technologies used for heating and their market share. In this case, the market share of collective heat pumps with thermal storage and geothermal heat in the district heating supply cause the deviation in load profiles. The geothermal heat supply provides a constant amount of heat year round, resulting to a lower demand for other electrified heat sources in the summer. As the profiles present the portion of the total demand for that specific application and per scenario, the reduction of electricity demand in the summer results in a relative increase in electricity demand in the winter.

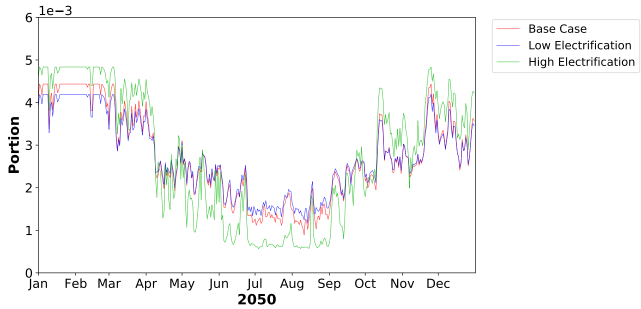

(a) Electricity demand for heating applications in the buildings sector for all demand scenarios. The load profile is shown as a portion per time step of the total load in a year, and is calculated by dividing the load per day by the total load in a year.

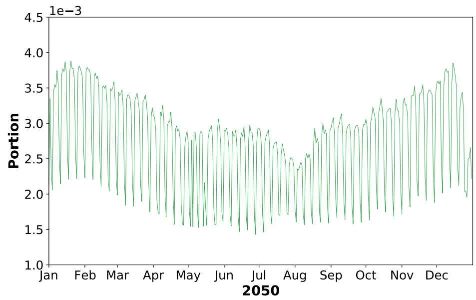

(b) Electricity demand for cooling applications in the buildings sector for all demand scenarios. The load profile is shown as a portion per time step of the total load in a year, and is calculated by dividing the load per day by the total load in a year.

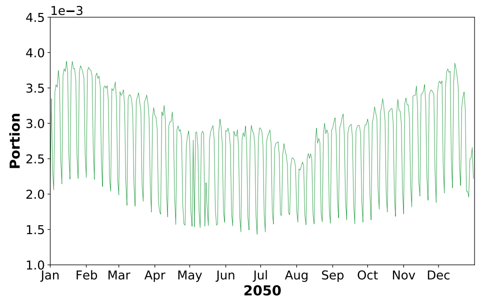

(c) Electricity demand for other applications in the buildings sector for all demand scenarios. The load profile is shown as a portion per time step of the total load in a year, and is calculated by dividing the load per day by the total load in a year.

Figure 5.5: **Electricity demand profiles in the buildings sector for all demand scenarios.**

It can be observed that the load profile of electricity used for cooling applications is similar to the other electricity demand and is lower during summer months and higher during winter months. The justification for the cooling profile is similar to the arguments presented for the cooling profile of the households sector. The varying levels of electrification of the heating sector result in a varying total electricity demand in the buildings sector. The monthly electricity demand per application and per scenario is shown in Figure 5.6.

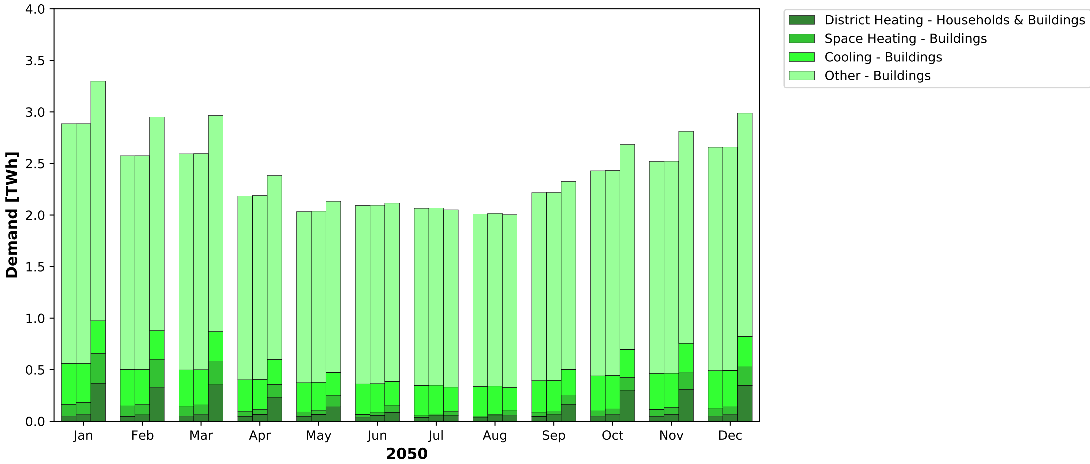

Figure 5.6: **Monthly electricity demand in the buildings sector for all demand scenarios.**
From left to right: base case, low electrification, and high electrification

Transport Sector

The main energy carriers in the transport sector are electricity, petrol, hydrogen, and Liquefied Natural Gas (LNG). The transport sector is not responsible for heating and cooling demand. As there is no heating and cooling demand, the only electricity demand in the transport sector originates from other applications. Aviation, heavy transport, and long-haul transport are difficult to electrify applications in the transport sector and are mainly responsible for the energy carrier demand of petrol, hydrogen, and LNG. Electric vehicles in passenger and freight transport are largely electrified according to the scenario study by Berenschot and Kalavasta [134]. Electric vehicles comprise trucks, cars, trains, trams, metros, buses, motorcycles, and bicycles. For this thesis, this translates to the level of electrification to be maintained the same for all three load scenarios. The resulting load profile from the Energy Transition Model is obtained. Figure 5.7 shows the load profiles for all three scenarios.

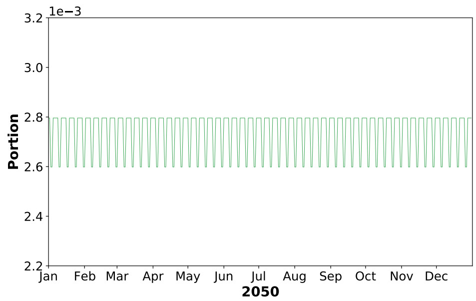

Figure 5.7: **Electricity demand profile in the transport sector for all demand scenarios.**
Electricity demand for all applications in the transport sector. The load profile is shown as a portion per time step of the total load in a year, and is calculated by dividing the load per day by the total load in a year.

It can be observed that the electricity load profile is equal in all three scenarios. As a result of identical levels of electrification of vehicles for all scenarios and no changes in growth factors of the individual transportation technologies for all scenarios, the total monthly electricity demand of the transport sector is equal for all three scenarios. Figure 5.8 presents the total demand per scenario.

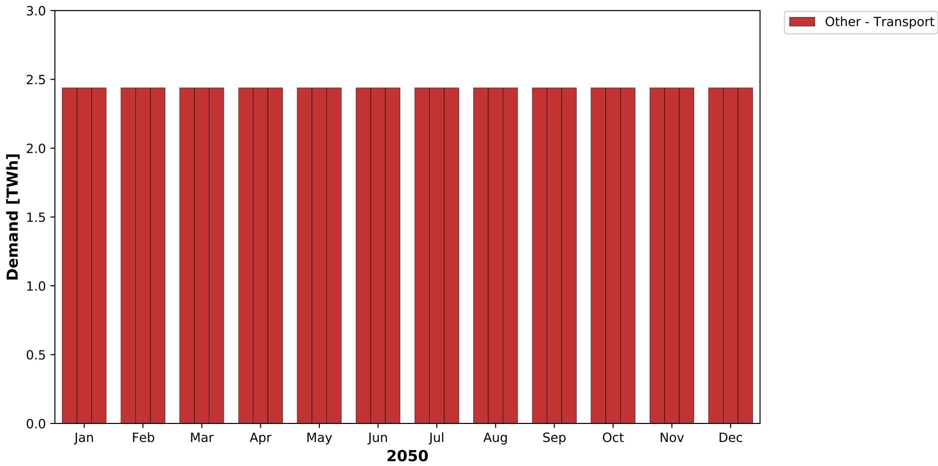

Figure 5.8: **Monthly electricity demand in the transport sector for all demand scenarios.**
From left to right: base case, low electrification, and high electrification

Agriculture Sector

The heat generation pool for the agriculture sector comprises all-electric heat pumps, biomass-, gas-, oil-, and hydrogen-fired heaters, and geothermal heat supply. The heat pumps are a suitable technology for electrifying the agriculture sector. A substantial part of the heat demand in the agriculture sector originates from greenhouses. Due to the size of individual heat pump installations needed for heating these greenhouses, they are often installed with thermal storage capacity for providing flexibility to the grid and the farmers. Geothermal heat can supply heat to individual greenhouses.

According to the study on climate-neutral thermal grids in the Netherlands, the potential heat demand in the agriculture sector of low-temperature heat supplied by geothermal sources is 40 PJ per year [136]. In the scenarios developed for this thesis, this amounts to 60% of the total heating demand in the agriculture sector. A smaller market share than its potential is chosen as a result of the viability of geothermal sources. The scenario study by Berenschot and Kalavasta states that a market share of geothermal heat of 40% of the total demand is viable without subsidies [134]. For this thesis, this translates to the market share of geothermal heat in the low and high electrification scenarios to be maintained the same and is set at 40%. The market share of all-electric heat pumps in the low electrification scenario is maintained from the base case. The remaining assets in the heat generation pool for the low electrification scenario comprise hydrogen-, gas-, and biomass-fired heaters.

The heat generation pool for the high electrification scenario consists of all-electric heat pumps, geothermal heat, and hydrogen-fired heaters. The market share of all-electric heat pumps is based on the scenario with the highest level of electrification in the scenario study by Berenschot and Kalavasta [134]. For this thesis, this translates to a market share of 45% for all-electric heat pumps and hydrogen-fired heaters completing the heat generation pool. The hydrogen-fired heaters are used as supply for peak loads. Table 5.7 gives an overview of the market share per heat generation technology in the agriculture sector for all three scenarios.

Table 5.7: **Overview of heat generation technologies in the agriculture sector per scenario. ETM parameters.**

	Base case	**Low electrification**	**High electrification**
District heating	34%	-	-
Electrified heating	4% all-electric heat pump with thermal storage	4% all-electric heat pump with thermal storage	45% all-electric heat pump with thermal storage
Non-electrified heating	9% geothermal 38% gas-fired heater 13% oil-fired heater 2% biomass-fired heater	40% geothermal 16% hydrogen-fired heater 25% gas-fired heater 15% biomass-fired heater	40% geothermal 15% hydrogen-fired heater

The load profiles resulting from loading the parameters from Table 5.7 in the Energy Transition Model are obtained. Figure 5.9 shows the load profiles for all three scenarios divided by electricity for heating, and electricity for other applications. The load profiles are presented as portions of the total load size for the individual applications.

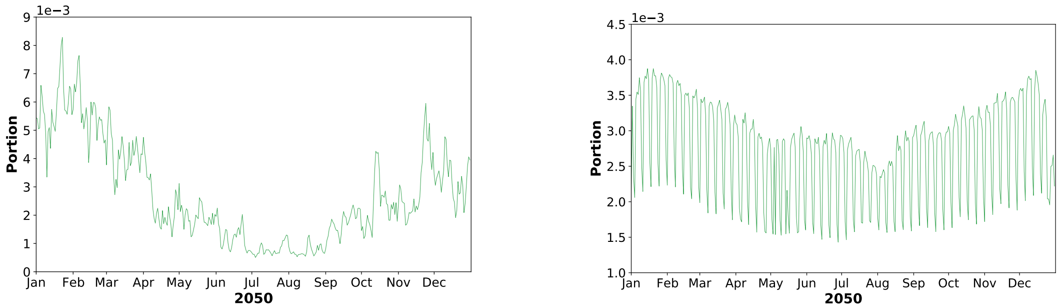

(a) Electricity demand for heating applications in the agriculture sector for all demand scenarios. The load profile is shown as a portion per time step of the total load in a year, and is calculated by dividing the load per day by the total load in a year.

(b) Electricity demand for other applications in the agriculture sector for all demand scenarios. The load profile is shown as a portion per time step of the total load in a year, and is calculated by dividing the load per day by the total load in a year.

Figure 5.9: **Electricity demand profiles in the agriculture sector for all demand scenarios.**

It can be observed that the heating profiles and the other electricity profiles are similar in all three scenarios. The varying levels of electrification of the heating sector result in a varying total electricity demand in the agriculture sector. The monthly electricity demand per application and per scenario is shown in Figure 5.10. The heat demand is expected to decrease with one percent per year and electricity demand is expected to increase with three percent per year. As a result, the percentage of electricity demand for heating applications in the agriculture sector is small for all scenarios.

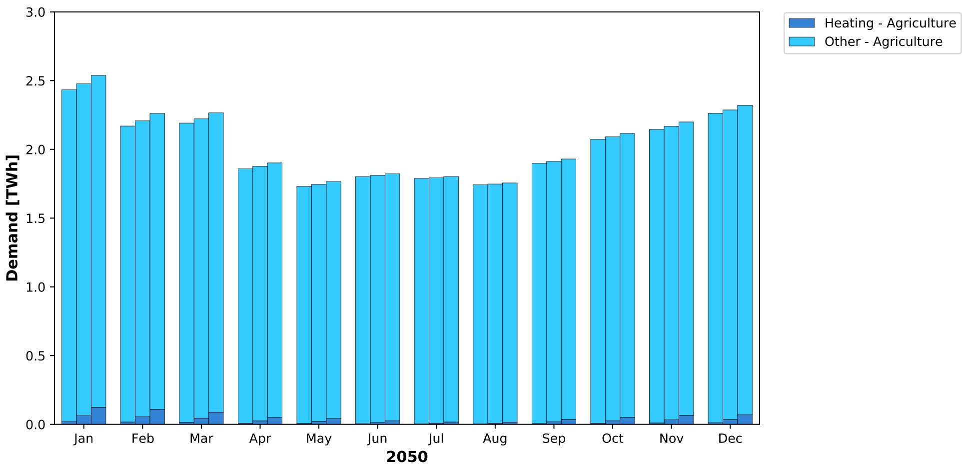

Figure 5.10: **Monthly electricity demand in the agriculture sector for all demand scenarios.**
From left to right: base case, low electrification, and high electrification

Industry - Other Sector

The other industry sector encompasses all industry sectors, apart from the ICT, paper, food, and uncategorised sectors. The biggest contributors to the final energy demand of this sector are: (a) the metal production and processing sector (e.g., steel and aluminium), and (b) the chemical production and processing sector (e.g., refineries and fertilisers). The heat generation pool for the industry sector comprises all-electric heat pumps, electric boilers, biomass-, gas-, oil-, and hydrogen-fired heaters, mechanial vapour recompression, and geothermal heat supply. The heat pumps and electric boilers are suitable technologies for electrifying these industry sectors. Geothermal heat can supply heat to the industrial district heating networks.

The heat generation pool of all industry subsectors can be adjusted in the ETM. The market shares of district heating networks, electric boilers, and hydrogen- and oil-fired heaters for every subsector are based on the scenario study by Berenschot and Kalavasta [134]. The heat generation pool of the scenario with the lowest and the scenario with the highest level of electrification of heating supply is duplicated to create the generation pool for the low and high electrification scenarios for this thesis. Table 5.8 gives an overview of the market share per heat generation technology in the other industry sector for all three scenarios.

Table 5.8: **Overview of heat generation technologies in the other industry sector per scenario. ETM parameters.**

	Base case	Low electrification	High electrification
District heating	22%	9%	9%
Electrified heating	3% all-electric heat pump	-	21% electric boiler
Non-electrified heating	24% hydrogen-fired heater 33% oil-fired heater 9% gas-fired heater 6% biomass-fired heater 3% mechanical vapour recompression	70% hydrogen-fired heater 21% oil-fired heater	70% hydrogen-fired heater

The load profiles resulting from loading the parameters from Table 5.8 in the Energy Transition Model are obtained. Figure 5.11 shows the load profiles for all three scenarios divided by electricity for heating, and electricity for other applications. The load profiles are presented as portions of the total load size for the individual applications.

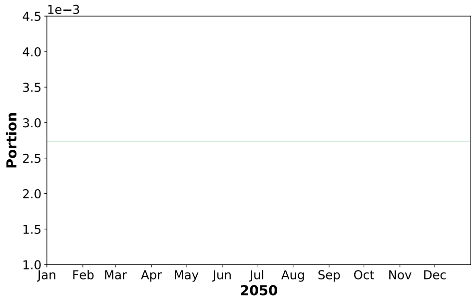

(a) Electricity demand for heating applications in the other industry sector for all demand scenarios. The load profile is shown as a portion per time step of the total load in a year, and is calculated by dividing the load per day by the total load in a year.

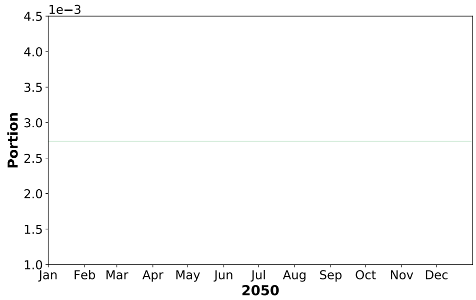

(b) Electricity demand for other applications in the other industry sector for all demand scenarios. The load profile is shown as a portion per time step of the total load in a year, and is calculated by dividing the load per day by the total load in a year.

Figure 5.11: **Electricity demand profiles in the other industry sector for all demand scenarios.**

It can be observed that the heating profiles and the other electricity profiles are similar in all three scenarios. The varying levels of electrification of the heating sector result in a varying total electricity demand in the industry sector. The monthly electricity demand per application and per scenario is shown in Figure 5.12.

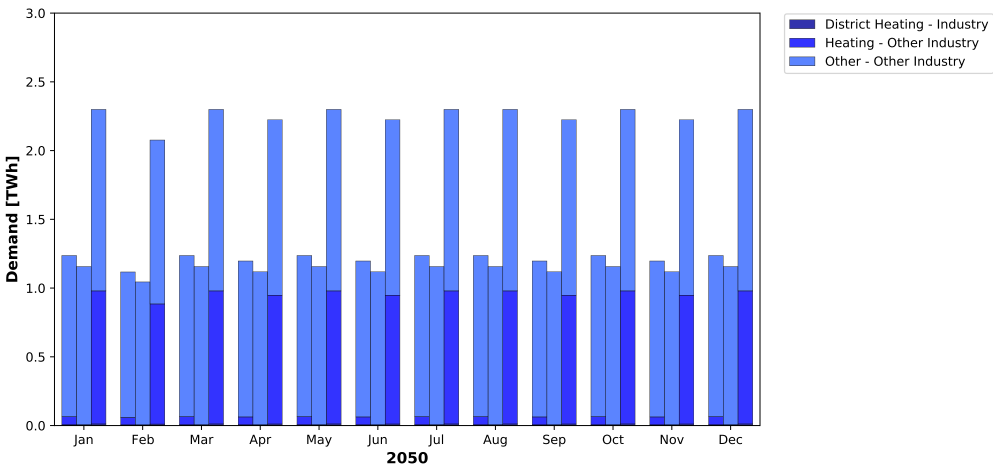

Figure 5.12: **Monthly electricity demand in the other industry sector for all demand scenarios.**
From left to right: base case, low electrification, and high electrification

The thermal grids used for district heating supply of all industry sectors and the corresponding heat generation pool for industrial district heating networks are combined in the ETM. The pool for the low electrification scenario is based on the geothermal capacity provided in the base case. The pool for the high electrification scenario is based on a report published by IEA. The report estimates that low-temperature heat demand accounts for 30% of the total industrial heat demand and can be supplied by district heating sources [53]. For this thesis, this translates to the capacities of the renewable technologies shown in Table 5.9. The capacities are calculated based on that 30% market share. Table 5.9 gives an overview of the renewable technologies in the generation pool for the three scenarios.

Table 5.9: **Overview of heat generation technologies for district heating in the industry sectors per scenario. ETM parameters.**

	Base case	Low electrification	High electrification
Electrified heating	-	-	-
Non-electrified heating	440 MW geothermal	440 MW geothermal	900 MW geothermal

Industry - PFO Sector

The PFO industry sector encompasses the paper, food, and uncategorised sectors. The heat generation pool for the PFO industry sector comprises electric boilers, biomass-, gas-, coal-, and hydrogen-fired heaters, and geothermal heat supply. The electric boilers are a suitable technology for electrifying these industry sectors. Geothermal heat can supply heat to the industrial district heating networks.

The heat generation pool of all industry subsectors can be adjusted in the ETM. The market shares of district heating networks, electric boilers, and hydrogen- and gas-fired heaters for every subsector are based on the scenario study by Berenschot and Kalavasta [134]. The heat generation pool of the scenario with the lowest and the scenario with the highest level of electrification of heating supply are duplicated to create the generation pool for the low and high electrification scenarios for this thesis.

The uncategorised industry comprises all industry sectors that are not explicitly defined in the ETM. As the specific technologies used in these sectors are unknown, the market share of the energy carriers themselves can be adjusted. Berenschot and Kalavasta state in their scenario study that the heating demand of industrial buildings account for 25% - 30%, other electrical and mechanical applications account for 35% - 45%, and thermal processing for 25% - 30% of the final energy demand in these sectors [134]. They predict a 10% market share for heat as energy carrier. For this thesis, this translates to the market share of heat as energy carrier to be maintained for both the low and high electrification scenario. The market share of electricity as energy carrier for the low electrification scenario is based on the value provided in the base case. The market share of electricity for the high electrification scenario is based on the low electrification scenario, and adjusted for high electrification of the heating demand of industrial buildings and a high electrification of the heating demand for thermal processing. Table 5.10 gives an overview of the market share per heat generation technology in the PFO industry sector for all three scenarios.

Table 5.10: **Overview of heat generation technologies in the PFO industry sector per scenario. ETM parameters.**

	Base case	Low electrification	High electrification
District heating	12%	12%	14%
Electrified heating	22% electric boiler	22% electric boiler	39% electric boiler
Non-electrified heating	58% gas-fired heater 6% biomass-fired heater 2% coal-fired heater	55% hydrogen-fired heater 11% gas-fired heater	47% hydrogen-fired heater
Energy carriers in the uncategorised industry	28% electricity 3% heat	28% electricity 10% heat	80% electricity 10% heat

The load profiles resulting from loading the parameters from Table 5.10 in the Energy Transition Model are obtained. Figure 5.13 shows the load profiles for all three scenarios divided by electricity for heating, and electricity for other applications. The load profiles are presented as portions of the total load size for the individual applications.

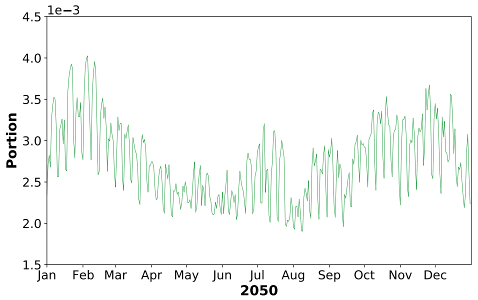

(a) Electricity demand for heating applications in the PFO industry sector for all demand scenarios. The load profile is shown as a portion per time step of the total load in a year, and is calculated by dividing the load per day by the total load in a year.

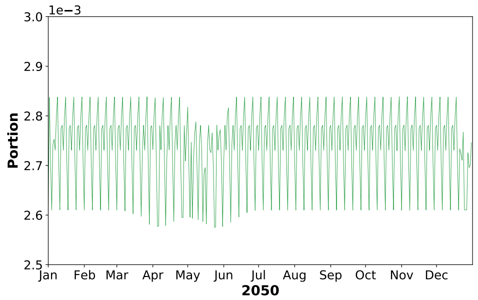

(b) Electricity demand for other applications in the PFO industry sector for all demand scenarios. The load profile is shown as a portion per time step of the total load in a year, and is calculated by dividing the load per day by the total load in a year.

Figure 5.13: **Electricity demand profiles in the PFO industry sector for all demand scenarios.**

It can be observed that the heating profiles and the other electricity profiles are similar in all three scenarios. The varying levels of electrification of the heating sector result in a varying total electricity demand in the PFO industry sector. The monthly electricity demand per application and per scenario is shown in Figure 5.14.

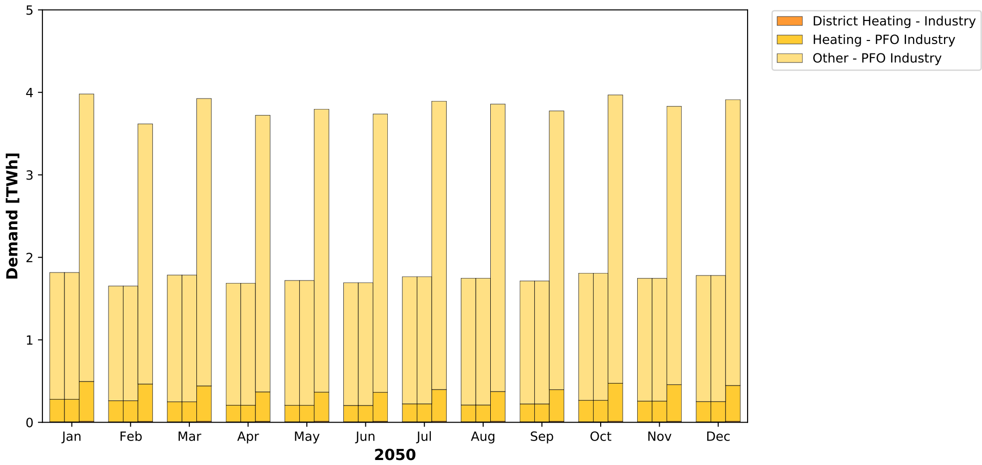

Figure 5.14: **Monthly electricity demand in the PFO industry sector for all demand scenarios.**
From left to right: base case, low electrification, and high electrification

Industry - ICT Sector

The sole energy carrier in the ICT industry sector is electricity. The ICT sector is not responsible for heating and cooling demand. The load profile is obtained from the Energy Transition Model. Figure 5.15 shows the load profiles for all three scenarios.

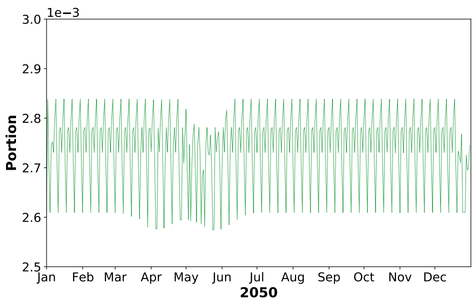

Figure 5.15: **Electricity demand profile in the ICT industry sector for all demand scenarios.**
Electricity demand for all applications in the ICT industry sector. The load profile is shown as a portion per time step of the total load in a year, and is calculated by dividing the load per day by the total load in a year.

It can be observed that the electricity load profile is equal in all three scenarios. As a result of no changes in growth factors for all scenarios, the total monthly electricity demand of the ICT sector is equal for all three scenarios. Figure 5.16 presents the total monthly electricity demand of the ICT sector.

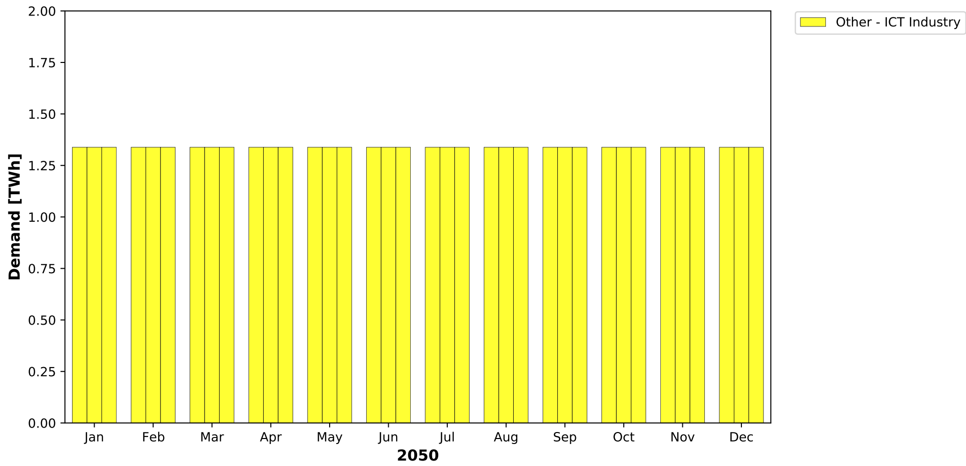

Figure 5.16: **Monthly electricity demand in the ICT industry sector for all demand scenarios.** From left to right: base case, low electrification, and high electrification

5.2.3. Generation Scenarios

Three different generation scenarios are studied: (a) base case, (b) low penetration of VRES, and (c) high penetration of VRES. The base case revolves around business as usual from 2030 onwards. The year 2030 is chosen as basis due to the long timeline of project development in the power sector and the intermediate objectives set by the climate agreements. Large project development in the power sector often takes years to a decade to progress from policies to drawing board to reality. Therefore, the envisaged generation pool for 2030 presented in recent studies by the Dutch government and the RES regions will be an reasonably accurate representation of the actual generation pool. The generation pool and the generation mapping for low and high penetration of VRES will be based on the power sector outlook presented in the scenario study by Berenschot and Kalavasta [134], the offshore outlook published by DNV GL [104], and the exploration study of offshore grid landing in 2030 [138]. Apart from the penetration of VRES, the biggest difference lies in the balancing and peaking supply of electricity. The scenario based on high penetration of VRES foresees a power sector based entirely on renewable sources, the low penetration scenario foresees a small portion of supply originating from non-renewable generators. This section presents the assets and the total capacity in the generation pool of the individual scenarios.

Renewable Generation

The renewable generation pool comprises offshore and onshore wind turbines, small scale and large scale solar PV systems, and hydrogen SCGT and CCGT generators. The assets in the generation pool and their capacity are mainly based on the scenario study published by Berenschot and Kalavasta [134]. The generation pool of the scenario with the lowest level of VRES penetration is adopted for creating the low penetration of VRES scenario for this thesis. The generation pool of the scenario with the highest level of VRES penetration is adopted for creating the high penetration of VRES scenario for this thesis. Table 5.11, shows an overview of the combined renewable generation capacity for the three different generation scenarios.

Table 5.11: **Overview of renewable power plants for all generation scenarios.**

	Base case	Low penetration of VRES	High penetration of VRES
Wind turbines [GW]	18.4	37.5	71.5
Onshore [GW]	7.0	10.0	20.0
Offshore [GW]	11.4	27.5	51.5
Solar PV [GW]	35.0	47.6	92.6
Large scale (> 15 kWp) [GW]	28.0	34.6	57.6
Small scale (< 15 kWp) [GW]	7.0	13.0	35.0
Hydrogen plant [GW]	0.0	29.0	35.0
Hydrogen CCGT [GW]	0.0	11.0	17.0
Hydrogen SCGT [GW]	0.0	18.0	18.0

The renewable generation capacity per generation scenario is known and the maximum available generation capacity per time step can be calculated using the solar and wind profiles presented in Section 5.3. The maximum available capacity per time step is incorporated in the pandapower model for executing the optimal power flow per scenario. The total monthly capacity per generation scenario and per variable renewable generation type can be observed in Figure 5.17

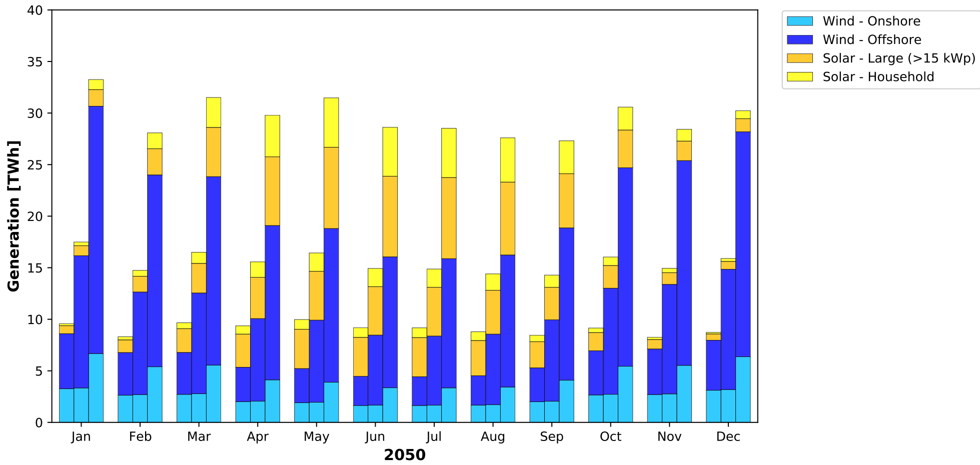

Figure 5.17: **Monthly renewable electricity generation capacity for all generation scenarios, based on the solar and wind profiles for 2050.**
From left to right: base case, low penetration of VRES, and high penetration of VRES.

Non-Renewable Generation

The non-renewable generation pool comprises natural gas SCGT, CCGT, and CHP generators. The assets in the generation pool and their capacity are mainly based on the scenario study published by Berenschot and Kalavasta [134]. The non-renewable generation pool of the scenario with the lowest level of VRES penetration is adopted for creating the low penetration of VRES scenario for this thesis. The non-renewable generation pool of the scenario with the highest level of VRES penetration is adopted for creating the high penetration of VRES scenario for this thesis. Table 5.12, shows an overview of the combined non-renewable generation capacity for the three different generation scenarios.

Table 5.12: **Overview of non-renewable power plants for all generation scenarios.**

	Base Case	Low penetration of VRES	High penetration of VRES
Gas plants [GW]	12.9	6.7	0.0
Gas CCGT [GW]	5.4	5.0	0.0
Gas SCGT [GW]	5.4	0.0	0.0
Gas CHP [GW]	2.1	1.7	0.0
Nuclear [GW]	0.5	0.0	0.0

The non-renewable generation capacity is assumed to be available at full capacity for all time steps of the year. Maintenance on the power plants is not considered in this study. The total non-renewable generation capacity per time step is combined with the maximum available renewable generation capacity per time step to create the input on the supply side of the pandapower model. The total monthly capacity per generation scenario and per generation type can be observed in Figure 5.18.

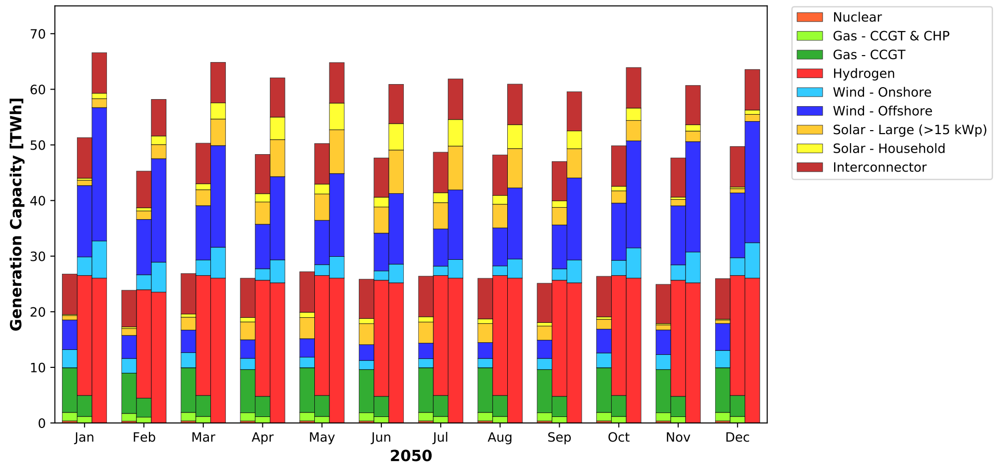

Figure 5.18: **Monthly electricity generation capacity for all generation scenarios, divided in nine generation types.** From left to right: base case, low penetration of VRES, and high penetration of VRES.

5.3. Modelling for Scenario Study

The objective of this thesis is to analyse the effects of power and heating sector integration on the Dutch high-voltage electricity grid. As the effects of sector integration will solely be analysed for the electricity grid, the electrified heating demand is isolated. The non-electrified heating demand will not be considered. Thus, the model in this thesis purely ensures security of energy supply for the electrified heating demand. The remaining energy demand for heating applications is assumed to be covered by other external energy sources, such as hydrogen and biogas. The high-voltage stations, lines, external grids, and transformers, as modelled in the aggregated pandapower network model presented in Section 4.1 and shown in Figure 4.6, are used as a bases for creating the model of the future electricity grid. This section describes the adjustments made to the generator and load capacities, their profiles, and the spatial mapping based on the scenario specifics.

5.3.1. pandapower Network Adjustments

TenneT TSO B.V. publishes all ongoing and upcoming grid expansion and maintenance projects on their web page. Additionally, they publish their quality and capacity document once every couple years, where grid expansion projects and expected future bottlenecks are discussed. The quality and capacity document from 2017 presents critical investments needed up until 2027 [64]. This document and the projects published on their web page are used as a guideline for the pandapower network adjustments. A summary of the aggregated pandapower network representing the Dutch high-voltage electricity grid in 2050 is given in Table 5.13 and is visualised in Figure 5.19. The following projects deriving from the documents are marked as interesting and form the basis of the adjustments made to create the future aggregated pandapower network model:

- **Eemshaven Oudeschip (EOS380) - Vierverlaten (VVL380)** - addition of a high-voltage station and transformer, and an upgrade of high-voltage lines:
  - VVL380 - new high-voltage station at Vierverlaten [139].
  - VVL380–VVL220 - new transfomer connecting the new 380 kV station with the existing 220 kV station. Installation of six transformers of 750 MVA each.
  - Existing 220 kV lines between Eemshaven (EEM220) and Vierverlaten (VVL220), and Eemshaven (EEM220) and Robbenplaat (RBB220) are upgraded to 380 kV lines consisting of 4 separate circuits.

- **Meeden (MEE380) - Zwolle (ZL380)** - addition of two high-voltage stations to reinforce the 380 kV grid in the North-East of the Netherlands.
- **Rilland (RLL380) - Tilburg (TBN380)** - addition of a high-voltage station and high-voltage lines:
  - TBN380 - new high-voltage station at Tilburg Noord.
  - RLL380–TBN380 - new high-voltage lines directly connecting Rilland to Tilburg for reinforcing the Southern part of the Dutch electricity grid.
- **Eemshaven (EEM380) - Eemshaven (EEM220)** – addition of a transformer, increasing the transformer capacity with 750 MVA to 2250 MVA [135].
- **Ens (ENS380) - Ens (ENS220)** - potential upgrade of the two 500 MVA transformers to two transformers with a capacity of 750 MVA each [64]. Uncertain if it is necessary to upgrade. First iteration of the scenario study this upgrade is excluded.

Table 5.13: **Overview of aggregated pandapower network used for the scenario study.**

Buses	
Number of 220 kV buses	10
Number of 380 kV buses (excluding external grid buses)	29
External grid buses	10
Lines	
Number of lines	102
Length of lines [km]	3,236
Transformers	
Number of transformers	4

(a) Aggregated Dutch high-voltage grid in 2050. Black dots represent high-voltage stations. Green and red lines represent 220 kV and 380 kV lines, respectively. Map data obtained from TenneT's ArcGIS assets [75]. Basemap obtained from Esri [76]

(b) Aggregated Dutch high-voltage grid in 2050 as modelled in pandapower. Black dots represent high-voltage stations. Green and red lines represent 220 kV and 380 kV lines, respectively. Prints use map data from Mapbox and OpenStreetMap and their data sources.

Figure 5.19: **Aggregated Dutch high-voltage grid in 2050.**

5.3.2. Generation and Load Mapping

The solar and wind profiles used for simulating the renewable generation capacity per time step in 2050, the methods used for obtaining these profiles, and the methods used for determining the generation and load mapping for the scenario study are presented. The final generation and load mapping per scenario can be seen in Appendix A.

Solar and Wind Profiles

The solar and wind profiles used for modelling the scenario studies are obtained from renewables.ninja and consist of corrected MERRA-2 profiles [88, 89]. The MERRA-2 data sets consists of hourly corrected capacity factors for 1980 - 2019 in the case of the wind data set, and hourly corrected capacity factors for 1985 - 2016 in the case of the solar data set. For this thesis, the obtained wind data set is divided in capacity factors for onshore and offshore wind turbines. The daily averaged capacity factor profiles for 2018 are shown in Figure 4.3 and Figure 4.4. However, due to the weather-dependency and seasonal variation of available solar and wind energy, the capacity factor profiles of 2018 are not necessarily an accurate representation of the average yearly output. In order to create more accurate solar and wind profiles, the data sets are analysed in Python to find the monthly average capacity factor. A 32-year averaged monthly capacity factor is obtained for the solar profile and a 40-year averaged monthly capacity factor is obtained for the wind profiles. The Python script returns the year with the smallest deviation from the mean for every month. The corresponding data points are merged in one data set per generation type. The capacity factor profiles for offshore wind, onshore wind, and solar PV are established. The capacity factor profiles for wind generation are shown on the left side in Figures 5.20 and 5.21. The capacity factor profile for solar PV generation is shown in Figure 5.22. The filled area in the figures present the bandwidth of the capacity factor at that specific time step over all years in the corrected MERRA-2 data set. The yearly average capacity factor for offshore wind turbines lies around 33%, for onshore wind turbines the yearly average capacity factor lies around 24%. Solar PV panels have a yearly average capacity factor of around 11%.

Studies show an expected increase in capacity factor for offshore and onshore wind turbines. The expected increase derives from the continuous development in efficiency improvements of energy conversion for low and high wind speeds, the increasing hub heights (less affected by turbulence from ground objects), and the increasing distance of offshore wind parks to land area. In a study commissioned by the IEA, expected offshore and onshore wind capacity factors per European country are presented for 2030 - 2049 [63]. The study predicts the yearly average capacity factor for offshore wind turbines to increase to 45% and for onshore wind turbines to increase to 32%. For this thesis, this translates to adjusting the capacity factor profiles obtained from the corrected MERRA-2 data set. The final capacity factor profiles for wind generation are shown on the right side in Figures 5.20 and 5.21. The final capacity factor profiles are used to calculate the maximum renewable generation capacity per time step per scenario. To give an idea of the general trend in one year, the hourly capacity factors are averaged per day to create the profiles shown in the figures.

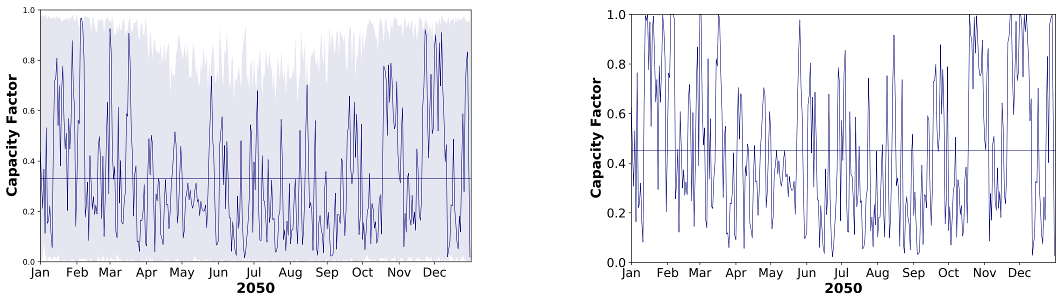

(a) Original MERRA-2 capacity factor profile for offshore wind turbines in 2050. The light blue represents the range in the capacity factor per time step in the MERRA-2 data set.

(b) Adjusted MERRA-2 capacity factor profile for offshore wind turbines in 2050.

Figure 5.20: **Averaged daily capacity factor profiles for offshore wind turbines in 2050.**

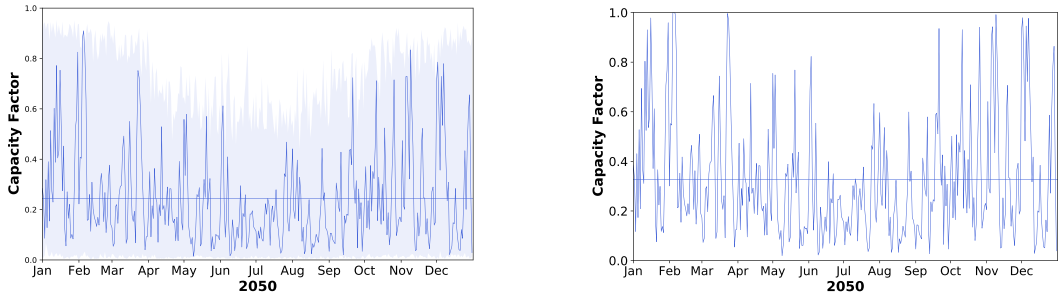

(a) Original MERRA-2 capacity factor profile for onshore wind turbines in 2050. The light blue represents the range in the capacity factor per time step in the MERRA-2 data set.

(b) Adjusted MERRA-2 capacity factor profile for onshore wind turbines in 2050.

Figure 5.21: **Averaged daily capacity factor profiles for onshore wind turbines in 2050.**

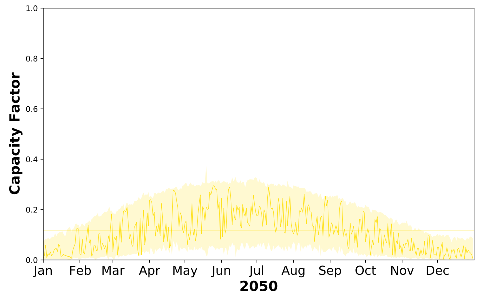

Figure 5.22: **Averaged daily capacity factor profile for solar PV panels in 2050.**

Generation Mapping

The mapping of the generators differs slightly per generation scenario, as each scenario comprises a different generator pool. Nevertheless, the base case generation mapping functions as the bases for the low and high VRES penetration scenarios. The non-renewable power plants from the 2018 validation study are copied to the non-renewable power plant pool of the base case. From this pool, a selection is made based on the preferred fuel and generator types for the 2050 base case scenario. The oldest power plants are shutdown until the defined non-renewable generation capacity is reached.

The mapping of the non-renewable generators included in the base case is used to establish the potential mapping locations of future non-renewable power plants. It is assumed that the current locations of large non-renewable power plants are maintained for future electricity generation. Therefore the non-renewable power plant pool of the low and high VRES penetration scenarios is mapped on the same nodes as the base case power plants. The division in capacity per node is based on the percentage of current non-renewable generation capacity per node, divided by the total non-renewable generation capacity.

The renewable power plants can be divided in four main categories: large offshore wind power, aggregated onshore wind power, aggregated large solar power (larger than 15 kWp per system), and aggregated small solar power (smaller than 15kWp per system). The division is based on the objectives set by a national program dividing the Netherlands in 30 RES regions. Every region is responsible for defining their renewable generation objectives for 2030 and 2050 and was asked to publish the first report stating the objectives for 2030 in July 2021. The objectives are split into onshore wind power and large solar power. The RES regions are not responsible for the small solar power systems and thus these are excluded in the objectives. The division of the Netherlands in the 30 RES regions can be seen in Figure 5.23.

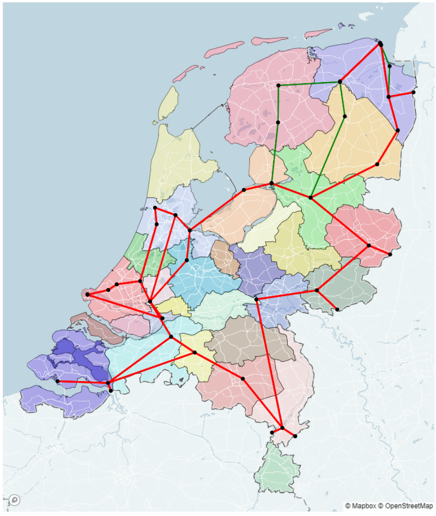

(a) Aggregated Dutch high-voltage grid in 2050, mapped on the RES regions. Black dots represent high-voltage stations. Green and red lines represent 220 kV and 380 kV lines, respectively. Prints use map data from Mapbox and OpenStreetMap and their data sources. RES regions geodata obtained from Esri [76] and CBS.

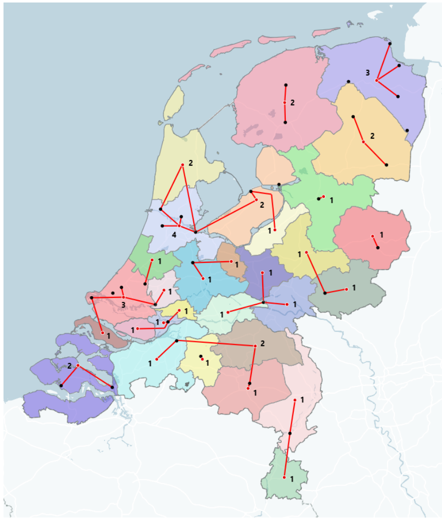

(b) Connecting nodes per RES region. Black dots represent high-voltage stations. Red dots represent the RES regions. Red lines represent the connecting nodes per RES region. The number denotes the connecting nodes per region. Prints use map data from Mapbox and OpenStreetMap and their data sources. RES regions geodata obtained from Esri [76] and CBS.

Figure 5.23: **Aggregated Dutch high-voltage grid in 2050, mapped on the RES regions.** Use zoom for more detail. Check Appendix A for the enlarged printed version.

The generation mapping assumptions per generation type are:

- **Large offshore wind power** - the location of future offshore wind power plants and their onshore connection hub are defined up to the year 2030 in an investment plan published by TenneT TSO B.V. [140]. The Ministry of Economic Affairs and Climate Policy envisaged offshore wind power capacity and locations past the year of 2030 [141]. Based on that document and the 72 GW offshore wind power potential, the Ministry instructed Witteveen+Bos to perform an effect analyses of onshore landing locations [138]. The most promising locations are used for this thesis to map the offshore wind power on.

- **Aggregated onshore wind power** - the locations of onshore wind power plants are based on the RES 1.0 documents published by the RES regions [142]. Per RES region, the node connecting the onshore wind power plants to the high-voltage grid is established by looking at the planned generation locations presented by the region. If the RES region encompasses multiple nodes and the generation locations are spread-out, the generation capacity is split over multiple nodes.

- **Aggregated large solar power** - the locations of large solar power plants are based on the RES 1.0 documents published by the RES regions. The mapping method is similar to the aggregated onshore wind power plants.

- **Aggregated small solar power** - as most small solar power plants are located on the rooftops of households, the locations of small solar power plants are assumed to be in urban areas. For every province, at least one node located close to a large urban area is selected. The division in capacity mapped onto the nodes is made based on number of households at every node. The number of households per province is obtained from CBS [143].

The aggregated onshore wind power and aggregated large scale solar power are mapped based on the information presented by the RES regions in their RES 1.0 documents. The document presents the 2030 installed capacity objectives per RES region. The capacities obtained from the RES 1.0 documents are converted to percentages of the total capacity mapped per node. The total generation capacity defined per scenario is multiplied by those percentages to define the generation capacity mapped per node in that specific scenario. Table 5.14 shows an overview of the percentages used for generation mapping. The ID's of the nodes and the corresponding location and province are specified in more detail in Appendix B.

Table 5.14: **Overview of renewable generation capacity per RES region for generation mapping**

RES regions	**Connecting Nodes**		**Onshore Wind**		**Large Scale Solar**	
			[GWh]	[% of total]	[GWh]	[% of total]
Achterhoek [105]	Doetichem	DTC380	546	1.95%	804	2.85%
Alblasserwaard [106]	Crayestein	CST380	156	0.56%	163	0.58%
Amersfoort [107]	Breukelen	BKK380	181	0.65%	381	1.35%
Arnhem-Nijmegen [108]	Dodewaard	DOD380	471	1.69%	1145	4.06%
Cleantech Regio [109]	Doetichem	DTC380	110	0.39%	960	3.41%
Drechtsteden [110]	Crayestein	CST380	11	0.04%	349	1.24%
Drenthe [111]	Veenoord	VB380	562	2.01%	1071	3.80%
	Zeijerveen	ZYV220	562	2.01%	1071	3.80%
Flevoland [112]	Lelystad	LLS380	2320	8.30%	585	2.08%
	Diemen	DIM380	2320	8.30%	585	2.08%
Foodvalley [113]	Dodewaard	DOD380	254	0.91%	710	2.52%
Friesland [114]	Louwsmeer	LSM220	1102	3.94%	396	1.41%
	Oudehaske	OHK220	1102	3.94%	396	1.41%
Goeree-Overflakkee [115]	Maasvlakte	MVL380	710	2.54%	142	0.50%
Groningen [18]	Meeden	MEE220	1200	4.29%	2230	7.91%
	Weiwerd	WEW220	1100	3.94%	100	0.35%
	Robbenplaat	RBB220	1710	6.12%	50	0.18%
Hart van Brabant [116]	Tilburg-Noord	TBN380	344	1.23%	656	2.33%
Hoeksche Waard [117]	Crayestein	CST380	348	1.25%	141	0.50%
Holland Rijnland [118]	Bleiswijk	BWK380	445	1.59%	695	2.47%
Metropoolregio Eindhoven [119]	Eindhoven	EHV380	1000	3.58%	1000	3.55%
Midden-Holland [120]	Capelle a/d IJssel	KIJ380	9	0.03%	435	1.54%
Noord- en Midden-Limburg [121]	Maasbracht	MBT380	458	1.64%	647	2.30%
Noord-Holland Noord [122]	Beverwijk	BVW380	1012	3.62%	838	2.97%
	Diemen	DIM380	1012	3.62%	838	2.97%
Noord-Holland Zuid [123]	Beverwijk	BVW380	50	0.18%	400	1.42%
	Diemen	DIM380	72	0.26%	521	1.85%
	Vijfhuizen	VHZ380	37	0.13%	660	2.34%
	Oostzaan	OZN380	333	1.19%	750	2.66%
Noord-Oost Brabant [124]	Geertruidenberg	GT380	290	1.04%	510	1.81%
	Eindhoven	EHV380	290	1.04%	510	1.81%
Noord-Veluwe [125]	Lelystad	LLS380	223	0.80%	307	1.09%
Rivierenland / Fruitdelta [126]	Dodewaard	DOD380	750	2.68%	584	2.07%
Rotterdam-Den Haag [127]	Maasvlakte	MVL380	574	2.05%	432	1.53%
	Wateringen	WTR380	574	2.05%	432	1.53%
	Capelle a/d IJssel	KIJ380	574	2.05%	432	1.53%
Twente [128]	Hengelo	HGL380	625	2.24%	875	3.11%
U16 [129]	Breukelen	BKK380	542	1.94%	1460	5.18%
West-Brabant [130]	Geertruidenberg	GT380	1200	4.29%	800	2.84%
West-Overijssel [131]	Zwolle	HSW220	651	2.33%	979	3.48%
Zeeland [132]	Borssele	BSL380	975	3.49%	485	1.72%
	Rilland	RLL380	975	3.49%	485	1.72%
Zuid-Limburg [133]	Maasbracht	MBT380	168	0.60%	1166	4.14%

Table 5.15 provides an example of the data available in a RES 1.0 document. The example is based on the document published by RES region Groningen. The province encompasses several nodes and the generation locations are spread-out. The installed capacity is divided per municipality and per generation type. The closest node per municipality is obtained from the ArcGIS map and is used to calculate the total mapped capacity per node for the RES region [75].

Table 5.15: **Example of RES 1.0 spatial analysis for generation capacity mapping in Groningen** [18].

Municipalities	**Closest Node**		**Onshore Wind** [GWh]	**Large Scale Solar** [GWh]
Eemsdelta	Weiwerd	WEW220	1100	100
Groningen	Meeden	MEE220	197	303
Het Hogeland	Robbenplaat	RBB220	1710	50
Midden-Groningen	Meeden	MEE220	531	419
Oldambt	Meeden	MEE220	103	57
Pekela	Meeden	MEE220	0	80
Stadskanaal	Meeden	MEE220	0	430
Veendam	Meeden	MEE220	120	30
Westerkwartier	Meeden	MEE220	149	191
Westerwolde	Meeden	MEE220	0	450
Small scattered	Meeden	MEE220	100	270

Load Mapping

The mapping of the loads is the same for all three load scenarios, the sole difference is the total load capacity. The mapping of the different energy end-use sectors is derived with two different methods. The first methods is similar to the method used for mapping the aggregated small solar power. It is assumed that the households, buildings, and transport sector load originates from the urban areas. Therefore, at least one node located close to a large urban area is selected per province. The division in capacity mapped onto the nodes is based on the number of households at every node divided by the total number of households. The second method for mapping the agriculture and industry sector loads is based on the mapping of those sectors in the 2018 validation study. The percentages of the total load per energy end-use sector per node are copied for mapping the agriculture and industry loads.

6
Results

This chapter presents the results of the individual simulation runs for the generation and load scenarios. Furthermore, the sensitivity and robustness of the representative model of the Dutch high-voltage grid is discussed. First, Section 6.1 explores the bottlenecks originating from varying levels of VRES penetration and heating sector electrification per scenario and calculates the corresponding grid investments. Then, Section 6.2 determines the sensitivity of the model to a variation of the input data and examines the robustness of the future high-voltage electricity grid.

6.1. Bottleneck Analysis

In this section the high-voltage grid components causing the bottlenecks are identified. The methodology used for identifying and resolving the bottlenecks is discussed and the results of the bottleneck analysis are presented.

6.1.1. Methodology for Bottleneck Analysis

By executing a DC optimal power flow calculation over a time series, the pandapower package searches for the paths of least resistance to balance load and generation on every bus. All generators in the network are modelled as controllable generators, including the renewable generators, and thus can be curtailed when there is an abundance of renewable generation capacity. Before executing the optimal power flow, one slack node needs to be defined. The slack node is responsible for providing for system losses and balancing the active and reactive power in a system by emitting or absorbing power to and from the system. Basically functioning as an electricity sink or source. The nodes capable of functioning both as a sink and source are the external grid nodes. It is common practice to define the slack node for power flow calculations as the node with highest balancing capacity. The designated slack node with the highest balancing capacity in the Dutch aggregated electricity system is the external grid node connecting Zandvliet, located in Belgium, to the Dutch grid in Rilland, located in Zeeland.

The two limiting factors in maintaining a balance on the electricity grid are the capacities of all the generators per time step and the line and transformer loading limits. If the total load exceeds the available generator capacity for a specific time step, the calculation will not converge due to an electricity shortage. Similarly, if the line and/or transformer loading limits are exceeded and no alternate power flow route is available, the calculation will not converge due to a grid congestion.

When an optimal power flow calculation does not converge for a specific time step, the pandapower package returns a message stating the time step for which the calculation could not convergence. All output data for that time step will be stored as zero values and the model continues the calculation for the following time step. The calculation output data and the bottlenecks causing non-convergence of the optimal power flow calculations are identified and resolved by following the steps mentioned below.

Step 1: Check for Electricity Shortages

The first step is to check if the non-convergence of the optimal power flow calculation occurs due to electricity shortages. An electricity shortage occurs when the total demand minus the available variable renewable generation capacity—calculated by multiplying the capacity factor profiles with the installed generation capacity—exceeds the total dispatchable generation capacity. The dispatchable generation capacity comprises the interconnection capacity, non-renewable generation capacity, and non-variable renewable generation capacity. All dispatchable generation capacity is assumed to fully available at all time steps, generator or line maintenance is not taken into account.

The python script running the pandapower simulation determines the total load and total available variable renewable generation capacity per time step. The script returns if and how often an electricity shortage occurs and creates a plot to visualise the available variable renewable generation capacity per time step. If no electricity shortages occur, the next step can be analysed. If they do occur, the generation pool must be extended and the simulation must be rerun.

Step 2: Check Lines and Transformers for Congestion and Increase Transmission Capacity
The second step for analysing the bottlenecks in the future power system is to check the high-voltage lines and transformers for congestion. The capacity of the high-voltage lines is limited by the voltage level and the maximum current. The capacity of the transformers is limited by the number of installed transformers and the capacity per installed transformer. Congestion occurs when the loading limits on one of the lines and/or transformers is exceeded. The capacity of the congested line and/or transformer can be adjusted in the pandapower model by increasing the line loading parameter and/or transformer loading parameter. The default setting for both parameters for all lines and transformers is 100%, referring to the max capacity determined by the line- and transformer-specific parameters.

The python script running the pandapower simulation determines the loading percentages of all lines and transformers for all individual time steps. If the optimal power flow does not converge, all output variables are saved as zeros. As a result, the origin of the non-convergence of the power flow calculation can not be found. Therefore, a workaround is found to identify the congested lines and/or transformers. First, after the simulation is completed, the python script saves the individual line and transformer loading percentages of that simulation run. Then, the scenario is rerun with the individual line and transformer loading percentages of the previous run as input. Before the script executes the simulation run, it looks for lines and/or transformers that are within 0.1% of their loading limit for at least one time step. The capacity of the lines and/or transformers that meet that requirement is increased with an additional 50% of the original value. Finally, the simulation run is executed by the python script and the individual line and transformer loading percentages are saved. This process is repeated until the optimal power flow calculations converges for all time steps or no congested components can be identified.

Step 3: Calculate the Necessary Grid Investments
The final step is to calculate the grid investments related to capacity expansion of the congested components. The capacity increase over all iterations in the second step of the bottleneck analysis is found by running a python script. The script returns the identifiers of the congested components and the corresponding total capacity increase. The unit investment costs for high-voltage lines and transformers is obtained from the Infrastructure Unit Investment Costs (UIC) report published by the Agency for the Cooperation of Energy Regulators (ACER) [15]. In the Infrastructure UIC report, a database was populated with historical data provided by 25 National Regulatory Authorities (NRA) in Europe and their respective TSOs. The assets populating the database were commissioned between 2005 - 2014 and are adjusted by ACER for inflation with 2014 as base year. Furthermore, ACER states that the derived UIC are based solely on total asset costs, excluding the financing costs and that the outliers were removed if they were above the upper or under the lower quartile values by a factor of 1.5 of the interquartile range. Table 6.1 gives an overview of the UIC in Euro [€/p.u.]. The UIC presented in the table are used for calculating the grid investment costs in this thesis.

Table 6.1: **Unit Investment Costs (UIC) of AC high-voltage overhead lines and transformers** [15]. Costs are adjusted for inflation up to 2014.

Component	Mean [€/p.u.]	Minimum - Maximum interquartile range [€/p.u.]	Median [€/p.u.]
380 kV, 2 circuit	1,060,919	579,771 - 1,401,585	1,023,703
380 kV, 1 circuit	598,231	302,664 - 766,802	597,841
220 kV, 2 circuit	407,521	354,696 - 461,664	437,263
220 kV, 1 circuit	288,289	157,926 - 298,247	218,739
Transformer	9,903	6,865 - 12,709	9,500

Figures 6.1 and 6.2 present the UIC of the high-voltage lines and transformers in interquartile box-plots. The unit is determined by the type of component: kilometre for lines and MVA for transformers. It can be observed that the high-voltage lines are divided by the voltage level and the number of circuits. A circuit is defined in the pandapower model by one high-voltage line. Most high-voltage lines run in parallel and therefore consist of two circuits. The parallel lines can be distinguished from the single or triple lines by their component ID. The ID of high-voltage lines contains the ID's of connected high-voltage stations plus a letter denoting the direction of connection. For instance, the parallel high-voltage lines connecting Borssele (BSL380) and Rilland (RLL380) are referred to as BSL380-RLL380-W and BSL380-RLL380-Z. As both lines have equal lengths and parameters, neither or both of the lines will be congested. If a congestion is resolved for parallel high-voltage lines by increasing their capacity with 50% of the original value, it results in the need for one extra circuit. However, if a congestion is resolved for a single high-voltage line by increasing its capacity with 50% of the original value, it results in a similar need for one extra circuit, on the grounds that the capacity of a high-voltage line is not a significant factor for the UIC. The UIC per MVA for a transformer is based solely on the installation of a transformer at an existing high-voltage station. The approach for analysing the bottlenecks is summarised in Figure 6.3.

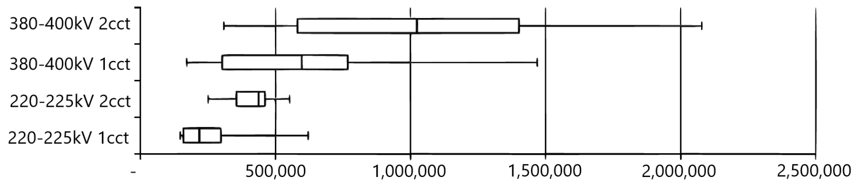

Figure 6.1: **Unit Investment Costs (UIC) of AC high-voltage overhead lines** [15].

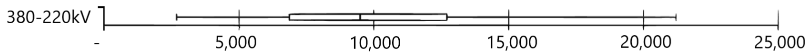

Figure 6.2: **Unit Investment Costs (UIC) of AC high-voltage transformers** [15].

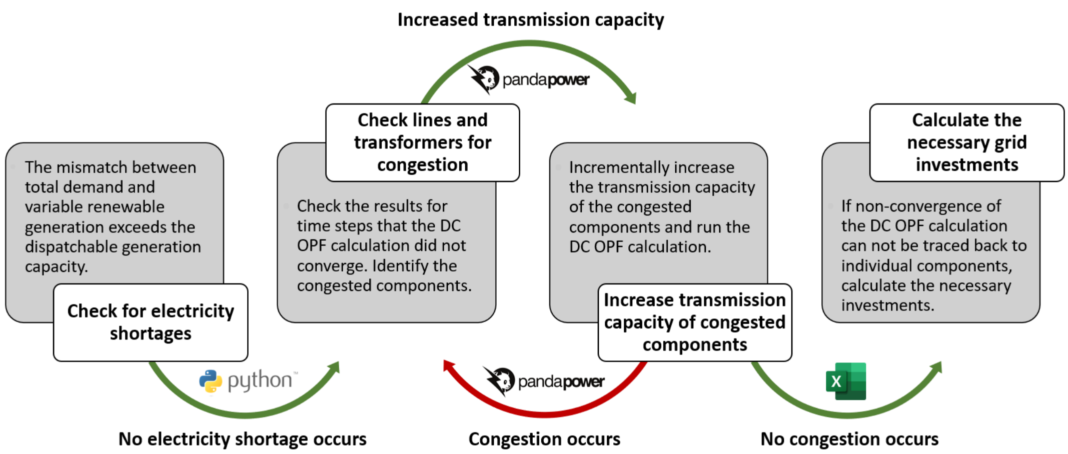

Figure 6.3: **Workflow of the bottleneck analysis.**

6.1.2. Base Case

The base case is based on the objectives set by the Dutch government for 2030. The electricity generation pool for the base case is entirely based on operational generation capacity in 2030. The electrified heat generation pool and corresponding electricity demand is based on the objectives set for 2030. The remaining electricity demand is based on predicted growth factors for 2050 as presented in the scenario study by Berenschot and Kalavasta [134]. This results in a substantial difference in available generation capacity in the base case compared to the four other scenarios.

Step 1: Check for Electricity Shortages

The first step is to check the model for electricity shortages. This is determined by subtracting the variable renewable generation capacity per time step—based on the capacity factor profiles and the installed capacity—from the electricity demand per time step. Figure 6.4 presents the demand minus VRES electricity profile. It can be observed that shortages of VRES can be balanced by the dispatchable generation capacity for all time steps and thus no electricity shortages occur. The abundance of VRES generation must either be curtailed or exported, but will not cause convergence problems for the optimal power flow calculation.

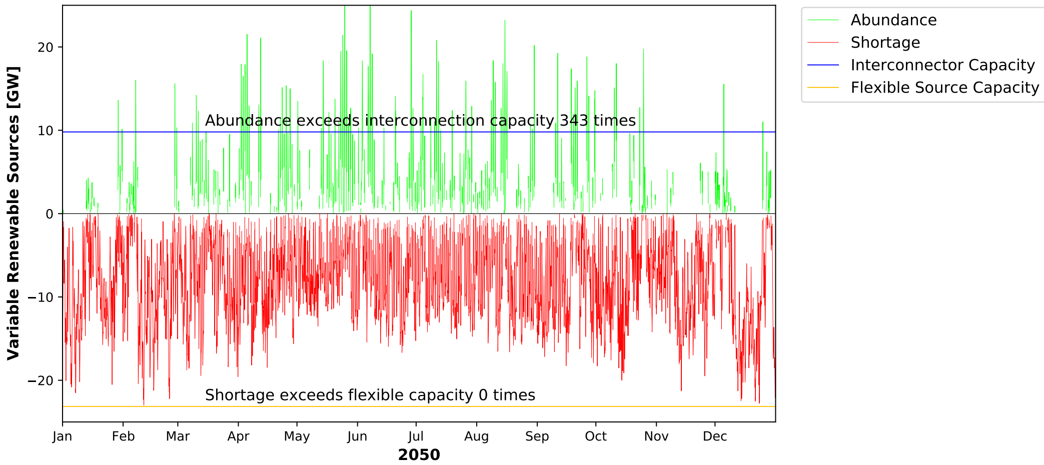

Figure 6.4: **Electricity shortage in the base case**

Step 2: Check for Line and Transformer Congestion and Increase Transmission Capacity

The second step is to identify the congested components causing the optimal power flow to not converge. The capacity of the congested components is incrementally increased until none of the convergence problems in the optimal power flow can be traced back to individual components. The number of iterations performed, the congested components and their relevant parameters for calculating the investment costs, and the number of time steps the optimal power flow could not converge per iteration are presented in Table 6.2. It can be observed that three congested components cause the optimal power flow calculation to not converge for almost 9% of the total number of time steps. The remaining twelve non-converged time steps can not be traced back to individual components.

Table 6.2: **Congested components per simulation run of the base case.**
The location and names corresponding to the component ID's can be found in Appendix B.

	1st run		**2nd run**	
	Component ID	**Length [km]**	**Component ID**	**Length [km]**
Congested lines	BSL380-RLL380-G	38.9	-	-
	BSL380-RLL380-Z	38.9	-	-
	OZN380-DIM380-G	15.2	-	-
	Component ID	**Capacity [MVA]**	**Component ID**	**Capacity [MVA]**
Congested transformers	-	-	-	-
Time steps OPF calculation did not convergence	754		12	

The maximum line loading percentages of all high-voltage lines are illustrated in Figure 6.5. The gradient represents line loading percentages of 0% - 100%. In the base case, the congestion occurs in Zeeland and near the city of Amsterdam. The former most likely originates from the grid landing of large renewable power plants in Zeeland. The latter most likely originates from the connection of the Northern part of the high-voltage grid to the node near Amsterdam, that is subsequently responsible for distributing the electricity to the nodes in the North- and South-Western parts of the grid. The connection with the North-Western nodes is a single high-voltage line connection with limited capacity. The corresponding grid investments are calculated after the analysis of the remaining scenarios.

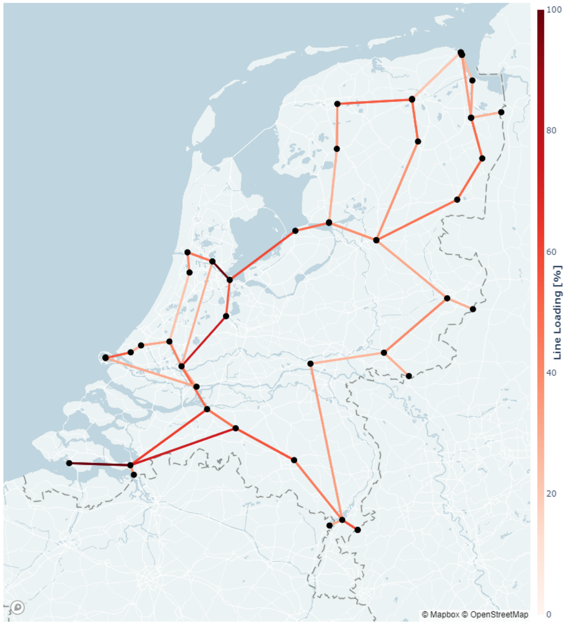

Figure 6.5: **Line congestion in the base case**.

6.1.3. Scenario 1 - Low Electrification and Low VRES Penetration

The first scenario is based on a low level of heating sector electrification and low VRES penetration. It assumes low future levels of electrification of the district heating sources and other non-industrial heat demand. Furthermore, it assumes the industrial heat demand and large parts of the electricity demand are supplied by generation technologies running on hydrogen. The remaining electricity generation pool consists of a low level of VRES penetration capacity, based on the lower limits stated in the power sector outlook studies, and a small dispatchable pool of SCGT and CCGT generators running on natural gas. The location of the dispatchable hydrogen and natural gas generators are based on the current locations of large power plants. The grid landing nodes of offshore wind energy are based on research performed by Witteveen+Bos. The mapping of the remaining VRES generation is similar to the four other scenarios.

Step 1: Check for Electricity Shortages

First, the scenario is checked for electricity shortages similarly to the base case. It is concluded that no electricity shortages occur in this scenario. A similar figure to Figure 6.4 is created and can be observed in Appendix D.

Step 2: Check for Line and Transformer Congestion and Increase Transmission Capacity

The congested components causing the optimal power flow to not converge are identified similarly to the base case. The number of iterations performed, the congested components and their relevant parameters for calculating the investment costs, and the number of time steps the optimal power flow could not converge per iteration are presented in Table 6.3. For resolving the bottlenecks in this scenario, three iterations were needed. It can be observed that the single line connecting two nodes near Amsterdam is congested for this scenario as well. Furthermore, a transformer connecting the 220 kV grid with the 380 kV grid in Flevoland is congested.

Table 6.3: **Congested components per simulation run of scenario 1.**
The location and names corresponding to the component ID's can be found in Appendix B.

	1st run		**2nd run**		**3rd run**	
	Component ID	**Length [km]**	**Component ID**	**Length [km]**	**Component ID**	**Length [km]**
Congested lines	OZN380-DIM380-G	15.2	OZN380-DIM380-G	15.2	-	-
	Component ID	**Capacity [MVA]**	**Component ID**	**Capacity [MVA]**	**Component ID**	**Capacity [MVA]**
Congested transformers	ENS380-ENS220	1000	-	-	-	-
Time steps OPF calculation did not convergence	22		5		4	

The maximum line loading percentages of all high-voltage lines are illustrated in Figure 6.6. The gradient represents line loading percentages of 0% - 100%. In the first scenario, the congestion occurs near the city of Amsterdam, most likely due to the connection of the Northern part of the high-voltage grid to the node near Amsterdam, that is subsequently responsible for distributing the electricity to the nodes in the North- and South-Western parts of the grid. The connection with the North-Western nodes is a single high-voltage line connection with limited capacity. It can be observed that the line loading percentages in the Northern part of the grid are substantially higher than in the base case, most likely as a result of an increase in the grid landing of offshore wind farms and an increase in the total capacity of large hydrogen and natural gas power plants in the Eemshaven area. The same can be observed for the lines connecting the Maasvlakte area to the electricity grid. The grid investments related to the capacity increase are calculated after the analysis of the remaining scenarios.

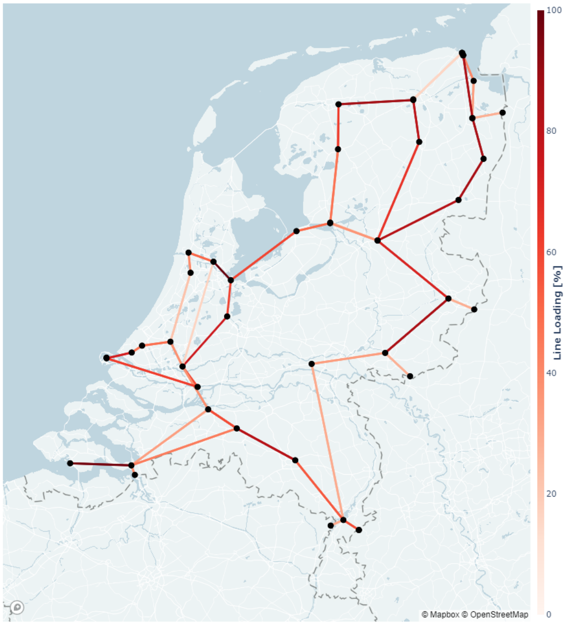

Figure 6.6: **Line congestion in scenario 1**.

6.1.4. Scenario 2 - Low Electrification and High VRES Penetration

The second scenario is based on a low level of heating sector electrification and high VRES penetration. It assumes low future levels of electrification of the district heating sources and other non-industrial heat demand. Furthermore, it assumes the industrial heat demand is largely supplied by generation technologies running on hydrogen. The dispatchable electricity generation pool is solely based on renewable electricity generators, in which hydrogen-fired SCGT and CCGT generators are used for balancing supply and demand, and as fast-responding generators for providing electricity during peak loads. The remaining electricity generation pool consists of a high level of VRES penetration, based on the upper limits stated in the power sector outlook studies. The locations of dispatchable generators, the grid landings of offshore wind parks, and the mapping of the remaining VRES generation is similar to the first scenario.

Step 1: Check for Electricity Shortages

First, the scenario is checked for electricity shortages similarly to the base case. It is concluded that no electricity shortages occur in this scenario. A similar figure to Figure 6.4 is created and can be observed in Appendix D.

Step 2: Check for Line and Transformer Congestion and Increase Transmission Capacity

The congested components causing the optimal power flow to not converge are identified similarly to the base case. The number of iterations performed, the congested components and their relevant parameters for calculating the investment costs, and the number of time steps the optimal power flow could not converge per iteration are presented in Table 6.4. For resolving the bottlenecks in this scenario, three iterations were needed. It can be observed that the single line connecting two nodes near Amsterdam and the parallel lines connecting Borssele to the grid are congested in this scenario, similar to the base case. Furthermore, two transformers connecting the 220 kV grid with the 380 kV grid in Flevoland and Groningen are congested.

Table 6.4: **Congested components per simulation run of scenario 2.**
The location and names corresponding to the component ID's can be found in Appendix B.

	1st run		2nd run		3rd run	
	Component ID	**Length [km]**	**Component ID**	**Length [km]**	**Component ID**	**Length [km]**
Congested lines	BSL380-RLL380-G	38.9	OZN380-DIM380-G	15.2	-	-
	BSL380-RLL380-Z	38.9	-	-	-	-
	OZN380-DIM380-G	15.2	-	-	-	-
	Component ID	**Capacity [MVA]**	**Component ID**	**Capacity [MVA]**	**Component ID**	**Capacity [MVA]**
Congested transformers	ENS380-ENS220	1000	ENS380-ENS220	1000	-	-
	MEE380-MEE220	750	-	-	-	-
Time steps OPF calculation did not convergence	40		4		1	

The maximum line loading percentages of all high-voltage lines are illustrated in Figure 6.7. The gradient represents line loading percentages of 0% - 100%. In the second scenario, the congestion occurs in Zeeland, near the city of Amsterdam, and in the Northern part of the grid. The line congestion in Zeeland and the transformer congestion in the Northern part of the grid most likely result from the substantial increase of grid landing of large offshore wind parks, compared to the first scenario and base case. The congestion near the city of Amsterdam is most likely caused by the same reason described for the first scenario. The grid investments related to the capacity increase are calculated after the analysis of the remaining scenarios.

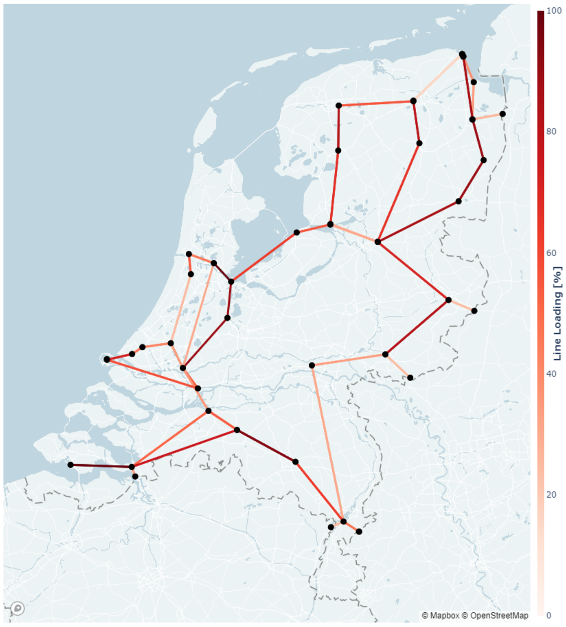

Figure 6.7: **Line congestion in scenario 2**.

6.1.5. Scenario 3 - High Electrification and Low VRES Penetration

The third scenario is based on a high level of heating sector electrification and low VRES penetration. It assumes a high electrification of technologies used for the supply of heat in the district heating sector, the non-industrial sector, and the industrial sector. The upper limits of electrified heating sources in the heating sector are implemented for this scenario and are based on the heating sector outlook. Furthermore, it assumes that large parts of the electricity demand are supplied by generation technologies running on hydrogen. The remaining electricity generation pool consists of a low level of VRES penetration capacity, based on the lower limits stated in the power sector outlook studies, and a small dispatchable pool of SCGT and CCGT generators running on natural gas. The locations of dispatchable generators, the grid landings of offshore wind parks, and the mapping of the remaining VRES generation is similar to the first scenario.

Step 1: Check for Electricity Shortages

First, the scenario is checked for electricity shortages similarly to the base case. It is concluded that no electricity shortages occur in this scenario. A similar figure to Figure 6.4 is created and can be observed in Appendix D.

Step 2: Check for Line and Transformer Congestion and Increase Transmission Capacity

The congested components causing the optimal power flow to not converge are identified similarly to the base case. The number of iterations performed, the congested components and their relevant parameters for calculating the investment costs, and the number of time steps the optimal power flow could not converge per iteration are presented in Table 6.5. For resolving the bottlenecks in this scenario, three iterations were needed. It can be observed that the single line connecting two nodes near Amsterdam and the parallel lines connecting Borssele to the grid are congested in this scenario, similar to the base case. Furthermore, a transformer connecting the 220 kV grid with the 380 kV grid in Flevoland is congested. No congested components could be found for the third iteration. However, the number of time steps with a non-converged optimal power flow increased compared to the second run.

Table 6.5: **Congested components per simulation run of scenario 3.**
The location and names corresponding to the component ID's can be found in Appendix B.

	1st run		2nd run		3rd run	
	Component ID	**Length [km]**	**Component ID**	**Length [km]**	**Component ID**	**Length [km]**
Congested lines	BSL380-RLL380-G	38.9	OZN380-DIM380-G	15.2	-	-
	BSL380-RLL380-Z	38.9	-	-	-	-
	OZN380-DIM380-G	15.2	-	-	-	-
	Component ID	**Capacity [MVA]**	**Component ID**	**Capacity [MVA]**	**Component ID**	**Capacity [MVA]**
Congested transformers	ENS380-ENS220	1000	ENS380-ENS220	1000	-	-
Time steps OPF calculation did not convergence	32		4		5	

The maximum line loading percentages of all high-voltage lines are illustrated in Figure 6.8. The gradient represents line loading percentages of 0% - 100%. In the third scenario, the congestion occurs in Zeeland, near the city of Amsterdam, and in the Northern part of the grid. The line congestion in Zeeland and the transformer congestion in the Northern part of the grid most likely result from the substantial increase of grid landing of large offshore wind parks, compared to the first scenario and base case. The congestion near the city of Amsterdam is most likely caused by the same reason described for the first scenario. Furthermore, an increase in the maximum line loading percentages of all lines can be observed compared to the first and second scenario, as a result of the increase in electricity demand due to the electrification of heating sources. The grid investments are calculated after the analysis of the remaining scenarios.

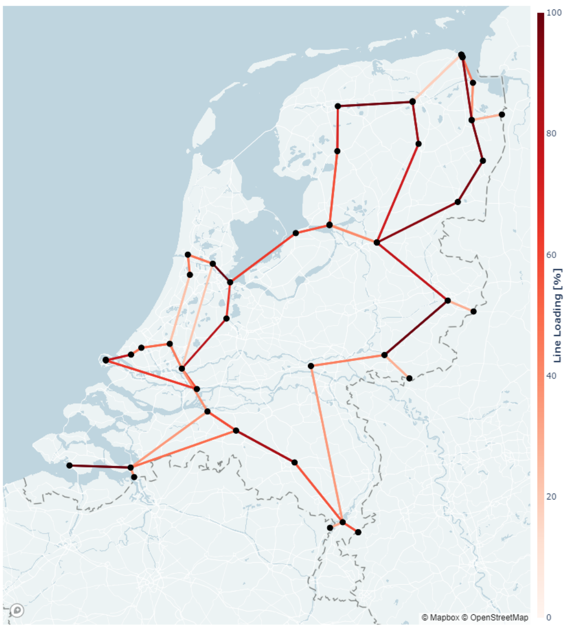

Figure 6.8: **Line congestion in scenario 3**.

6.1.6. Scenario 4 - High Electrification and High VRES Penetration

The fourth scenario is based on a high level of heating sector electrification and high VRES penetration. It assumes a high electrification of technologies used for the supply of heat, similar to the third scenario. Furthermore, it assumes that the dispatchable generation pool is solely based on renewable electricity generators, similar to the second scenario. The locations of dispatchable generators, the grid landings of offshore wind parks, and the mapping of the remaining VRES generation is similar to the first scenario.

Step 1: Check for Electricity Shortages

First, the scenario is checked for electricity shortages similarly to the base case. It is concluded that no electricity shortages occur in this scenario. A similar figure to Figure 6.4 is created and can be observed in Appendix D.

Step 2: Check for Line and Transformer Congestion and Increase Transmission Capacity

The congested components causing the optimal power flow to not converge are identified similarly to the base case. The number of iterations performed, the congested components and their relevant parameters for calculating the investment costs, and the number of time steps the optimal power flow could not converge per iteration are presented in Table 6.6. For resolving the bottlenecks in this scenario, four iterations were needed. It can be observed that the single line connecting two nodes near Amsterdam and the parallel lines connecting Borssele to the grid are congested in this scenario, similar to the base case. Furthermore, a line connecting Utrecht to the central grid, lines connecting the external grid nodes in Gelderland to each other, and lines connecting the Northern part of the grid to the central and 220 kV grid are congested. Additionally, two transformers connecting the 220 kV grid with the 380 kV grid in Flevoland and Groningen are congested. Furthermore, it can be observed that the number of congested components in the third iteration increased after resolving the congestion near Amsterdam. The congested components in the third iteration are partly responsible of distributing the electricity from the Northern part of the grid to the central grid.

Table 6.6: **Congested components per simulation run of scenario 3.**
The location and names corresponding to the component ID's can be found in Appendix B.

	1st run		2nd run		3rd run		4th run	
	Component ID	**Length [km]**	**Component ID**	**Length [km]**	**Component ID**	**Length [km]**	**Component ID**	**Length [km]**
Congested lines	BSL380-RLL380-G	38.9	OZN380-DIM380-G	15.2	MEE380-TAK380-W	23.5	-	-
	BSL380-RLL380-Z	38.9	-	-	MEE380-TAK380-Z	23.5	-	-
	DTC380-HGL380-W	58.7	-	-	TAK380-VB380-W	30.0	-	-
	DTC380-HGL380-Z	58.7	-	-	TAK380-VB380-Z	30.0	-	-
	KIJ380-BKK380-W	20.0	-	-	-	-	-	-
	OZN380-DIM380-G	15.2	-	-	-	-	-	-
	Component ID	**Capacity [MVA]**	**Component ID**	**Capacity [MVA]**	**Component ID**	**Capacity [MVA]**	**Component ID**	**Capacity [MVA]**
Congested transformers	ENS380-ENS220	1000	ENS380-ENS220	1000	ENS380-ENS220	1000	-	-
	MEE380-MEE220	750	-	-	-	-	-	-
Time steps OPF calculation did not convergence	140		23		1		1	

The maximum line loading percentages of all high-voltage lines are illustrated in Figure 6.9. The gradient represents line loading percentages of 0% - 100%. In the fourth scenario, an overall increase in maximum line loading percentages can be observed compared to the third scenario. Most likely as a result of additional grid landing nodes in Friesland, Groningen, Zeeland, and Zuid-Holland compared to the third scenario.

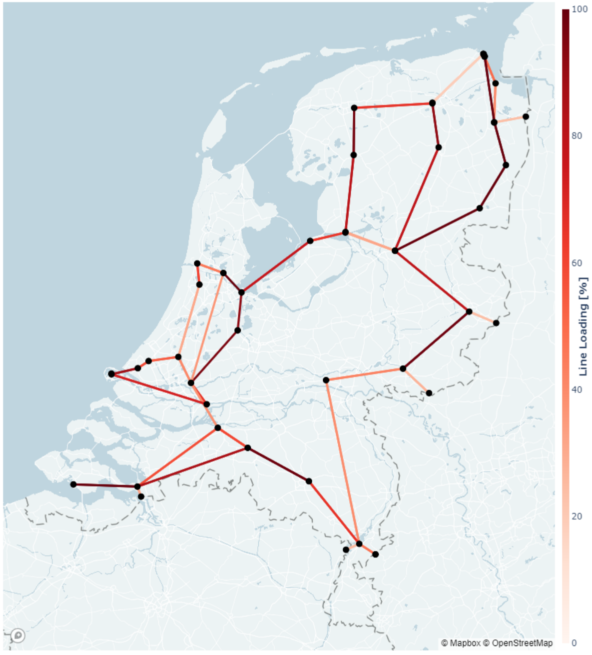

Figure 6.9: **Line congestion in scenario 4**.

Once all congestions are resolved and the capacity increase of all components per scenario are determined, the grid investment costs can be calculated. The investment costs per component are derived from a report published by the Agency for the Cooperation of Energy Regulators (ACER) in 2015 [15]. The UIC from the report are used in this thesis to calculate the total grid investment costs per scenario. The results are shown in Table 6.7.

Table 6.7: **Comparison of grid investment costs per scenario**.
Based on the UIC data shown in Table 6.1 and obtained from a report by ACER [15].

	Mean [Million €]	Minimum - Maximum interquartile range [Million €]
Base Case	32.4	16.4 - 41.5
Scenario 1	14.0	8.0 - 18.0
Scenario 2	46.0	25.8 - 59.0
Scenario 3	42.3	23.2 - 54.2
Scenario 4	130.0	69.3 - 166.7

6.2. Sensitivity Analysis

One of the goals of creating a representative model based on open data is to give other researchers the possibility to utilise this model for further analysis or other case studies. One of the downsides of creating a model based on open data is that it is highly likely that not all the necessary data will be available. On the input side of the model it leads to a need to make assumptions for unavailable parameters. On the output side, the assumptions cause uncertainty in the results. Therefore, a sensitivity analysis is performed. In this section the methodology used for performing the sensitivity analysis is discussed and the results are presented based on the robustness and sensitivity of the power system model.

6.2.1. Methodology for Sensitivity Analysis

The sensitivity analysis is described in Section 4.2 as a validation technique that analyses the effect of an adjustment in input or internal parameter on the model's behaviour or output. The accuracy of the sensitive parameters determine the accuracy of the model itself. The pandapower model discussed in this research is based on a combination of large assumptions, output of other models, and detailed parameters obtained from research. Most of the internal parameters of the pandapower model are derived from research. The input is predominantly based on large assumptions and output of other models. Therefore, the latter is most likely to be the root of inaccuracies in the model's behaviour and output. The large assumptions primarily relate to: (1) the spatial aggregation of generation and load, (2) the mapping of generation and load on the network, and (3) the availability of high-voltage assets and interconnection capacity throughout the year. The sensitivity of these assumptions on the model's behaviour and output are not analysed in this research due to time constraints. The effects of variations in input on the pandapower model is researched by performing an extreme case analysis.

Section 5.3 discusses the methodology for establishing the load input for the scenario study. The load size per time step and load profiles are obtained from the Energy Transition Model. The output of the model is based on historical temporal load profiles and weather data. The weather data is used to determine the heating demand in the households, buildings and agriculture sectors and establish the available generation capacity of the weather-dependent sources (e.g., solar and wind). The ETM provides an option for extreme weather analysis, in which historical data is used from specific years with anomalous weather conditions.

Two extreme weather cases are created by adjusting the weather conditions in the ETM and obtaining the corresponding load profiles and capacity factor profiles for offshore wind, onshore wind, and solar PV. The capacity factor profiles of offshore and onshore wind turbines are adjusted for predicted capacity factor improvements over the years. The full-load hours of the extreme weather cases are provided by the ETM relative to the default weather case. The ratio between the full-load hours and the predicted future full load-hours are the basis of calculating the adjusted extreme weather profile. The extreme weather cases are imported in the model and the effects of input adjustments on the model's output is analysed for the five individual scenarios. The pandapower model used for simulation of the extreme weather cases differs for each of the five scenarios and is based on the final non-congested version obtained from the bottleneck analysis. This section presents the load profiles obtained from the ETM and the capacity factor profiles.

Extreme Weather Case 1

The first extreme weather case is based on the year 1987. According to the ETM, the Netherlands faced an extreme cold period from 6 - 21 January 1987, which resulted in a significant heat demand increase. In the second week of January 1987 a Dunkelflaute event occurred, when little to no wind resulted in scarce renewable electricity generation. The capacity factor profiles are shown in Figures 6.10, 6.11 and 6.12. It can be observed that the yearly averaged capacity factors of the first extreme weather case are lower than the standard weather case.

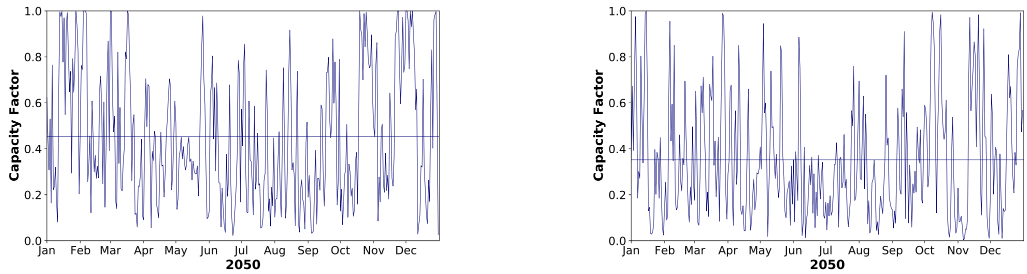

(a) Adjusted MERRA-2 capacity factor profile for offshore wind turbines in 2050.

(b) 1987 MERRA-2 capacity factor profile adjusted for offshore wind turbines in 2050.

Figure 6.10: **Averaged daily capacity factor profiles for offshore wind turbines for extreme weather case 1.**

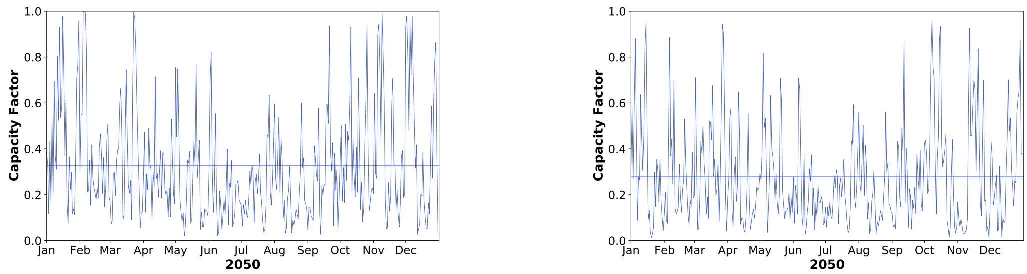

(a) Adjusted MERRA-2 capacity factor profile for onshore wind turbines in 2050.

(b) 1987 MERRA-2 capacity factor profile adjusted for onshore wind turbines in 2050.

Figure 6.11: **Averaged daily capacity factor profiles for onshore wind turbines in 2050 for extreme weather case 1.**

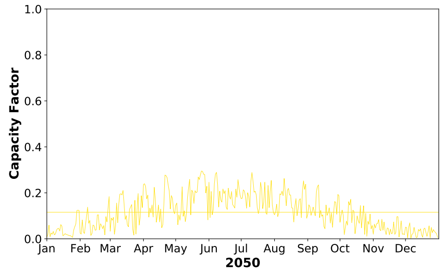

(a) MERRA-2 capacity factor profile for solar PV panels in 2050.

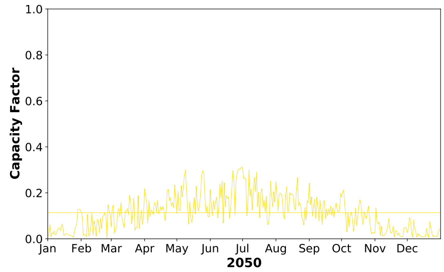

(b) 1987 MERRA-2 capacity factor profile adjusted for solar PV panels in 2050.

Figure 6.12: **Averaged daily capacity factor profile for solar PV panels in 2050 for extreme weather case 1.**

Extreme Weather Case 2

The second extreme weather case is based on the year 2004. According to the ETM, the Netherlands had several periods with scarce renewable electricity generation and in September periods with excess renewable electricity generation. The capacity factor profiles are shown in Figures 6.13, 6.14 and 6.15. It can be observed that the yearly averaged capacity factors for offshore and onshore wind turbines are lower in the second extreme weather case than the in standard weather case. The capacity factor for solar PV panels in the second extreme weather case is higher than in the standard weather case.

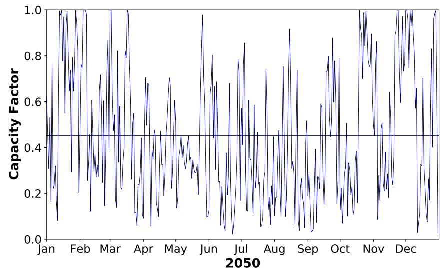

(a) Adjusted MERRA-2 capacity factor profile for offshore wind turbines in 2050.

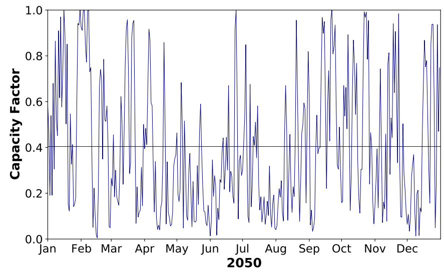

(b) 2004 MERRA-2 capacity factor profile adjusted for offshore wind turbines in 2050.

Figure 6.13: **Averaged daily capacity factor profiles for offshore wind turbines for extreme weather case 2.**

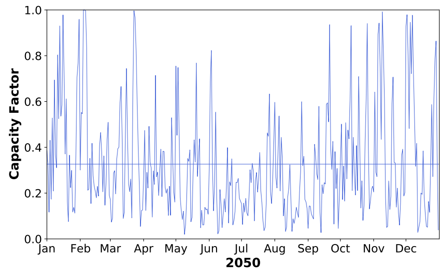

(a) Adjusted MERRA-2 capacity factor profile for onshore wind turbines in 2050.

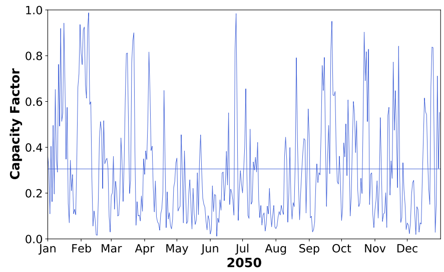

(b) 2004 MERRA-2 capacity factor profile adjusted for onshore wind turbines in 2050.

Figure 6.14: **Averaged daily capacity factor profiles for onshore wind turbines in 2050 for extreme weather case 2.**

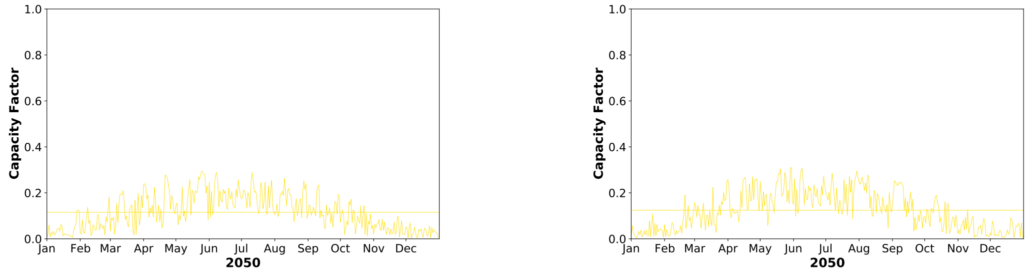

(a) MERRA-2 capacity factor profile for solar PV panels in 2050.

(b) 2004 MERRA-2 capacity factor profile adjusted for solar PV panels in 2050.

Figure 6.15: **Averaged daily capacity factor profile for solar PV panels in 2050 for extreme weather case 2.**

Load Profiles for Extreme Weather Cases

The ETM uses weather data to determine the heating demand in the households, buildings and agriculture sectors. The load size and profiles of the remaining sectors are not adjusted for the extreme weather cases. Chapter 5 provides a detailed explanation of the load scenarios modelled in the ETM and the load profiles obtained per scenario. The effects of extreme weather cases per energy end-use sector are illustrated by showing the electricity load profiles for heating application for the base case. The load profiles for the low and high electrification scenarios are shown in Appendix C. Figures 6.16, 6.17 and 6.18 represent the load profiles for heating applications of the households, buildings, and agriculture sector, respectively.

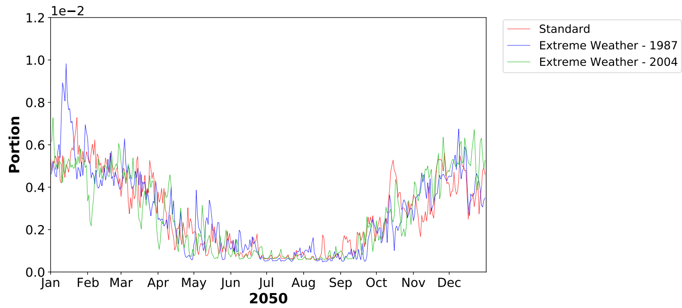

Figure 6.16: **Base case load profiles for heating applications in the households sector in 2050 for all weather cases**. The load profiles are shown as a portion per time step of the total load in a year, and is calculated by dividing the load per day by the total load in a year.

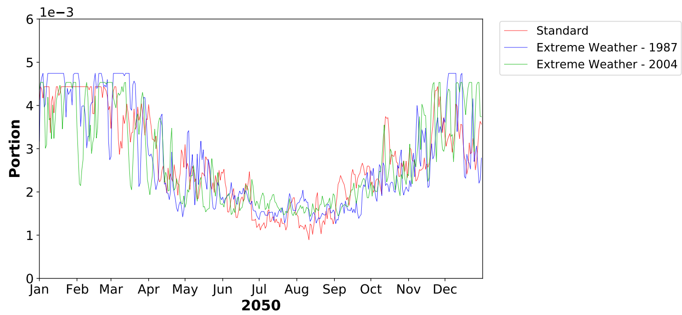

Figure 6.17: **Base case load profiles for heating applications in the buildings sector in 2050 for all weather cases**. The load profiles are shown as a portion per time step of the total load in a year, and is calculated by dividing the load per day by the total load in a year.

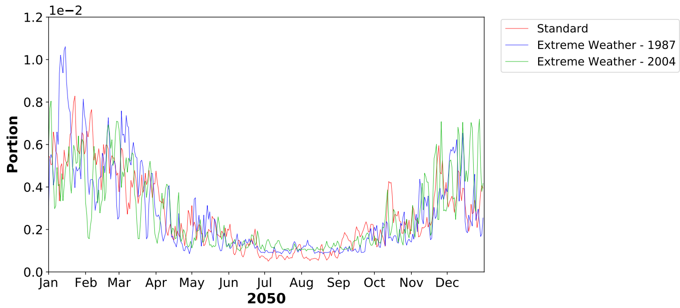

Figure 6.18: **Base case load profiles for heating applications in the agriculture sector in 2050 for all weather cases**. The load profiles are shown as a portion per time step of the total load in a year, and is calculated by dividing the load per day by the total load in a year.

6.2.2. Results of the Sensitivity Analysis

The optimal power flow is calculated for all five scenarios with both extreme weather cases. The robustness of the high-voltage electricity grid is reviewed based on the number of congested time steps. An increase in the number of time steps that a congestion occurs is attributed to the change in load and generation profiles. The sensitivity of the model to an adjustment in the input is analysed by reviewing the line loading percentages. The percentage change of the average line loading percentage per time step is calculated for both extreme weather cases. Similarly, the percentage change of the total load per time step is calculated for both extreme weather cases. The reference line loading percentages and load are defines as the data for the standard weather case.

Robustness

The robustness of the model and envisaged future electricity grid is explored by determining their effects on extreme weather cases. The models with increased transmission capacity created as a result of the bottleneck analysis are used. If no electricity shortages and no congestion occurs, the model and envisaged electricity grid is determined to be sufficiently robust for anomalous and extreme weather cases. The extreme weather cases used for the sensitivity analysis are within reason and are based on measured data. As a result of the unavailability of accurate historical data for other extreme weather years, this must suffice.

Table 6.8 presents the number of time steps per weather case for which the optimal power flow calculation did not converge. The origin of the increase or decrease in time steps is determined and a decision is made on the robustness of the model. The generation pool in the base case is not sufficient for balancing periods with scarce renewable electricity generation, as a result the increase of non-converged time steps all originate from a period with electricity shortage. As the base case is based on the 2030 electricity generation pool and the 2050 expected electricity demand, this problem is foreseen. The robustness of the base case is of least importance for the proposed scenario study in this work. The increase in non-converged time steps for the four other scenarios in both extreme weather cases can not be traced back to either electricity shortages or individual components. As the increase in number of time steps remains relatively small, this is assumed to be negligible. Therefore, the scenario models and corresponding envisaged electricity grids are determined sufficiently robust for this work.

Table 6.8: **Total time step for which the OPF calculation does not converge per weather scenario.**

	Standard weather	Extreme weather case 1	Extreme weather case 2
Base case	12	31	24
Scenario 1	4	8	7
Scenario 2	1	1	0
Scenario 3	5	10	8
Scenario 4	1	2	1

Sensitivity

The sensitivity of the model to a variation in input is analysed by determining the percentage change of the average line loading percentage per time step and the percentage change of the average load per time step. Two separate analysis are performed, one for each extreme weather case. The percentage changes are visualised in boxplots. The boxplot visualises the data by showing: (a) the median—orange line in the middle of the boxes—, (b) the InterQuartile Range (IQR)—the boundaries of the boxes—, (c) the IQR x 1.5—the so-called whiskers or lines to the left and right of the boxes—, and (d) the outliers—plotted as separate dots.

In both figures the data is grouped per scenario. The upper boxplot per scenario represents the percentage change of total load per time step for the extreme weather case versus the standard weather case. The lower boxplot per scenario represents the percentage change of the average line loading percentage per time step.

Figure 6.19 shows the sensitivity of the model to the first extreme weather case and Figure 6.20 shows the sensitivity of the model to the second extreme weather case. A similar effect can be observed in both the figures, a change in input severely affects the model's output. As the optimal power flow calculated the past of least resistance, it can be expected that a small change in nodal load can shift the power flow. Therefore, the sensitivity of the model to a varying input is not necessarily a problem. However, it shows that the assumptions made for the aggregation of loads and the mapping on the nodes can affect the accuracy of the model's output.

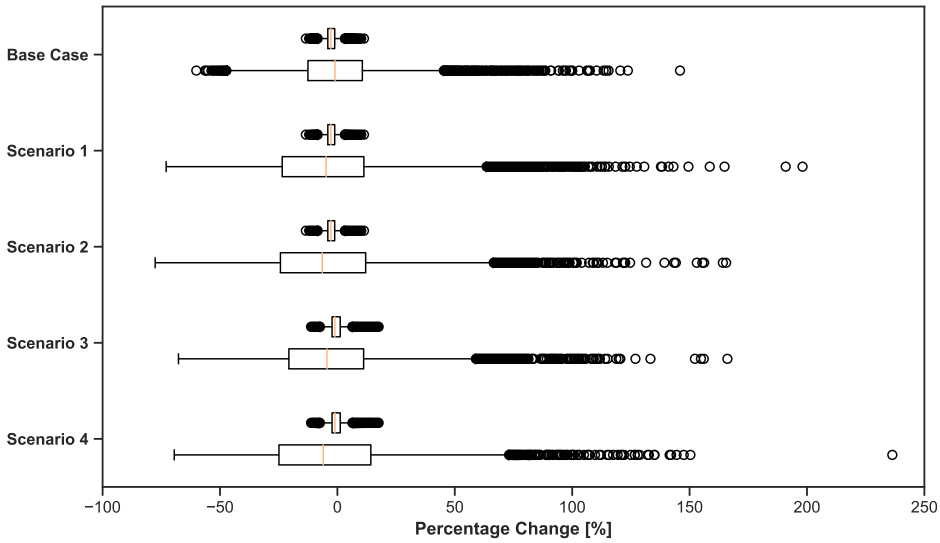

Figure 6.19: **Sensitivity of the line loading percentages to varying input parameters, based on extreme weather case 1**. The upper boxplot per scenario represents the percentage change of total load per time step for the extreme weather case versus the standard weather case. The lower boxplot per scenario represents the percentage change of the average line loading percentage per time step.

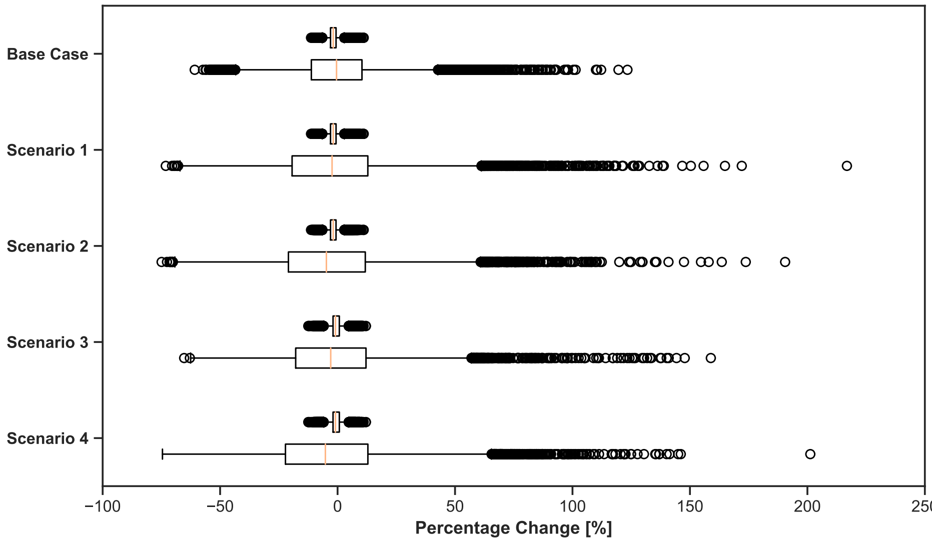

Figure 6.20: **Sensitivity of the line loading percentages to varying input parameters, based on extreme weather case 2**. The upper boxplot per scenario represents the percentage change of total load per time step for the extreme weather case versus the standard weather case. The lower boxplot per scenario represents the percentage change of the average line loading percentage per time step.

7 Concluding Remarks

This chapter concludes the thesis by answering the research questions posed in Section 1.4. Furthermore, the assumptions underlying the aggregated model of the Dutch high-voltage grid are discussed. The potential effects of the assumptions on the accuracy of the model are explored. Finally, this chapter will propose future lines of work.

7.1. Conclusion

The first research question relates to the methodology of energy system modelling and is extensively discussed in Chapter 4. The second research question relates to the future scenarios for heating sector integration and is comprehensively covered in Chapter 5. The third and final research question relates to the grid investments for future scenarios and is based on the results presented in Chapter 6. This section presents the approach for answering the individual research questions and provides detailed answers for each of the research questions.

7.1.1. Research Question 1 – How do we create a representative model of the Dutch high-voltage electricity grid for assessing energy system integration?

The methodology for modelling, the underlying assumptions, the validation methods, and the necessary input data are extensively discussed in Chapter 4. The research question essentially comprises two components: (1) how do we create a model of the Dutch high-voltage electricity grid that can assess energy system integration and (2) how do determine the accuracy of the model and what is sufficiently accurate for assessing energy system integration. The former concerns the assets in the electricity grid, their parameters, and the ability to include other energy systems. The latter concerns the accuracy of the input data and the degree of confidence that can be established based on the available data. The research question is answered by answering the two components of the question separately.

How do we create a model of an electricity grid at a national scale?

One of the goals of this thesis was to create a representative model of the Dutch high-voltage electricity grid based on open data. The idea behind using open data is to give other researchers the possibility to utilise this model for further analysis or other case studies. However, the downside of creating a model based on open data is that not all the necessary data will be available. The unavailability of data led to several assumptions that will be discussed in Section 7.2.

The first step for creating a model of an electricity grid is to decide on the software package suitable for the anticipated application. The software package determines the type of input parameters for the model and the model's ability for co-modelling and energy system integration. We chose the pandapower package, as it is an open source programming tool and their claim is that all element behaviour is tested against commercial energy system modelling tools. Since pandapower is a power system modelling tool, it must be noted that any energy system integration studies using pandapower can only be performed from the perspective of the electricity grid.

The second step is to gather all the necessary element data. If element data is unavailable, the pandapower package provides standard element types with preset parameters. All high-voltage assets in the

Dutch electricity system are maintained by TenneT TSO B.V. in an open source ArcGIS map. The asset parameters can be largely obtained from documents published by TenneT TSO B.V. Once all the data is gathered, it can be converted to create a pandapower network model.

The third step is to decide on the level of detail in the pandapower network model. The ArcGIS map provides basic data on all high-voltage assets of 110 kV and up. Open data on technical parameters are hardly available for the 110 kV and 150 kV assets, but are mostly available for the 220 kV and 380 kV assets. Furthermore, the 220 kV and 380 kV assets are responsible for most of the nationwide transmission of electricity. Therefore, the electricity grid model is aggregated to only include 220 kV assets and up.

The fourth step is to update the model for planned grid expansions. In investment planning documents published by TenneT TSO B.V., they present a roadmap for the grid investments in the pipeline up until 2030.

How do we validate a model of the Dutch electricity grid?
Once the model is created, the accuracy of the model must be determined. In Section 4.2 several validation methods for simulation models are proposed. The validation and verification of a simulation model is often divided in three steps: (1) conceptual model validation, (2) computerised model verification, and (3) operational validation. The preferred validation method for a simulation model based on a non-observable system—a system where no data is available on the system operations—is face validation. This entails that an expert on the system evaluates the model by examining the modelling principles. If face validation is not an option and other models on the system are not available, it is unlikely that a high degree of confidence in the model's behaviour can be achieved.

The methods used to obtain a sufficient degree of confidence in the model's behaviour are traces, structured walk-throughs, historical data validation and sensitivity analysis. The underlying assumptions of the model are validated against assumptions made by TenneT TSO B.V. to create a similar model for sector integration analysis [23]. Traces entail the tracking of elements in the conceptual model and the pandapower computerised model to determine the modelling accuracy. Structured walk-throughs entail the correct use of the programming language for creating the model. For historical data validation the model is simulated for 2018 based on historical available data (e.g., capacity factor profiles for solar and wind generation, load). The output of the model is graphically compared to market analysis documents published by the TSO. Finally, a sensitivity analysis is performed to check for the robustness and sensitivity of the model to varying input data. The basic validation methods result in an sufficiently accurate model for future scenario analysis. Therefore, the model is referred to as a 'representative model of the Dutch high-voltage electricity grid'.

7.1.2. Research Question 2 – How do we create scenarios for power and heating sector integration?

The second research question relates to the future scenarios for heating sector integration and is comprehensively covered in Chapter 5. The research question comprises two components: (1) what are the outlooks for heat sector integration and (2) which end-use sectors can be considered for heat sector integration. The former concerns the general outlook of the heating sector and the technologies suitable for heat sector integration. The latter concerns the end-use sectors that heat sector integration can be applied to. The research question is answered by answering the two components of the question separately.

What are the national outlooks for the heating sector?
Four fundamental proposals that contribute to the efficiency, decarbonisation, and affordability of the future heating sector are mentioned in Chapter 5. The first proposal is the expansion of the thermal grids, to accommodate a market share of the total low-temperature heat demand in the range of 60% - 75%. The second proposal is excess heat recovery from the industrial sector, which can account for at least 21% of the district heating demand. The third proposal is integration of short-term thermal storage units in the thermal grids. The fourth and final proposal is further increase of individual heat pumps, to accommodate a market share of the total low-temperature heat demand of up to 24%.

An enormous potential for geothermal heat sources is foreseen by the Netherlands Environmental Assessment Agency. They estimate the geothermal heat potential to be in the range of 85 - 1000 PJ per year depending on the investment policies proposed by the Dutch government. This potential can be used to cover between 40% - 60% of the heating demand in the agricultural sector, around 30% of the heating demand in the industrial sector, and around 25% of the heating demand in the households and buildings sector. Large-scale heat pumps are predicted to cover around 25% of the district heating demand.

This thesis focuses on power and heating sector integration. The pandapower model is used to analyse the effects of electrification in the heating sector and therefore solely the electrified heating sources in the heating sector outlook are of interest for this thesis. Two levels of power and heating sector integration are analysed based on the lower and upper limits mentioned above.

Which energy sectors need to be considered for future heating sector electrification?
The scenarios created for this thesis relate to the power and heating sector integration by electrifying the heating supply. Due to technical limitations, only low-temperature heat supply can be electrified. The households, buildings, agriculture, and industry sector have a demand for low-temperature heat. Low-temperature heat demand constitute a great portion of the households, buildings, and agriculture heat demand. In the industry sector it constitutes around 30% of the total heat demand. As full electrification of the low-temperature heat demand is not viable, the levels of electrification are based on the scenarios proposed by Berenschot and Kalavasta.

7.1.3. Research Question 3 – How does heating sector electrification impact the investments in the electricity grid?

The third research question relates to the electricity grid investments for future scenarios and is based on the results presented in Chapter 6. The research question consists of two components: (1) the identification of the bottlenecks in the model and (2) calculating the investments necessary to overcome these bottlenecks. The former concerns the methodology for bottleneck analysis presented in Section 6.1. The latter concerns the grid investments needed to resolve the bottlenecks based on the Unit Investment Costs (UIC) obtained from a study from the Agency on the Cooperation of Energy Regulators. The research question is answered by answering the two components of the question separately.

What are the bottlenecks of heating sector electrification for the Dutch high-voltage electricity grid?
The approach for identifying the bottlenecks is comprehensively discussed in Chapter 4. The results of the bottleneck analysis are presented in Chapter 6. The effects of heating sector electrification are analysed by simulating four scenarios, ranging from low to high for the level of heating sector electrification and VRES penetration. As a result of the decarbonisation of the power sector and the envisaged offshore renewable generation capacities, large portions of the electricity demand is supplied by offshore wind. The identified bottlenecks mainly relate to the grid landing locations of offshore wind farms and the high-voltage lines distributing the electricity from these locations to the central part of the grid. In the scenarios with a high level of VRES penetration, more bottlenecks are identified than in the scenarios with a low level of VRES penetration. The number of bottlenecks further increase for the scenarios with a high level of heating sector electrification. The high level of electrification leads to an increase in demand that most likely will be supplied by variable renewable energy sources.

Will grid investments be needed to overcome these bottlenecks in 2050?
All scenarios needed grid investments to overcome the bottlenecks. The investments are discussed in Chapter 6 and are based on a report on UIC in the European electricity grid. The calculated grid investments costs per scenario are shown in Figure 7.1.

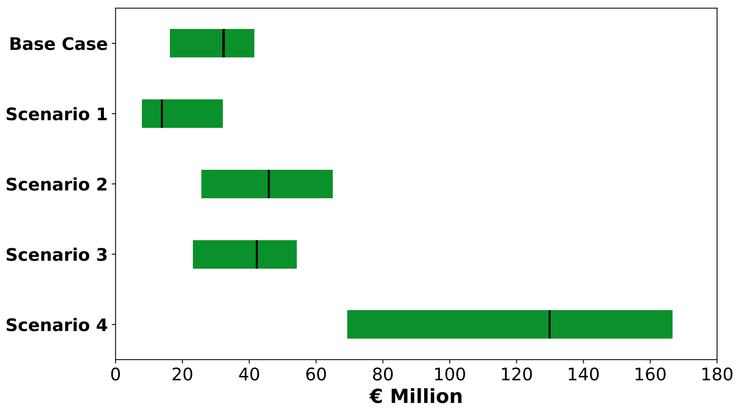

Figure 7.1: **Comparison of grid investment costs per scenario.**

7.2. Discussion

The representative model of the Dutch high-voltage electricity grid is partly based on open technical parameters and open data for the Dutch grid. The remaining part is based on assumptions, general knowledge and research. The assumptions can lead to unexpected model behaviour and atypical model output. From the results of the sensitivity analysis it can be observed that small variations in input of the pandapower model can lead to large variations in output. On the one hand, it is highly likely that part of the large variations can be assigned to the assumptions made on e.g., the aggregation and mapping of the loads and generators. On the other hand, part of the large variations are expected and can be contributed to the fact that a small change in nodal load can alter the power flow, and thus change the line loading percentages. Nonetheless, it shows that incorrect assumptions can alter the output and behaviour of the model. However, most of the assumptions made on the aggregation and mapping of the loads and generators are supported by research and by the modelling approach of TenneT TSO B.V. in their Infrastructure Outlook 2050 for creating a power system model of the Dutch high-voltage electricity grid. Therefore, the bigger portion of the variations can be contributed to the nature of an optimal power flow instead of the assumptions. As a result, the model was deemed to be a representative model of the Dutch high-voltage electricity grid.

The methodology used for identifying the bottlenecks in the pandapower network model for five different scenarios was based on analysing the results of a DC optimal power flow. The results were analysed for line and transformer loading percentages per time step. As the non-convergence of the optimal power flow calculation can not directly be traced back to one or several components, it was decided to look for components close to their operating limits. These components were referred to as congested components and their transmission capacity was incrementally increased until the components were operating safely within their limits. This led to a basic bottleneck and grid investment analysis. However, not all non-converged time steps were resolved by applying this methodology, due to the inability to trace the non-convergence of the optimal power flow back to one or several specific components. As the primary objective of this thesis was to create a representative model of the Dutch high-voltage electricity grid and the bottleneck and investment analysis was a secondary objective to showcase the created model, the methodology used was sufficient. When the model is utilised in future research, it is recommended to check if the methodology is sufficient for the intended use.

The heating sector outlook for 2050 shows an enormous potential for geothermal heat sources in the agricultural, industrial, and households and buildings sector. Large scale heat pumps with thermal storage are expected to cover a substantial part of the district heating supply and small scale heat pumps are expected to cover a substantial part of the decentralised heating supply for households and buildings. The three above mentioned renewable heating technologies have a major technical limitations: they can solely generate low-temperature heat. The higher temperature heat demand is expected to be mostly covered by hydrogen-fired boilers. The transition of the current heating system to the future heating system, primarily comprising the four renewable heating technologies, is subject to uncertainties related to the proposed policies, transition subsidies, and technology improvements. The current bottlenecks in the heating system transition are mostly related to the substantially higher investments costs for both large and small scale heat pumps compared to non-renewable heating technologies, and the lack of policies on and investments in the geothermal heating technologies. Technology improvements can lead to an increase in temperature of the heat produced by the renewable heating technologies, creating new opportunities for heating demand of energy sectors to be electrified. Thus, the rate of change in the heating system and the penetration of electrified and decarbonised heating supply highly depends on the proposed policies in the coming years and decades. The created model of the Dutch high-voltage electricity grid can be used to analyse the effects of all heating decarbonisation strategies on the electricity system.

7.3. Recommendations and Future Work

The research performed in this thesis and the model created are subject to assumptions and discussion. Some of the assumptions are interesting to further research and implement. Additionally, the created model can be used as a basis for other studies. Future lines of work are presented below.

- **Aggregation:** The aggregation of loads and the mapping of the loads on the model are the main assumptions for the current version of the pandapower network model. Further research in the spatial aggregation of loads in the Netherlands are the key to obtain a higher degree of confidence in the model's output and behaviour.

- **Dynamic line loading:** As the dynamic line loading is weather-dependent, an extra controller per high-voltage line can be added to the model to accurately depict a change in line loading as a result of a change in temperature. The implementation of such a controller can possibly decrease the number of congested time steps.
- **Energy system model integration:** The pandapower network model solely simulates the electricity system. It assumes uncontrollable loads, and readily available non-renewable and sustainable fuels for electricity production. Integration with other energy system models can increase the level of detail that can be obtained when analysing the effects of proposed policies on the Dutch energy system.
- **External grids/Interconnectors:** The interconnection capacity is assumed to be available at full capacity throughout the year in the current pandapower network model. As the interconnection lines are rarely operational at full capacity in reality, the balancing power provided as a result of this assumption is inaccurate. Further research in a more representative method to model external grids can increase the degree of confidence in the model behaviour.
- **Grid landing nodes:** Documents regarding the grid landing nodes and corresponding offshore generation capacity for 2030 are recently published and form the basis for the 2050 grid landing assumptions. As the grid landing nodes of offshore wind farms and the generation capacity per node are of high importance for the accuracy of the model, further research in the potential locations of the grid landing nodes and the optimal capacity per node is needed.
- **Minimum up- and down-time:** The minimum up- and down-times of generators are of importance when looking at hourly simulations. Incorporating minimum up- and down-times in a future version of the pandapower network model can increase the level of detail of the model.
- **Power-to-Hydrogen:** Another key component of energy sector integration is Power-to-Hydrogen ($P2H_2$). This process can provide flexibility to the electricity grid. The substantiation of the amount of flexibility provided, and the optimal production capacity and location of hydrogen plants to decrease the curtailment of offshore wind farms can be an interesting topic for further research.
- **Slack node:** It is common practice to define the slack node for power flow calculations as the node with highest balancing capacity. However, the location of the node relative to the other generators can affect the calculated load flow. The effects of the location of the slack node on the power flow can be an interesting topic for further research.

Bibliography

[1] Ministry of Economic Affairs and Climate Policy. Noord-West 380kV verbinding: Startnotitie voor de milieueffectrapportage. Technical Report 09ET16, Ministry of Economic Affairs and Climate Policy, The Hague, August 2009. URL https://www.rvo.nl/sites/default/files/2017/02/startnotitie%20NW380kV%20webversie%2009_ET_16.pdf.

[2] B. Najafi, S. Moaveninejad, and F. Rinaldi. Chapter 17 - Data Analytics for Energy Disaggregation: Methods and Applications. In R. Arghandeh and Y. Zhou, editors, Big Data Application in Power Systems. Elsevier, 2018. ISBN 978-0-12-811968-6. URL https://doi.org/10.1016/B978-0-12-811968-6.00017-6.

[3] European Commission. EU strategy on energy system integration, April 2020. URL https://ec.europa.eu/energy/topics/energy-system-integration/eu-strategy-energy-system-integration_en.

[4] European Commission. The European Green Deal. Technical Report COM(2019) 640 final, European Commission, Brussels, December 2019. URL https://eur-lex.europa.eu/legal-content/EN/TXT/?qid=1576150542719&uri=COM%3A2019%3A640%3AFIN.

[5] E. Taibi, T. Nikolakakis, L. Gutierrez, C. Fernandez, J. Kiviluoma, T.J. Lindroos, and S. Rissanen. Summary of power system flexibility for the energy transition. Part 2: IRENA FlexTool methodology. Technical report, International Renewable Energy Agency, 2019. URL https://www.irena.org/-/media/Files/IRENA/Agency/Publication/2018/Nov/IRENA_Power_system_flexibility_2_2018.pdf?la=en%26hash=B7028E2E169CF239269EC9695D53276E084A29AE.

[6] J. Osborn and C. Kawann. Reliability of the U.S. electricity system: Recent trends and current issues. Technical Report LBNL-47043, LBNL, Berkeley, August 2001. URL https://eta-publications.lbl.gov/sites/default/files/report-lbnl-47043.pdf.

[7] Ministry of Economic Affairs and Climate Policy. National Climate Agreement. Technical report, Ministry of Economic Affairs and Climate Policy, The Hague, June 2019. URL https://www.klimaatakkoord.nl/documenten/publicaties/2019/06/28/national-climate-agreement-the-netherlands.

[8] P. Schavemaker and L. van der Sluis. Electrical Power System Essentials. John Wiley & Sons Ltd, 2008. ISBN 978-0-470-51027-8.

[9] United Nations Framework Convention on Climate Change. The Paris Agreement, 2020. URL https://unfccc.int/process-and-meetings/the-paris-agreement/the-paris-agreement.

[10] IRENA. Innovation landscape for a renewable-powered future: Solutions to integrate variable renewables. Technical report, International Renewable Energy Agency, Abu Dhabi, 2019. URL https://www.irena.org/-/media/Files/IRENA/Agency/Publication/2019/Feb/IRENA_Innovation_Landscape_2019_report.pdf.

[11] European Parliament and Council of the European Union. Regulation (EU) 2019/941 on risk-preparedness in the electricity sector, June 2019. URL https://eur-lex.europa.eu/eli/reg/2019/941/oj.

[12] Gregor Erbach. Underestanding electricity markets in the EU. Technical Report PE 593.519, European Parliamentary Research Service, Brussels, November 2016. URL https://www.europarl.europa.eu/RegData/etudes/BRIE/2016/593519/EPRS_BRI(2016)593519_EN.pdf.

[13] Netbeheer Nederland. Basisinformatie over energie-infrastructuur, May 2019. URL https://www.netbeheernederland.nl/_upload/Files/Basisdocument_over_energie-infrastructuur_143.pdf.

[14] Baerbel Epp. Support for renewable district heating in Slovenia, 2019. URL https://www.solarthermalworld.org/news/support-renewable-district-heating-slovenia.

[15] Agency for the Cooperation of Energy Regulators. Electricity Infrastructure. Report on unit investment cost indicators and corresponding reference values for electricity and gas infrastructure. Technical Report ELEC-2015, ACER, Ljubljana, August 2015. URL https://documents.acer.europa.eu/Official_documents/Acts_of_the_Agency/Publication/UIC%20Report%20%20-%20Electricity%20infrastructure.pdf.

[16] K. van den Bergh and E. Delarue. Cycling of conventional power plants: Technical limits and actual costs. Energy Conversion and Management, 97:70–77, June 2015. ISSN 0196-8904. doi: https://doi.org/10.1016/j.enconman.2015.03.026.

[17] R.G. Sargent. Verification and validation of simulation models. In Proceedings of the 2010 Winter Simulation Conference, volume 37, pages 166–183, Baltimore, December 2010. WSC. doi: https://doi.org/10.1109/WSC.2010.5679166.

[18] Stuurgroep RES Groningen. Regionale Energie Strategie 1.0 - Regio Groningen. Technical report, RES Regio Groningen, July 2021. URL https://www.provinciegroningen.nl/fileadmin/user_upload/Documenten/Downloads/Downloads_2021/RES_1.0_Groningen__versie_08-04-2021_.pdf.

[19] UN General Assembly. United Nations Framework Convention on Climate Change. Technical report, United Nations, New York, 1992. URL https://unfccc.int/files/essential_background/background_publications_htmlpdf/application/pdf/conveng.pdf.

[20] UN General Assembly. Paris Agreement to the United Nations Framework Convention on Climate Change. Technical report, United Nations, Paris, December 2015. URL https://unfccc.int/sites/default/files/english_paris_agreement.pdf.

[21] European Commission. Nationally Determined Contribution (NDC) of the European Union and its Member States. Technical report, European Commission, Berlin, December 2020. URL https://www4.unfccc.int/sites/ndcstaging/PublishedDocuments/European%20Union%20First/EU_NDC_Submission_December%202020.pdf.

[22] European Commission. Long-Term Low greenhouse gas Emission Development Strategy (LT-LEDS) of the European Union and its Member States. Technical report, European Commission, Zagreb, March 2020. URL https://unfccc.int/sites/default/files/resource/HR-03-06-2020%20EU%20Submission%20on%20Long%20term%20strategy.pdf.

[23] TenneT TSO B.V. and N.V. Nederlandse Gasunie. Infrastructure outlook 2050. Technical report, TenneT TSO B.V. and N.V. Nederlandse Gasunie, Arnhem, February 2019. URL https://www.tennet.eu/fileadmin/user_upload/Company/News/Dutch/2019/Infrastructure_Outlook_2050_appendices_190214.pdf.

[24] TenneT TSO B.V. and N.V. Nederlandse Gasunie. Infrastructure outlook 2050. Phase II: Pathways to 2050. Technical report, TenneT TSO B.V. and N.V. Nederlandse Gasunie, Arnhem, February 2020. URL https://www.tennet.eu/fileadmin/user_upload/Company/Publications/Technical_Publications/200115_Phase_II_Executive_summary.pdf.

[25] Paardekooper, S., Lund, R. S., Mathiesen, B. V., Chang, M., Petersen, U. R., Grundahl, L., David, A.,, Dahlbæk, J., Kapetanakis, I. A., Lund, H., Bertelsen, N., Hansen, K., Drysdale, D. W., and Persson, U. Heat Roadmap Netherlands: Quantifying the Impact of Low-Carbon Heating and Cooling Roadmaps. Technical report, Aalborg University, Aalborg, 2018. URL https://vbn.aau.dk/ws/portalfiles/portal/287931509/Country_Roadmap_Netherlands_20181005.pdf.

[26] IRENA. Innovation landscape brief: Renewable power-to-hydrogen. Technical report, International Renewable Energy Agency, Abu Dhabi, 2019. URL https://www.irena.org/-/media/Files/IRENA/Agency/Publication/2019/Sep/IRENA_Power-to-Hydrogen_Innovation_2019.pdf.

[27] K. Kavvadias, J.P. Jimenez Navarro, and G. Thomassen. Decarbonising the EU heating sector: Integration of the power and heating sector. Technical Report EUR 29772 EN, Publications Office of the European Union, Luxembourg, 2019. URL https://doi.org/10.2760/943257.

[28] European Commission. EU Strategy on Energy System Integration, July 2021. URL https://ec.europa.eu/energy/topics/energy-system-integration/eu-strategy-energy-system-integration_en.

[29] J.C. Koj, C. Wulf, and P. Zapp. Environmental impacts of power-to-X systems - A review of technological and methodological choices in Life Cycle Assessments. Renewable and Sustainable Energy Reviews, 112:865–879, September 2019. ISSN 1364-0321. doi: https://doi.org/10.1016/j.rser.2019.06.029.

[30] C. Wulf, J. Linßen, and P. Zapp. Review of Power-to-Gas Projects in Europe. Energy Procedia, 155: 367–378, November 2018. ISSN 1876-6102. doi: https://doi.org/10.1016/j.egypro.2018.11.041.

[31] G. Buffo, P. Marocco, D. Ferrero, A. Lanzini, and M. Santarelli. Chapter 15 - Power-to-X and power-to-power routes. In F. Calise, M.D. D'Accadia, M. Santarelli, A. Lanzini, and D. Ferrero, editors, Solar Hydrogen Production, pages 529–557. Academic Press, January 2019. ISBN 978-0-12-814853-2. URL https://doi.org/10.1016/B978-0-12-814853-2.00015-1.

[32] C. Wulf, P. Zapp, and A. Schreiber. Review of Power-to-X Demonstration Projects in Europe. Frontiers in Energy Research, 8:191, September 2020. ISSN 2296-598X. doi: https://doi.org/10.3389/fenrg.2020.00191.

[33] Z. Chehade, C. Mansilla, P. Lucchese, S. Hilliard, and J. Proost. Review and analysis of demonstration projects on power-to-X pathways in the world. International Journal of Hydrogen Energy, 44(51): 27637–27655, October 2019. ISSN 0360-3199. doi: https://doi.org/10.1016/j.ijhydene.2019.08.260.

[34] J. Salpakari, J. Mikkola, and P.D. Lund. Improved flexibility with large-scale variable renewable power in cities through optimal demand side management and power-to-heat conversion. Energy Conversion and Management, 126:649–661, October 2016. ISSN 0196-8904. doi: https://doi.org/10.1016/j.enconman.2016.08.041.

[35] A. Bloess, W.P. Schill, and A. Zerrahn. Power-to-heat for renewable energy integration: A review of technologies, modeling approaches, and flexibility potentials. Applied Energy, 212:1611–1626, February 2018. ISSN 0306-2619. doi: https://doi.org/10.1016/j.apenergy.2017.12.073.

[36] D. Fischer and H. Madani. On heat pumps in smart grids: A review. Renewable and Sustainable Energy Reviews, 70:342–357, April 2017. ISSN 1364-0321. doi: https://doi.org/10.1016/j.rser.2016.11.182.

[37] IRENA. Innovation landscape brief: Renewable power-to-heat. Technical report, International Renewable Energy Agency, Abu Dhabi, 2019. URL https://www.irena.org/-/media/Files/IRENA/Agency/Publication/2019/Sep/IRENA_Power-to-heat_2019.pdf?la=en&hash=524C1BFD59EC03FD44508F8D7CFB84CEC317A299.

[38] B. Zakeri, S. Rinne, and S. Syri. Wind Integration into Energy Systems with a High Share of Nuclear Power - What Are the Compromises. Energies, 8:2493–2527, March 2015. ISSN 996-1073. doi: https://doi.org/10.3390/en8042493.

[39] S. Pilpola and P.D. Lund. Effect of major policy disruptions in energy system transition: Case Finland. Energy Policy, 116:323–336, May 2018. ISSN 0301-4215. doi: https://doi.org/10.1016/j.enpol.2018.02.028.

[40] D. Böttger, M. Götz, N. Lehr, H. Kondziella, and T. Bruckner. Potential of the Power-to-Heat Technology in District Heating Grids in Germany. Energy Procedia, 46:246–253, January 2014. ISSN 1876-6102. doi: https://doi.org/10.1016/j.egypro.2014.01.179.

[41] D. Connolly, H. Lund, B. V. Mathiesen, S. Werner, B. Möller, U. Persson, T. Boermans, D. Trier, P. A. Østergaard, and S. Nielsen. Heat Roadmap Europe: Combining district heating with heat savings to decarbonise the EU energy system. Energy Policy, 65:475–489, January 2014. ISSN 0301-4215. doi: https://doi.org/10.1016/j.enpol.2013.10.035.

[42] A.C. Ince, C.O. Colpan, A. Hagen, and M.F. Serincan. Modeling and simulation of Power-to-X systems: A review. Fuel, 304:121354, November 2021. ISSN 0016-2361. doi: https://doi.org/10.1016/j.fuel.2021.121354.

[43] F.V. Vázquez, J. Koponen, V. Ruuskanen, C. Bajamundi, Antti Kosonen, P. Simell, J. Ahola, C. Frilund, J. Elfving, M. Reinikainen, N. Heikkinen, J. Kauppinen, and P. Piermartini. Power-to-X technology using renewable electricity and carbon dioxide from ambient air: SOLETAIR proof-of-concept and improved process concept. Journal of CO2 Utilization, 28:235–246, December 2018. ISSN 2212-9820. doi: https://doi.org/10.1016/j.apenergy.2018.12.028.

[44] Y. Chen, Z. Chen, P. Xu, W. Li, H. Sha, Z. Yang, G. Li, and C. Hu. Quantification of electricity flexibility in demand response: Office building case study. Energy, 188:116054, December 2019. ISSN 0360-5442. doi: https://doi.org/10.1016/j.energy.2019.116054.

[45] M. A. Ancona, M. Bianchi, L. Branchini, F. Catena, A. De Pascale, F. Melino, and A. Peretto. Numerical prediction of off-design performance for a Power-to-Gas system coupled with renewables. Energy Conversion and Management, 210:112702, April 2020. ISSN 0196-8904. doi: https://doi.org/10.1016/j.enconman.2020.112702.

[46] M. Münster, P.E. Morthorst, H.V. Larsen, L. Bregnbæk, J. Werling, H.H. Lindboe, and Hans Ravn. The role of district heating in the future Danish energy system. Energy, 48(1):47–55, December 2012. ISSN 0360-5442. doi: https://doi.org/10.1016/j.apenergy.2018.12.028.

[47] S.N. Petrović and K.B. Karlsson. Residential heat pumps in the future Danish energy system. Energy, 114:787–797, November 2016. ISSN 0360-5442. doi: https://doi.org/10.1016/j.energy.2016.08.007.

[48] H. Lund, J.Z. Thellufsen, P.A. Østergaard, P. Sorknæs, I.R. Skov, and B.V. Mathiesen. EnergyPLAN – Advanced analysis of smart energy systems. Smart Energy, 1:100007, February 2021. ISSN 2666-9552. doi: https://doi.org/10.1016/j.segy.2021.100007.

[49] D. Connolly, H. Lund, and B. V. Mathiesen. Smart Energy Europe: The technical and economic impact of one potential 100% renewable energy scenario for the European Union. Renewable and Sustainable Energy Reviews, 60:1634–1653, July 2016. ISSN 1364-0321. doi: https://doi.org/10.1016/j.rser.2016.02.025.

[50] N. Helistö, J. Kiviluoma, J. Ikäheimo, T. Rasku, E. Rinne, C. O'Dwyer, R. Li, and D. Flynn. Backbone—An Adaptable Energy Systems Modelling Framework. Energies, 12(17):3388, January 2019. doi: https://doi.org/10.3390/en12173388. Number: 17 Publisher: Multidisciplinary Digital Publishing Institute.

[51] J. Ikäheimo, R. Weiss, J. Kiviluoma, E. Pursiheimo, and T.J. Lindroos. Impact of power-to-gas on the cost and design of the future low-carbon urban energy system. Applied Energy, 305:117713, January 2022. ISSN 0306-2619. doi: https://doi.org/10.1016/j.apenergy.2021.117713.

[52] A. Herbst, F. Toro, R. Felix, and J. Eberhard. Introduction to energy systems modelling. Swiss Journal of Economics and Statistics, 148:111–135, April 2012. doi: https://doi.org/10.1007/BF03399363.

[53] C. Philibert. Renewable Energy for Industry. From green energy to green materials and fuels. Technical report, IEA, Paris, 2017. URL `https://iea.blob.core.windows.net/assets/48356f8e-77a7-49b8-87de-87326a862a9a/Insights_series_2017_Renewable_Energy_for_Industry.pdf`.

[54] EBN. Energy in the Netherlands, 2018. URL `https://www.ebn.nl/wp-content/uploads/2018/04/EBN-poster-numbers2016.pdf`.

[55] O. Ellabban, H. Abu-Rub, and F. Blaabjerg. Renewable energy resources: Current status, future prospects and their enabling technology. Renewable and Sustainable Energy Reviews, 39:748–764, November 2014. ISSN 1364-0321. doi: https://doi.org/10.1016/j.rser.2014.07.113.

[56] Brian Vad Mathiesen. 2015 Final Heating & Cooling Demand in the Netherlands., October 2017. URL `https://heatroadmap.eu/wp-content/uploads/2018/11/HRE4-Country_presentation-Netherlands.pdf`.

[57] CBS. Elektriciteitsbalans; aanbod en verbruik, 2020. URL https://opendata.cbs.nl/statline/#/CBS/nl/dataset/84575NED/table?dl=5C87B.

[58] CBS. Elektriciteit; productie en productiemiddelen, 2019. URL https://opendata.cbs.nl/statline/#/CBS/nl/dataset/37823wkk/table?dl=5C882.

[59] A.L. Polyzakis, C. Koroneos, and G. Xydis. Optimum gas turbine cycle for combined cycle power plant. Energy Conversion and Management, 49(4):551–563, April 2008. ISSN 0196-8904. doi: https://doi.org/10.1016/j.enconman.2007.08.002.

[60] A.J. Seebregts, H.J.M. Snoep, J. van Deurzen, S.M. Lensink, A.J. van der Welle, and W. Wetzels. Brandstofmix elektriciteit 2020. Inventarisatie, mogelijke problemen en oplossingsrichtingen. Technical Report ECN-E–09–046, ECN, Petten, December 2009. URL https://publicaties.ecn.nl/PdfFetch.aspx?nr=ECN-E--09-046.

[61] P.A. Pilavachi. Power generation with gas turbine systems and combined heat and power. Applied Thermal Engineering, 20(15-16):1421–1429, October 2000. ISSN 1359-4311. doi: https://doi.org/10.1016/S1359-4311(00)00016-8.

[62] I. Komusanac, G. Brindley, and D. Fraile. Wind energy in Europe in 2019. Trends and statistics. Technical report, Wind Europe, Brussels, February 2020. URL https://windeurope.org/intelligence-platform/product/wind-energy-in-europe-in-2019-trends-and-statistics/.

[63] Nordic Energy Research. Nordic Energy Technology Perspectives 2016: Cities, flexibility and pathways to carbon-neutrality. Technical report, IEA, Paris, 2016. URL https://www.nordicenergy.org/wp-content/uploads/2016/04/Nordic-Energy-Technology-Perspectives-2016.pdf.

[64] TenneT TSO B.V. KCD 2017. Kwaliteits- en Capaciteitsdocument 2017. Deel II: Investeringen Net op Land 2018 - 2027. Technical report, TenneT TSO B.V., Arnhem, December 2017. URL https://www.tennet.eu/fileadmin/user_upload/Company/Publications/Technical_Publications/Dutch/TenneT_KCD2017_Deel_II.pdf.

[65] Elia. Federaal ontwikkelingsplan van het transmissienet 2020-2030. Technical report, Elia Group, Brussels, February 2019. URL https://eliafederaalontwikkelingsplan.be/.

[66] L. Thurner, A. Scheidler, F. Schafer, J. H. Menke, J. Dollichon, F. Meier, S. Meinecke, and M. Braun. pandapower - an Open Source Python Tool for Convenient Modeling, Analysis and Optimization of Electric Power Systems. IEEE Transactions on Power Systems, 33(6):6510–6521, November 2018. ISSN 0885-8950. doi: https://doi.org/10.1109/TPWRS.2018.2829021.

[67] Van Rossum, G. and Drake, F.L. Python 3 Reference Manual. CreateSpace, 2009. ISBN 978-1-4414-1269-0.

[68] L.M.H. Hall and A.R. Buckley. A review of energy systems models in the UK: Prevalent usage and categorisation. Applied Energy, 169:607–628, May 2016. ISSN 0306-2619. doi: https://doi.org/10.1016/j.apenergy.2016.02.044.

[69] S. Jebaraj and S. Iniyan. A review of energy models. Renewable and Sustainable Energy Reviews, 10(4):281–311, August 2006. ISSN 1364-0321. doi: https://doi.org/10.1016/j.rser.2004.09.004.

[70] D. Connolly, H. Lund, B.V. Mathiesen, and M. Leahy. A review of computer tools for analysing the integration of renewabl energy into various energy systems. Applied Energy, 87(4):1059–1082, April 2010. ISSN 0306-2619. doi: https://doi.org/10.1016/j.apenergy.2009.09.026.

[71] N.M.J.P. van Beeck. Classification of Energy Models. Operations research, 777:25, May 1999. URL https://pure.uvt.nl/ws/portalfiles/portal/532108/777.pdf.

[72] W. Medjroubi, U.P. Müller, M. Scharf, C. Matke, and D. Kleinhans. Open data in power grid modelling: New approaches towards transparent grid models. Energy Reports, 3:14–21, November 2017. ISSN 2352-4847. doi: https://doi.org/10.1016/j.egyr.2016.12.001.

[73] B. Pfluger. Assessment of least-cost pathways for decarbonising Europe's power supply. Dissertation, Karlsruher Institut für Technologie, Kalsruhe, May 2013. URL https://d-nb.info/1053702175/34.

[74] S. Pfenninger, L. Hirth, I. Schlecht, E. Schmid, F. Wiese, T. Brown, C. Davis, M. Gidden, H. Heinrichs, C. Heuberger, S. Hilpert, U. Krien, C. Matke, A. Nebel, R. Morrison, B. Müller, G. Pleßmann, M. Reeg, J.C. Richstein, A. Shivakumar, I. Staffell, T. Tröndle, and C. Wingenbach. Opening the black box of energy modelling: Strategies and lessons learned. Energy Strategy Reviews, 19:63–71, January 2018. ISSN 2211-467X. doi: https://doi.org/10.1016/j.esr.2017.12.002.

[75] TenneT TSO B.V. Hoogspanningsnet Nederland - Asset gegevens TenneT TSO B.V., 2021. URL https://services3.arcgis.com/XWGZdevfTDjoWmwu/arcgis/rest/services/TenneT_Assets/FeatureServer.

[76] Esri. Topographic, 2021. URL https://services.arcgisonline.com/ArcGIS/rest/services/World_Topo_Map/MapServer.

[77] TenneT TSO B.V. Grid diagram. HV network of the Netherlands, November 2019. URL https://www.tennet.org/controls/DownloadDocument.ashx?documentID=40.

[78] HoogspanningsNet. EHV Network of the Netherlands, July 2021. URL https://www.hoogspanningsnet.com/netschema/.

[79] HoogspanningsNet. HoogspanningsNet Netkaart, 2021. URL https://webkaart.hoogspanningsnet.com/index2.php#8/52.112/5.098.

[80] TenneT TSO B.V. Static grid model NL. Overview of 380kV and 220kV grid components inclusive of technical data, November 2020. URL https://www.tennet.org/controls/DownloadDocument.ashx?documentID=41.

[81] TenneT TSO B.V. International connections, 2021. URL https://www.tennet.eu/our-grid/international-connections/.

[82] TenneT TSO B.V. KCD 2008. Kwaliteits- en Capaciteitsplan 2008 - 2014. Deel II. Technical report, TenneT TSO B.V., Arnhem, December 2007. URL https://www.tennet.eu/fileadmin/user_upload/Company/Publications/Technical_Publications/Dutch/TP_KCD2008_Deel_2.pdf.

[83] TenneT TSO B.V. KCD 2010. Kwaliteits- en Capaciteitsplan 2010 - 2016. Deel II A. Technical report, TenneT TSO B.V., Arnhem, November 2009. URL https://www.tennet.eu/fileadmin/user_upload/Company/Publications/Technical_Publications/Dutch/TP_KCD2010-2016_deel_2A.pdf.

[84] ENTSO-E. Installed capacity per production unit, 2018. URL https://transparency.entsoe.eu/generation/r2/installedCapacityPerProductionUnit/show.

[85] TenneT TSO B.V. System and transmission data: Installed capacity, 2018. URL https://www.tennet.org/bedrijfsvoering/Systeemgegevens_voorbereiding/Aangemeld_productievermogen/Opgesteld_vermogen.aspx.

[86] CBS. Windenergie op land; productie en capaciteit per provincie, June 2021. URL https://opendata.cbs.nl/statline/#/CBS/nl/dataset/70960ned/table?ts=1636628111301.

[87] CBS. Hernieuwbare energie; zonnestroom, windenergie, RES-regio, July 2021. URL https://opendata.cbs.nl/statline/#/CBS/nl/dataset/85004NED/table?ts=1630339841444.

[88] S. Pfenninger and I. Staffel. Long-term patterns of European PV output using 30 years of validated hourly reanalysis and satellite data. Energy, 114:1251–1265, 2016. ISSN 0360-5442. doi: https://doi.org/10.1016/j.energy.2016.08.060.

[89] I. Staffel and S. Pfenninger. Using Bias-Corrected Reanalysis to Simulate Current and Future Wind Power Output. Energy, 114:1224–1239, 2016. ISSN 0360-5442. doi: https://doi.org/10.1016/j.energy.2016.08.068.

[90] Quintel Intelligence. Energy Transition Model, 2021. URL https://pro.energytransitionmodel.com/.

[91] Commissie verbruiksprofielen. Profielen Elektriciteit 2018, 2018. URL https://www.nedu.nl/documenten/verbruiksprofielen/.

[92] Rijkswaterstaat. De Klimaatmonitor, 2021. URL https://klimaatmonitor.databank.nl/jive.

[93] Erik Koldenhof. Energy from Waste - Amsterdam, September 2013. URL https://www.ieabioenergy.com/wp-content/uploads/2013/09/Energy-from-Waste-Amsterdam-koldenhof.pdf.

[94] P.J. Zijlema. The Netherlands: list of fuels and standard CO2 emission factors. Technical Report 113569/BL2020, Netherlands Enterprise Agency, The Hague, January 2020. URL https://english.rvo.nl/sites/default/files/2020/03/The-Netherlands-list-of-fuels-version-January-2020.pdf.

[95] Markets Insider. CO2 European Emission Allowances, 2021. URL https://markets.businessinsider.com/commodities/co2-european-emission-allowances.

[96] Yahoo! Finance. Dutch TTF Natural Gas Price, 2021. URL https://finance.yahoo.com/quote/TTF%3DF?p=TTF%3DF.

[97] Yahoo! Finance. Coal (API2) Price, 2021. URL https://finance.yahoo.com/quote/MTFQ21.NYM?p=MTFQ21.NYM.

[98] Bosch & van Rijn. Statistieken, 2021. URL https://windstats.nl/statistieken/.

[99] Windenergie Nieuws. Windmolen & Windparken Kaart Nederland, 2016. URL https://www.google.com/maps/d/viewer?mid=1ivmLZBlPfpCjvBE8Qn3-2IQwlvw&ll=52.31034682457768%2C6.066631530648907&z=8.

[100] R. Holtkamp and R. Woolthuis. Midden- en grootverbruik van elektriciteit en gas, 2017, May 2019. URL https://www.cbs.nl/nl-nl/maatwerk/2019/23/midden-en-grootverbruik-van-elektriciteit-en-gas-2017.

[101] American Institute of Aeronautics and Astronautics. Guide for the Verification and Validation of Computational Fluid Dynamics Simulations. Technical Report AIAA G-077-1998 (2002), AIAA, Reston, 1998. URL https://arc.aiaa.org/doi/abs/10.2514/4.472855.001.

[102] J. Greunsven and M. Derks. Annual Market Update 2018. Electricity market insights. Technical report, TenneT TSO B.V., Arnhem, March 2019. URL https://www.tennet.eu/fileadmin/user_upload/Company/Publications/Technical_Publications/Dutch/Annual_Market_Update_2018_-_Final.pdf.

[103] J. Matthijsen, E. Dammers, and H. Elzenga. De toekomst van de Noorzee. De Noordzee in 2030 en 2050: een scenariostudie. Technical Report 2728, PBL Planbureau voor de Leefomgeving, The Hague, 2018. URL https://www.pbl.nl/sites/default/files/downloads/pbl-2018-toekomst-van-de-noordzee-2728.pdf.

[104] H. Cleijne, M. de Ronde, M. Duvoort, W. de Kleuver, and J. Raadschelders. Noordzee Energie Outlook. Technical report, DNV GL Netherlands B.V., Arnhem, September 2020. URL https://www.rijksoverheid.nl/documenten/kamerstukken/2020/09/01/rapport-noordzee-energie-outlook.

[105] Stuurgroep RES Achterhoek. Regionale Energie Strategie 1.0 - Regio Achterhoek. Technical report, RES Regio Achterhoek, July 2021. URL https://www.resachterhoek.nl/verzamelpagina+gepubliceerde+publiekelijke+documen/HandlerDownloadFiles.ashx?idnv=2004362.

[106] Gemeente Molenlanden and Gemeente Gorinchem. Regionale Energie Strategie 1.0 - Regio Alblasserwaard. Technical report, RES Regio Alblasserwaard, March 2021. URL https://www.molenlanden.nl/sites/default/files/2021-04/RES%201.0%20Alblasserwaard.pdf.

[107] Bestuurlijk Overleg RES Regio Amersfoort. Regionale Energie Strategie 1.0 - Regio Amersfoort. Technical report, RES Regio Amersfoort, July 2021. URL https://www.resregioamersfoort.nl/over+de+res/documenten-res-algemeen/default.aspx#folder=1960519.

[108] Team RES Regio Arnhem Nijmegen. Regionale Energie Strategie 1.0 - Regio Arnhem Nijmegen. Technical report, RES Regio Arnhem Nijmegen, June 2021. URL https://www.regioan.nl/media/RES-1-AN-v2-20210629-DEF.pdf.

[109] Stuurgroep RES Cleantech Regio. Regionale Energie Strategie 1.0 - Cleantech Regio. Technical report, RES Cleantech Regio, November 2021. URL https://cleantechregio.nl/res/images/Cleantech_Regio_RES10_1920x1080px_2104_8-2.pdf.

[110] Bestuurlijk Overleg RES Drechtsteden. Regionale Energie Strategie 1.0 - Regio Drechtsteden. Technical report, RES Regio Drechtsteden, May 2021. URL https://drechtstedenenergie.nl/downloads/res-drechtsteden.pdf.

[111] Drentse Energietafel. Regionale Energie Strategie 1.0 - Regio Drenthe. Technical report, RES Regio Drenthe, April 2021. URL https://energievoordrenthe.nl/res+10+regio+drenthe/default.aspx#folder=1937417.

[112] Stuurgroep RES Flevoland. Regionale Energie Strategie 1.0 - Regio Flevoland. Technical report, RES Regio Flevoland, July 2021. URL https://fea.nl/uploads/2021/07/RES-1.0-definitief.pdf.

[113] Regio Foodvalley. Regionale Energie Strategie 1.0 - Regio Foodvalley. Technical report, RES Regio Foodvalley, April 2021. URL https://www.regiofoodvalley.nl/fileadmin/energietransitie/Jul_2021/Formele_versie_rapport_RES_1.0_2021_volledig-print.pdf.

[114] Regiegroep Regionale Energie Strategie RES Fryslan. Regionale Energie Strategie 1.0 - Regio Fryslan. Technical report, RES Regio Fryslan, April 2021. URL https://www.resfryslan.frl/wp-content/uploads/2021/04/RES-1.0_RES-FRYSL%C3%82N_NL_DEF_digitaal.pdf.

[115] Stuurgroep RES Goeree-Overflakkee. Regionale Energie Strategie 1.0 - Regio Goeree-Overflakkee. Technical report, RES Regio Goeree-Overflakkee, April 2021. URL https://klimaatkrachtiggo.nl/wp-content/uploads/202124-A4-klein.pdf.

[116] Stuurgroep REKS Hart van Brabant. Regionale Energie- en Klimaatstrategie 1.0 - Regio Hart van Brabant. Technical report, REKS Regio Hart van Brabant, March 2021. URL https://www.regio-hartvanbrabant.nl/images/Nieuws/REKS/bijlagen-bod-1.0/reks-1_0-regio-hart-van-brabant.pdf.

[117] Stuurgroep RES Regio Hoeksche Waard. Regionale Energie Strategie 1.0 - Regio Hoeksche Waard. Technical report, RES Regio Hoeksche Waard, March 2021. URL https://www.gemeentehw.nl/direct-regelen/duurzaamheid/regionale-energiestrategie-res-hoeksche-waard/32212.

[118] Stuurgroep RES Holland Rijnland. Regionale Energie Strategie 1.0 - Regio Holland Rijnland. Technical report, RES Regio Holland Rijnland, April 2021. URL https://wijzijnon.nl/media/uploads/blocks/RES%2010_april%202021_def.pdf.

[119] Stuurgroep Regionale Energiestrategie Metropoolregio Eindhoven. Regionale Energie Strategie 1.0 - Metropoolregio Eindhoven. Technical report, RES Metropoolregio Eindhoven, September 2021. URL https://www.energieregiomre.nl/waar+staan+we+nu/documenten+res+10/handlerdownloadfiles.ashx?idnv=2053730.

[120] Stuurgroep RES Midden-Holland. Regionale Energie Strategie 1.0 - Regio Midden-Holland. Technical report, RES Regio Midden-Holland, April 2021. URL https://www.regiomiddenholland.nl/Strategische+agenda/duurzaamheid/regionale+energiestrategie/default.aspx#folder=1941146.

[121] Stuurgroep RES Noord- en Midden-Limburg. Regionale Energie Strategie 1.0 - Regio Noord- en Midden-Limburg. Technical report, RES Regio Noord- en Midden-Limburg, July 2021. URL https://www.resnml.nl/media/2021-07/RES-Noord--en-midden---1.0-Def.(1).pdf.

[122] Stuurgroep Regionale Energiestrategie Noord-Holland Noord. Regionale Energie Strategie 1.0 - Regio Noord-Holland Noord. Technical report, RES Regio Noord-Holland Noord, April 2021. URL https://energieregionhn.nl/res-downloaden.

[123] Stuurgroep Regionale Energiestrategie Noord-Holland Zuid. Regionale Energie Strategie 1.0 - Regio Noord-Holland Zuid. Technical report, RES Regio Noord-Holland Zuid, April 2021. URL https://energieregionhz.nl/res-downloaden.

[124] Stuurgroep RES Noordoost-Brabant. Regionale Energie Strategie 1.0 - Regio Noordoost-Brabant. Technical report, RES Regio Noordoost-Brabant, March 2021. URL https://www.energiewerkplaatsbrabant.nl/res/res+noordoost+brabant/publicaties+en+rapporten+overzicht/regionale+energiestrategie+10/default.aspx#folder=1929443.

[125] Stuurgroep Regionale Energie Strategie Noord-Veluwe. Regionale Energie Strategie 1.0 - Regio Noord-Veluwe. Technical report, RES Regio Noord-Veluwe, April 2021. URL https://energiestrategienv.nl/uploads/637546799608339084_RES-01%20Noord%20Veluwe%20-%20Bestuurlijk%20document.klein.pdf.

[126] Stuurgroep RES FruitDelta Rivierenland. Regionale Energie Strategie 1.0 - Regio FruitDelta Rivierenland. Technical report, RES Regio FruitDelta Rivierenland, April 2021. URL https://www.resrivierenland.nl/wp-content/uploads/RES-1.0-Rivierenland-6-april-2021.pdf.

[127] Stuurgroep Energiestrategie Regio Rotterdam Den Haag. Regionale Energie Strategie 1.0 - Regio Rotterdam Den Haag. Technical report, RES Regio Rotterdam Den Haag, March 2021. URL https://www.resrotterdamdenhaag.nl/wp-content/uploads/2021/04/RES-1.0-Regio-Rotterdam-Den-Haag.pdf.

[128] Coordinatieteam RES Twente. Regionale Energie Strategie 1.0 - Regio Twente. Technical report, RES Regio Twente, May 2021. URL https://energiestrategietwente.nl/assets/media/210518_RES-Twente-1.0.pdf.

[129] Stuurgroep RES Regio U16. Regionale Energie Strategie 1.0 - Regio U16. Technical report, RES Regio U16, May 2021. URL https://www.energieregioutrecht.nl/publicaties/default.aspx.

[130] Stuurgroep RES West-Brabant. Regionale Energie Strategie 1.0 - Regio West-Brabant. Technical report, RES Regio West-Brabant, January 2021. URL https://energieregiowb.nl/app/uploads/sites/3/2021/02/20210218-RES-West-Brabant-1.0.pdf.

[131] Werkgroep Elektriciteit. Regionale Energie Strategie 1.0 - Regio West-Overijssel. Bouwsteen Elektriciteit. Technical report, RES Regio West-Overijssel, May 2021. URL https://www.reswestoverijssel.nl/res1-0/default.aspx.

[132] Stuurgroep RES Zeeland. Regionale Energie Strategie 1.0 - Regio Zeeland. Technical report, RES Regio Zeeland, February 2020. URL https://www.zeeuwsenergieakkoord.nl/sites/default/files/2020-04/res-1.0.pdf.

[133] Stuurgroep RES Zuid-Limbug. Regionale Energie Strategie 1.0 - Regio Zuid-Limburg. Technical report, RES Regio Zuid-Limburg, May 2021. URL https://www.reszuidlimburg.nl/media/2021-06/RES-Zuid-Limburg---1.0---Def.pdf.

[134] B. den Ouden, J. Kerkhoven, J. Warnaars, R. Terwel, M. Coenen, T. Verboon, T. Tiihonen, and A. Koot. Klimaatneutrale energiescenario's 2050: Scenariostudie ten behoeve van de integrale infrastructuurverkenning 2030-2050. Technical Report 61689, Berenschot and Kalavasta, Utrect, March 2020. URL https://www.berenschot.nl/media/hl4dygfq/rapport_klimaatneutrale_energiescenario_s_2050_2.pdf.

[135] TenneT TSO B.V. KCD 2016. Kwaliteits- en Capaciteitsdocument 2016. Deel II: Investeringsplan 2016 - 2025. Technical report, TenneT TSO B.V., Arnhem, July 2016. URL https://www.tennet.eu/fileadmin/user_upload/Company/Publications/Technical_Publications/Dutch/TenneT_KCD_2016_Deel_II_DEF_M.pdf.

[136] N. Hoogervorst. Toekomstbeeld klimaatneutrale warmtenetten in Nederland. Technical Report 1926, PBL Planbureau voor de Leefomgeving, The Hague, 2017. URL https://www.pbl.nl/sites/default/files/downloads/pbl-2017-toekomstbeeld-klimaatneutrale-warmtenetten-in-nederland-1926_1.pdf.

[137] R. Geyer, D. Hangartner, M. Lindahl, and S.V. Pedersen. Heat Pumps in District Heating and Cooling Systems. Technical Report HPT-AN47-1, Research Institutes of Sweden, Boras, April 2020. URL https://heatpumpingtechnologies.org/publications/heat-pumps-in-district-heating-and-cooling-systems-final-report/.

[138] R. Colenbrander, M.M.K. Vanderschuren, and R. de Jong. Effectenanalyse: Verkenning aanlanding windenergie op zee (VAWOZ). Technical Report 124603/21-013.723, Witteveen+Bos, Deventer, September 2021. URL https://www.rvo.nl/sites/default/files/2021/09/Effectenanalyse-Verkenning-aanlanding-windenergie-op-zee-VAWOZ.pdf.

[139] TenneT TSO B.V. Hoogspanningsstations Vierverlaten en Oudeschip, 2021. URL https://www.eemshaven-vierverlaten380kv.nl/uitvoering/hoogspanningsstations-vierverlaten-en-oudeschip.

[140] TenneT TSO B.V. Investeringsplan 2020. Net op Zee 2020-2029. Technical report, TenneT TSO B.V., Arnhem, May 2020. URL https://www.tennet.eu/fileadmin/user_upload/Company/Publications/Investeringsplannen/IP2020_NOZ_201001.pdf.

[141] E.D. Wiebes. Structuurvisie Windenergie op Zee (SV WoZ). Routekaart windenergie op zee 2030. Kamerstuk kst-33561-42, Tweede Kamer der Staten-Generaal, The Hague, March 2018. URL https://zoek.officielebekendmakingen.nl/kst-33561-42.html.

[142] Nationaal Programma RES. RES Regio's op de kaart, 2021. URL https://www.regionale-energiestrategie.nl/resregios/default.aspx.

[143] CBS. Bevolkingsontwikkeling; regio per maand, October 2021. URL https://opendata.cbs.nl/statline/#/CBS/nl/dataset/37230ned/table?dl=5B752.

A

Generation and Load Mapping

RES Region Mapping

Figure A.1: **Aggregated Dutch high-voltage grid in 2050, mapped on the RES regions.**
Connecting nodes per RES region. Black dots represent high-voltage stations. Red dots represent the RES regions. Red lines represent the connecting nodes per RES region. The number denotes the connecting nodes per region. Prints use map data from Mapbox and OpenStreetMap and their data sources. RES regions geodata obtained from Esri [76] and CBS.

Base Case

(a) Total demand mapped per node. The larger the circle the larger the total yearly demand. Basemap obtained from Esri [76]

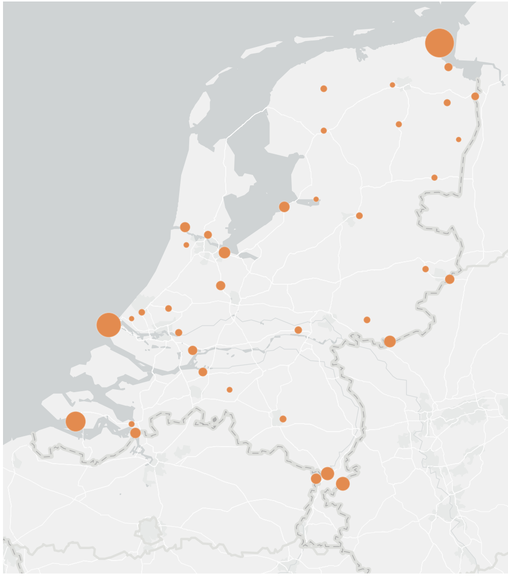

(b) Total generation mapped per node. The larger the circle the larger the total yearly generation capacity. Basemap obtained from Esri [76]

Figure A.2: **Spatial demand and generation in the base case.**

Scenario 1 - Low Electrification and Low Penetration of VRES

(a) Total demand mapped per node. The larger the circle the larger the total yearly demand. Basemap obtained from Esri [76]

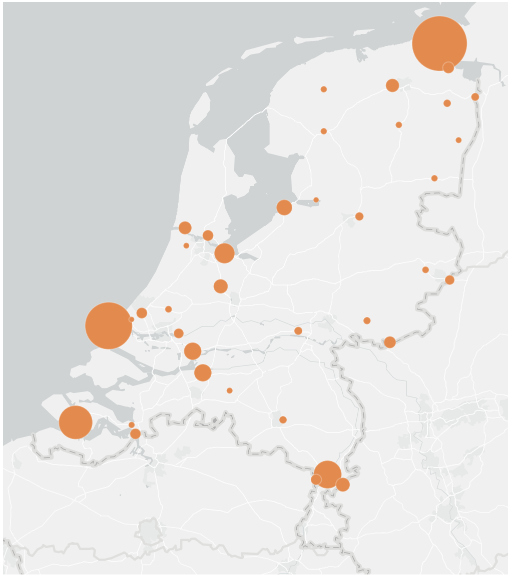

(b) Total generation mapped per node. The larger the circle the larger the total yearly generation capacity. Basemap obtained from Esri [76]

Figure A.3: **Spatial demand and generation in scenario 1.**

Scenario 2 - Low Electrification and High Penetration of VRES

(a) Total demand mapped per node. The larger the circle the larger the total yearly demand. Basemap obtained from Esri [76]

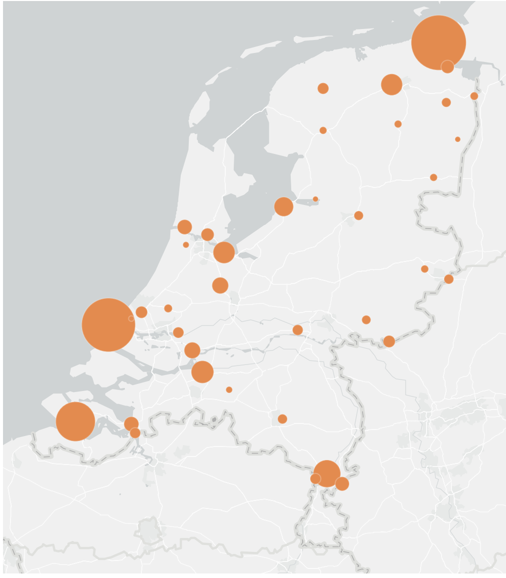

(b) Total generation mapped per node. The larger the circle the larger the total yearly generation capacity. Basemap obtained from Esri [76]

Figure A.4: **Spatial demand and generation in scenario 2.**

Scenario 3 - High Electrification and Low Penetration of VRES

(a) Total demand mapped per node. The larger the circle the larger the total yearly demand. Basemap obtained from Esri [76]

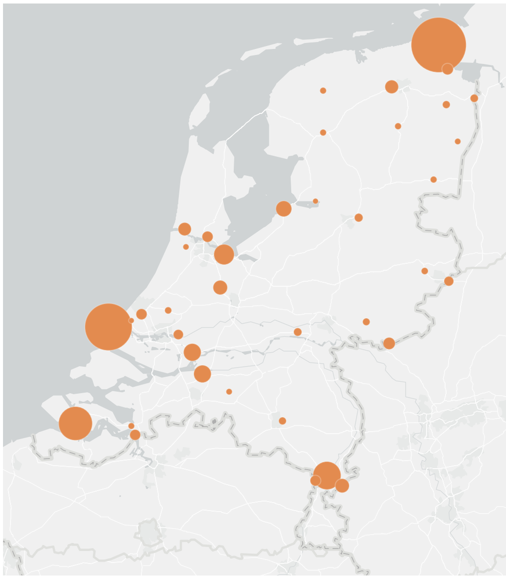

(b) Total generation mapped per node. The larger the circle the larger the total yearly generation capacity.Basemap obtained from Esri [76]

Figure A.5: **Spatial demand and generation in scenario 3.**

Scenario 4 - High Electrification and High Penetration of VRES

(a) Total demand mapped per node. The larger the circle the larger the total yearly demand. Basemap obtained from Esri [76]

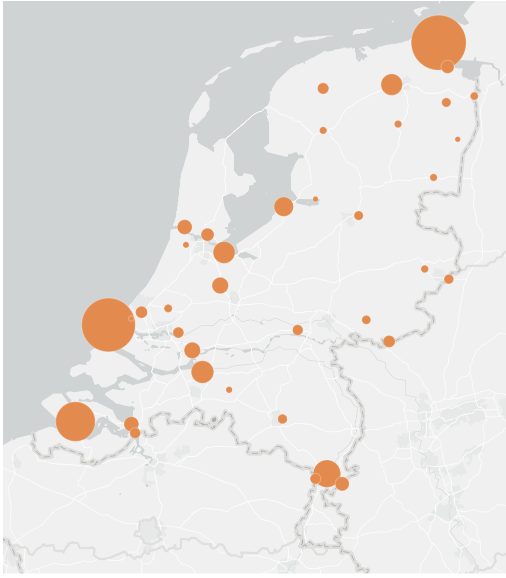

(b) Total generation mapped per node. The larger the circle the larger the total yearly generation capacity. Basemap obtained from Esri [76]

Figure A.6: **Spatial demand and generation in scenario 4.**

B

220 kV and 380 kV High-Voltage Stations

Table B.1: **220 kV and 380 kV high-voltage stations in the Dutch electricity grid.**

Station ID	Station name	Voltage level	Location	Province
EEM220	Station Eemshaven	220 kV	Eemshaven	Groningen
ENS220	Station Ens	220 kV	Ens	Flevoland
HSW220	Station Hessenweg	220 kV	Zwolle	Overijssel
LSM220	Station Louwsmeer	220 kV	Leeuwarden	Friesland
MEE220	Station Meeden	220 kV	Meeden	Groningen
OHK220	Station Oudehaske	220 kV	Heerenveen	Friesland
RBB220	Station Robbenplaat	220 kV	Eemshaven	Groningen
VVL220	Station Vierverlaten	220 kV	Groningen	Groningen
WEW220	Station Weiwerd	220 kV	Delfzijl	Groningen
ZYV220	Station Zeijerveen	220 kV	Assen	Drenthe
BKK380	Station Breukelen Kortrijk	380 kV	Breukelen	Utrecht
BSL380	Station Borssele	380 kV	Borssele	Zeeland
BVW380	Station Beverwijk	380 kV	Beverwijk	Noord-Holland
BWK380	Station Bleiswijk	380 kV	Bleiswijk	Zuid-Holland
CST380	Station Crayestein	380 kV	Dordrecht	Zuid-Holland
DIM380	Station Diemen	380 kV	Amsterdam	Noord-Holland
DOD380	Station Dodewaard	380 kV	Dodewaard	Gelderland
DTC380	Station Doetichem	380 kV	Doetichem	Gelderland
EEM380	Station Eemshaven	380 kV	Eemshaven	Groningen
EHV380	Station Eindhoven	380 kV	Eindhoven	Noord-Brabant
ENS380	Station Ens	380 kV	Ens	Flevoland
EOS380	Station Eemshaven Oudeschip	380 kV	Eemshaven	Groningen
GT380	Station Geertruidenberg	380 kV	Geertruidenberg	Noord-Brabant
HGL380	Station Hengelo	380 kV	Hengelo	Gelderland
KIJ380	Station Krimpen a/d IJssel	380 kV	Krimpen aan de IJssel	Zuid-Holland
LLS380	Station Lelystad	380 kV	Lelystad	Flevoland
MBT380	Station Maasbracht	380 kV	Maasbracht	Limburg
MEE380	Station Meeden	380 kV	Meeden	Groningen
MVL380	Station Maasvlakte	380 kV	Maasvlakte	Zuid-Holland
OZN380	Station Oostzaan	380 kV	Amsterdam	Noord-Holland
RLL380	Station Rilland	380 kV	Rilland	Zeeland
VHZ380	Station Vijfhuizen	380 kV	Haarlem	Noord-Holland
WL380	Station Westerlee	380 kV	Westland	Zuid-Holland
WTR380	Station Wateringen	380 kV	Wateringen	Zuid-Holland
ZL380	Station Zwolle	380 kV	Zwolle	Overijssel

C
Sensitivity Analysis

Households Sector

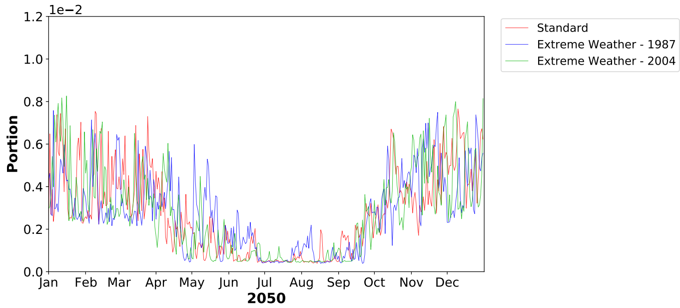

Figure C.1: **Low electrification load profiles for heating applications in the households sector in 2050 for all weather cases**.

The load profiles are shown as a portion per time step of the total load in a year, and is calculated by dividing the load per day by the total load in a year.

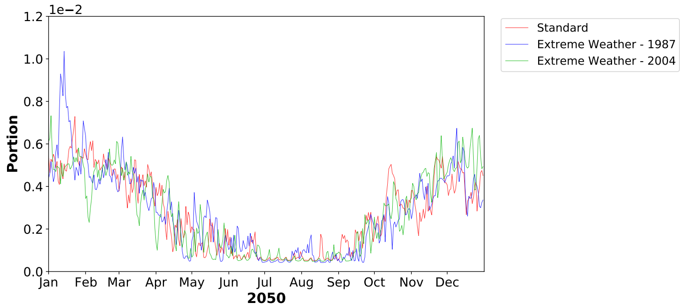

Figure C.2: **High electrification load profiles for heating applications in the households sector in 2050 for all weather cases**.

The load profiles are shown as a portion per time step of the total load in a year, and is calculated by dividing the load per day by the total load in a year.

Buildings Sector

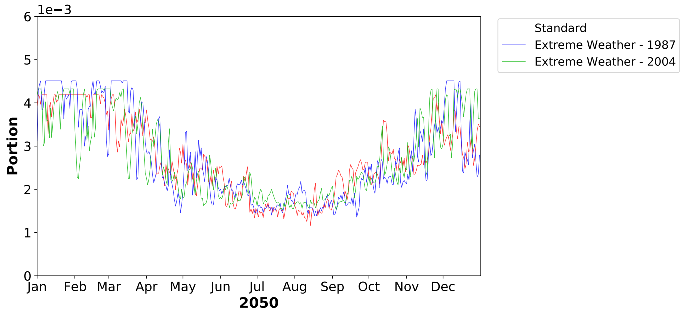

Figure C.3: **Low electrification load profiles for heating applications in the buildings sector in 2050 for all weather cases**.

The load profiles are shown as a portion per time step of the total load in a year, and is calculated by dividing the load per day by the total load in a year.

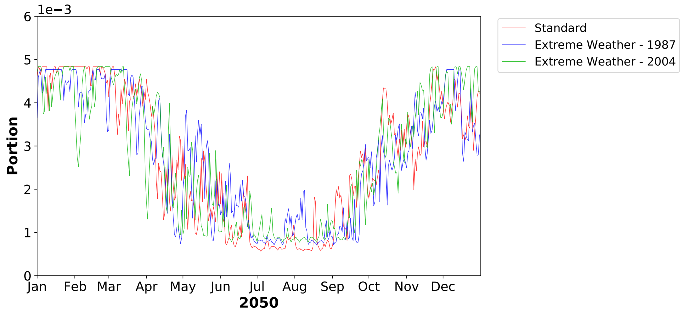

Figure C.4: **High electrification load profiles for heating applications in the buildings sector in 2050 for all weather cases**.

The load profiles are shown as a portion per time step of the total load in a year, and is calculated by dividing the load per day by the total load in a year.

Agriculture Sector

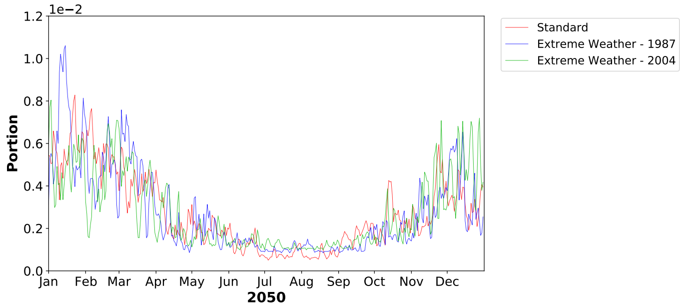

Figure C.5: **Low electrification load profiles for heating applications in the agriculture sector in 2050 for all weather cases**.

The load profiles are shown as a portion per time step of the total load in a year, and is calculated by dividing the load per day by the total load in a year.

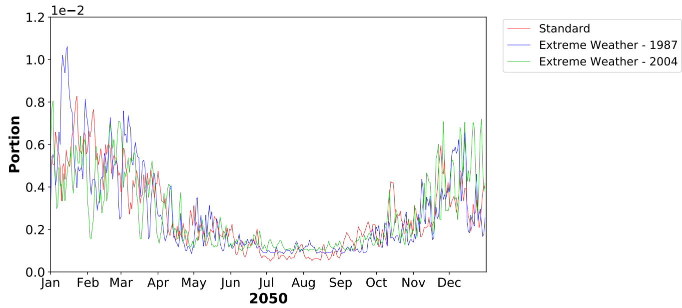

Figure C.6: **High electrification load profiles for heating applications in the agriculture sector in 2050 for all weather cases**.

The load profiles are shown as a portion per time step of the total load in a year, and is calculated by dividing the load per day by the total load in a year.

D
Bottleneck Analysis

Scenario 1 - Low Electrification and Low VRES Penetration

No electricity shortage occurs in scenario 1 as can be seen in Figure D.1.

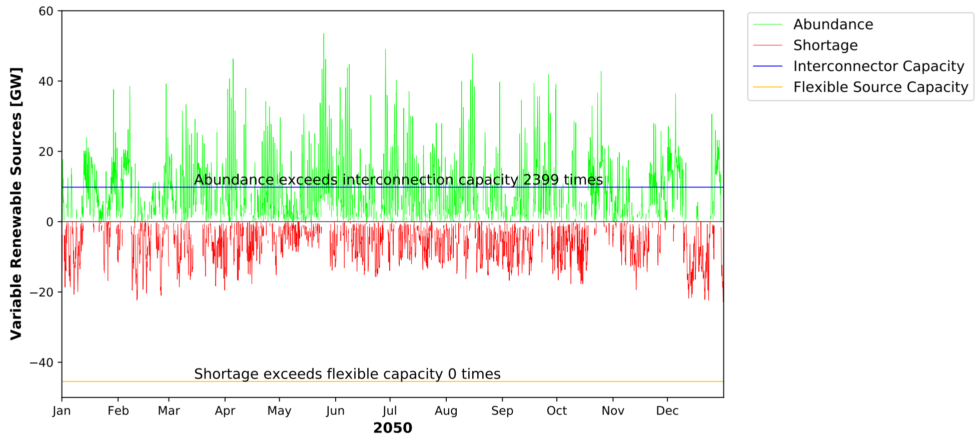

Figure D.1: **Electricity shortage in scenario 1**

Scenario 2 - Low Electrification and High VRES Penetration

No electricity shortage occurs in scenario 2 as can be seen in Figure D.2.

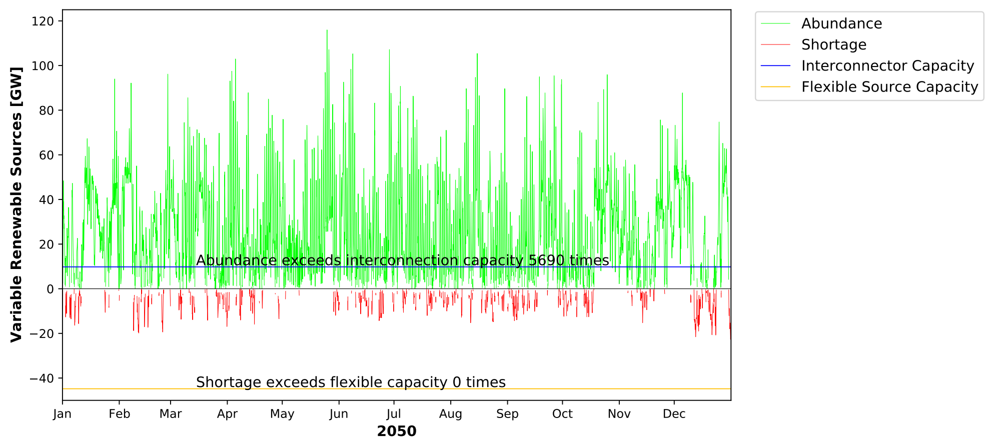

Figure D.2: **Electricity shortage in scenario 2**

Scenario 3 - High Electrification and Low VRES Penetration

No electricity shortage occurs in scenario 3 as can be seen in Figure D.3.

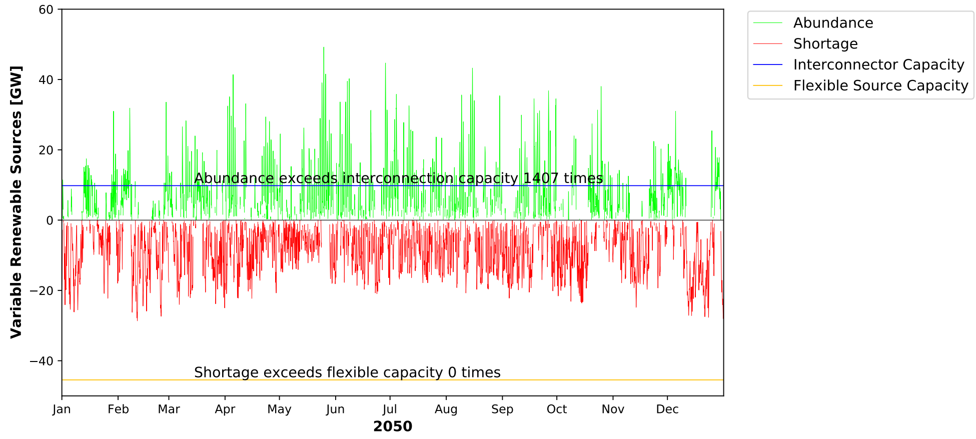

Figure D.3: **Electricity shortage in scenario 3**

Scenario 4 - High Electrification and High VRES Penetration

No electricity shortage occurs in scenario 4 as can be seen in Figure D.4.

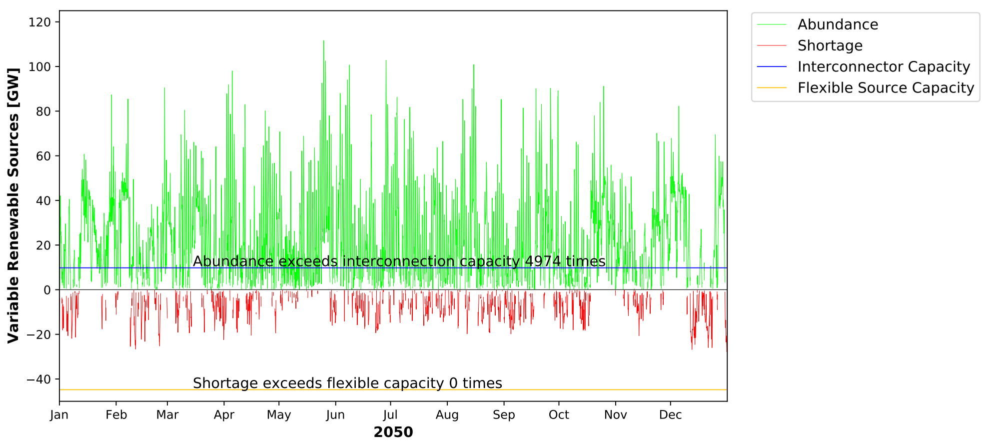

Figure D.4: **Electricity shortage in scenario 4**